uOttawa

L'Université canadienne
Canada's university

FACULTÉ DES ÉTUDES SUPÉRIEURES ET POSTOCTORALES

uOttawa

L'Université canadienne
Canada's university

FACULTY OF GRADUATE AND POSDOCTORAL STUDIES

David Saxby

AUTEUR DE LA THÈSE / AUTHOR OF THESIS

M.Sc. (Human Kinetics)

GRADE / DEGREE

School of Human Kinetics

FACULTÉ, ÉCOLE, DÉPARTEMENT / FACULTY, SCHOOL, DEPARTMENT

Three-dimensional Kinetic and Kinematic Analyses of the Olympic Snatch Lift

TITRE DE LA THÈSE / TITLE OF THESIS

Gord Robertson

DIRECTEUR (DIRECTRICE) DE LA THÈSE / THESIS SUPERVISOR

CO-DIRECTEUR (CO-DIRECTRICE) DE LA THÈSE / THESIS CO-SUPERVISOR

Blaine Hoshizaki

Daniel Benoit

Gary W. Slater

Le Doyen de la Faculté des etudes supérieures et postdoctorales / Dean of the Faculty of Graduate and Postdoctoral Studies

Three-dimensional kinetic and kinematic analyses of the Olympic snatch lift

David John Saxby

This thesis is submitted to the

Faculty of Graduate and Postdoctoral Studies

in partial fulfillment of the requirements

for the degree M.Sc. in Human Kinetics

Faculty of Health Sciences

School of Human Kinetics

University of Ottawa

Your file Votre référence
ISBN: 978-0-494-74193-1
Our file Notre référence
ISBN: 978-0-494-74193-1

Abstract

Olympic weightlifting has been subject to rigorous academic and applied sporting research for over 40 years. Biomechanists have concerned themselves with Olympic weightlifting due to the complex coordination requirements coupled with high levels of full-body muscular activity. Motivated by Enoka's (1988) research on load- and skill-related changes; we used modern three-dimensional motion capture to assess selected mechanical characteristics of the snatch lift across varied lifting intensities. Our research variables included peak moment powers about the joints of thelower extremity, bilateral shoulder symmetry, and range of anterior-posterior system centre of mass (COM) movement as barbell load was varied across 80, 85, and 90% of each lifter's maximum. The five subjects were elite-level Olympic weightlifters (mean age 23 +/- 4.18 years, mean mass 77.6 +/- 5.81 kg). Multiple dependent *t*-tests (one for each joint pair) with Bonferroni corrections were applied between left and right peak powers to assess symmetry in the lower extremities. No significant differences were found, t (df=14) = 0.068, 0.038, and 0.039. Significance statistics wereall > p (α/n) = 0.0167 about the ankle, knee, and hip joint pairs, respectively. This confirmed assumptions of previous researchers that peak moment powers in elite-level lifters were symmetrical between joint pairs of the lower extremity. Exploiting the symmetry results, we simplified further analyses by considering only the left side of the body. Repeated-measures ANOVA revealed no significant differences in average peak moment power in three dimensions about the joints of the left lower extremity across barbell intensities. In the flexion extension plane of motion, left ankle F (2, 8) = 2.594, p = 0.135, knee F (2, 8) = 0.133, p = 0.878, and hip F (2, 8) = 0.420, p = 0.671). Similar results followed for motion about the y and z axes of motion. Results indicated between 80-90% of maximal barbell load, no differences existed in average peak moment powers about the joints of the lower extremity. These results

confirmed the findings of Enoka (1988) and showed lifters do not accommodated heavier barbell loads through increased peak moment powers in the lower extremities.

Shoulder symmetry was assessed through graphical and numerical methods. All trials showed Pearson's correlations of $r > 0.95$, which indicated strong similarity between left and right shoulder trajectories. Bilateral shoulder position remained highly stable across barbell intensities, as participants did not modify shoulder symmetry across the tested intensity range. Range of anterior-posterior system COM movement showed no significant differences across barbell intensities ($F(2, 4) = 0.765$, $p = 0.523$). While the range of anterior-posterior system COM motion did not vary across barbell intensities, various motion trends were observed. The anterior-posterior range of system COM motion was quite small, but perturbations in system COM trajectory could be detrimental to subsequent lift phases as the barbell load approaches maximum.

In conclusion, peak moment powers about the joints of lower extremities did not vary significantly across snatch lifts of 80-90% maximal capacity. Thus, training programs designed to improve athletic power through the use of weightlifting movements should not exceed the 80% limit for snatch based exercises. Statistical tests revealed no significant differences between average peak moment powers between left and right joint pairs of the lower extremities. The peak moment powers during the snatch lift were not asymmetrical. Our research demonstrated elite-level weightlifters exhibiting strong linear correlation in shoulder position across the 80-90% range of barbell loads. System COM showed no significant variation in anterior-posterior range of motion across barbell intensities. This research confirmed the results previously established by Enoka (1988) regarding power response to load variation.

Table of Contents

List of Tables

List of Figures

Acknowledgements

A kind thank you is extended to the following:

- The weightlifting athletes and coach from Centre Sportif Claude Robillard, Montreal, QC, Canada.
- The University of Ottawa, for scholarship assistance to the Master's of Science program.

Introduction

Olympic Weightlifting is a sport requiring tremendous muscular effort in addition to excellent coordination and timing. The components of Olympic Weightlifting, the snatch and the clean & jerk, involve all large muscle groups of the body and are performed with an emphasis on speed of movement and technical mastery (Kauhanen, 2002; Vorobyev, 1978; Zatsiorsky, 1995). The performance of the component lifts in competitive environments, against substantial resistance and requiring maximal exertion, makes for ideal demonstrations of human strength, power and coordination. Few previousOlympic Weightlifting (OW) research efforts have provided three-dimensional kinetic data pertaining tothe snatch lift. OW research has largely been confined to two-dimensional (sagittal) kinetic research or detailed three-dimensional kinematic descriptions of segmental displacements and barbell trajectories. Only Baumann and colleagues (1985) provided 3-dimensional kinetic data from their analysis of the snatch lift. Their study did not, however, present data regarding joint specific moment powers.

The present study will investigate 3-dimensional kinetic variables, such as peak moment powers about joints, during the snatch lift at varied barbell loads. As well, an analysis of selected segmental kinematics will assess bilateral segmental symmetry and total system behaviour—path of centre of gravity during the snatch lift.

The results of the research may provide insight to the development of training systems for athletes within and outside the sport of Olympic weightlifting, as well as improving general knowledge of snatch lift mechanics.

Purpose

Stemming from the limited quantity of three-dimensional kinetic research on weightlifting, and to confirm the results of Enoka (1988) we sought to determine whether and the average 3D moment powers about the ankle, knee, and hip joints differed significantly as barbell load wasvaried during an Olympic snatch lift. As barbell load wasvaried, lift kinematics—specifically, bilateral shoulder symmetry and system centre of gravity—were analyzed to establish if lifting motions differed across barbell loads.

Hypotheses

Previous 2D kinetic analyses reported peak moment powers about joints of lower body remained constant, or slightly decreased, as barbell load increased above 70% of maximal capacity (Enoka, 1988). Enoka (1988) noted in his study of load- and skill- related changes during the clean pull, lower extremity powers remained largely constant between lifting conditions of 77% and 86% of maximal capacity. While external work and net moments of force varied positively with increased barbell load, segmental velocities decreased sufficiently such that muscle powers about the joints remained constant. Enoka (1988) concluded phase organization and timing of muscular contractions allowed skilled weightlifters to perform heavier lifts.

The first research hypothesis predicts that as barbell load increases, muscle powers about lower extremity joints would decreasesignificantly.

Regarding the kinematic analysis of lift mechanics, our second hypothesis predicted significant decreasesin system centre of mass (COM) anterior-posterior ranges of motion as barbell loads vary.

Pertaining to the behaviour of mean peak power values between left and right joint pairs in the lower extremities, our research hypothesis predicted no significant differences across between the left and right side pairs.

Finally, and stemming from the work of Rossi and colleagues (2007) on bilateral symmetry in barbell mechanics, shoulder position symmetry was assessed by correlation between left and right shoulder markers. Our contention was that there would exist a strong linear correlation between the left and right shoulder trajectories, indicating a high level of shoulder position symmetry.

Rationale

Limited three-dimensional kinetic data exists regarding snatch lift mechanics. Escamilla and colleagues (2001) argued limiting motion capture to two-dimensions (the sagittal plane) was appropriate when lifting stance was narrow and lower limbs oriented straight ahead. When stance was wide and lower limbs externally rotated, sagittal analysis alone does not completely capture all the motions. During first and second knee extensions of the snatch lift, the stance is typically narrow (defined by Escamilla as 87-118% of shoulder width), but the lower limbs are often substantially externally rotated. During drop-under, lifters adjust their base of support in three dimensions including substantial widening of their stance (Schilling, 2002; Vorobyev, 1978). We contend that due to the externally rotated orientation of the lower limbs during the snatch lift, two-dimensional motion capture would not fully capture the motion. Likely, it would underestimate flexion/extension motion as a component of this motion would not be orthogonal to the line of sight of two-dimensional motion capture system designed to assess sagittal plane motion. As we are interested in variables such as average peak moment power, and this variable is effected by the computation of joint angular velocity, the underestimation of the

flexion/extension signal would distort our analysis and weaken our strength in the conclusions drawn. Thus, three-dimensional motion capture was required for accurate mechanical analyses of the snatch lift.

Three-dimensional kinetics of snatch over varying intensities will provide valuable data to coaches and athletes participating in Olympic Weightlifting. In addition to benefiting the Olympic Weightlifting community, this research will inform the larger athletic community as Olympic Weightlifting movements and derivative exercises are commonly used training modalities to develop strength and power in athletes from a diverse range of sporting backgrounds (Bartonietz, 1996; Garhammer, 1984).

Assumptions and Limitations

The data collection environment was different from lifting environments to which participants are accustomed. In addition to introducing laboratory conditions (force plates, tracking markers, visual distracters such as lab equipment, etc.), the collection environment does not produce equivalent psychological and physiological responses elicited by competitions. During meaningful competitions, participants lift under a state of heightened physiological and psychological arousal. Elite athletes perform maximally under these aroused states (Gallucci, 2008; Jarvis, 1999). An assumption of this research design was, while personal best was improbable in laboratory environment, selected participants were elite caliber and hence could reliably reproduce their lifting techniques during data collection. This assumption was supported by McGuigan & Kane (2004) in their analysis of performance reliability over an 18 month period leading up to the 2000 Olympic Games in Sydney, Australia. They found elite lifters were capable of high fidelity repetition of lifting parameters (McGuigan, 2004) under laboratory conditions.

Previous kinetic research on Olympic Weightlifting modeled the lift system unilaterally (Garhammer, 1979; 1978; 1982; Naruhiro, 2007). Human bodies are not, however, perfectly symmetrical (Marieb, 2008). Hence the assumption of bilateral symmetry in lifting mechanics is not entirely valid. If weightlifters were to lift in a substantially asymmetrical manner this would impart undesirable torque to the barbell and disturb lift kinematics. Due to the large masses being lifted, an inefficient lift (one substantially asymmetrical) would likely result in an aborted or dropped lift (lifters often will simply abandon a poor lift rather than risk injury attempting to compensate). Recent research by Rossi and colleagues (2007) analyzed lift symmetry and barbell kinetics. Their results were in accordance with accepted athletic knowledge—successful or elite lifters lift in highly symmetrical fashion (Rossi, 2007). Rossi and colleagues (2007) found no significant differences in barbell trajectory or kinetic variables between left and right halves of the body during the clean and jerk and the snatch lift (Rossi, 2007). The present study analyzed selected kinetic and kinematic variables bilaterally to completely capture lift mechanics, and made statistical comparisons between left and right halves of the body to confirm or refute previous research regarding lift symmetry.

The current research modeled the lifting system to include both the lifter and the barbell. Previous researchers investigating the clean and jerk attempted to account for barbell deformation and elastic recoil in their models. Chui and colleagues (2008) showed barbell kinematics, and to a lesser degree kinetic variables (work, but not power), differed when using barbell centre compared to barbell ends as tracking points (Chui, 2008). The present study will not model the elastic properties of the barbell. Unlike the clean and jerk, which produces a three-point bending moment due to the narrow grip of the barbell, the snatch lift is performed using a wide grip (Vorobyev, 1978). In larger athletes, the snatch grip is often directly adjacent to the

mass plates at the barbell sleeves, thus producing a negligible moment arm between the forces of lifter and the force of gravity on the barbell.

The present study modeled the lifting system bilaterally. The lifter was divided into left and right halves; each half was comprised of an sevensegment dynamic rigid link chain. Segments included: single link foot, shank (lower leg), thigh (upper leg), hip, trunk, upper arm, lower arm, and head. This model was an extension of Garhammer's (1979) numerical approach. The barbell was explicitly represented in the kinematic chain; modelled as a uniform cylinder defined tracking markers placed at the barbell ends and an offset centre marker. Using ground-up inverse dynamics (Robertson, *et al.*, 2004; Winter, 1980; Zajac, 2002), net muscle moments of force about lower extremity joints in kinematic chain were resolved in three dimensions.

Conditional to lift kinematics being symmetrical, no moment of inertia or inertial tensors were used to model hand-mass link, as the barbell was assumed to have only translation (horizontally and vertically) and no rotation. Research has previously identified barbell trajectories to be confined to horizontal and vertical barbell displacements (Baumann, 1985; Brudett, 1982; Garhammer, 1985; Gourgoulis, 2002; 2004; 2009; Hiskia, 1997; Rossi, 2007; Salaami, 2008; Vorobyev, 1978).

The sleeve of the barbell rotated about a bearing system with friction assumed to be negligible. The barbell used in this study was an elite training bar and was in excellent condition (clean, well oiled and with no permanent deformation). As a result, we chose to ignore any resistance to rotation of hand-barbell complex around the barbell sleeve. Similarly, interaction between hand and mass was assumed to be fixed with no relative motion. Hence, hand and barbell were modeled as single rigid mass system.

This study used conventional kineticanalysis methods based on ground-up inverse dynamics (Robertson, 1980; Winter, 1980; Zajac, 2002). As such, several sources of errors were present in development of data.

Double differentiation of displacement histories amplified existing signal noise in displacement histories to subsequent velocity and acceleration histories. To address this issue biomechanists have utilized filters (both digital and analog) to remove noise from kinematic histories (Pezzack, 1977; Robertson, 2003; Robertson, *et al.*, 2004). The present research used a digital zero-lag low-pass Butterworth filter, with cut-off frequency of 8 Hz to filter kinematic histories and a high-pass version (10 Hz cutoff) to filter analog signals from force platforms. The strength of this particular filtering method was twofold. First, Butterworth filters are optimally flat in pass band (Robertson, 2003). Secondly, the zero-lag feature made this filtering method prudent for research which involved time sensitive analysis.

A first-order Butterworth filter does not have particularly competitive roll-off compared to other filtering methods (Chebyshev or elliptical), but this may compensated for by increased filtering order (Robertson, 2003).

Skin motion artifact, perhaps more appropriately labeled soft tissue artifact (STA), is caused by imposition of soft tissues between surface markers and rigid skeletal structure. Unlike filtering of kinematic and kinetic series above mentioned methods, STA has frequency spectrum embedded within frequency range of skeletal movement (Cappello, 2005). Therefore STA cannot be removed using analogous filtering techniques used on kinematic or kinetic histories (Cappello, 2005).Marker redundancy and various least-squares methods have been used to attempt to control for STA. Cappello (2005) outlined several mathematical approaches used to establish marker position and control for elements of STA. These approaches did not control for rigid

(relative to other segment tracking markers) translation of marker clusters and orientation with respect to the skeletal structure and hence did not fully eliminate STA (Cappello, 2005) Estimation of joint centres and segmental centres of mass are affected by STA STA is a pervasive and systematic source of error in motion analysis laboratories The impact of STA, and more generally, of proximal or distal segmental endpoint kinematics has been discussed by McGibbon & Krebs (1998) When rigid body assumptions were strictly adhered to, power imbalance (difference between segmental rate of energy change and segment moment power model) was zero When segmental displacements were calculated using marker tracking systems, segmental length changes occurred during motion due to influence of STA and residual errors in motion capture systems (McGibbon, 1998) Furthermore, when segmental velocities were calculated using finite difference calculus (routines based on Newtonian difference quotient), artifact was passed onto the subsequent velocity series (McGibbon, 1998), resulting in power imbalance Present research methods utilized tracking markers to indentify segmental endpoints and employed numerical methods to calculate segmental velocities and accelerations Thus, cautious interpretation of power calculations was necessary

A limitation of Newton-Euler inverse dynamics exists in its disregard for the action of biarticular muscles in mechanical power delivery to segments Net power about any given joint, computed by the product of net moment of force and angular velocity, represents "summed power to/from all the segments by all the net joint moments, and thus by all the muscles" (Zajac, 2002) As noted in the comprehensive review by Zajac (2002), a net muscle power does *not* represent summed mechanical power delivered to spanned segments about a specific joint by spanned musculature, because of presence of biarticular muscles and dynamic coupling Biarticular muscles (those muscles which span two joints) deliver mechanical power to other

segments, hence preventing simple summation of powers about a joint. As result, dot product of a muscle moment vector and joint angular velocity about which muscle spans cannot be used to determine net muscle power being delivered to spanned segments by muscle(s) in question.

$$\text{Moment power} = (\text{net moment of force}) \times (\text{joint angular velocity}) \quad (1)$$

As a result, the above equation does not account for effects of net moments of force on joint intersegmental forces nor the power delivered to non-spanned segments (Zajac, 2002). A more generalized expression expands Newton's summation of forces, with $\sum F = ma$, becoming,

$$\boldsymbol{I}(\mathbf{q})\ddot{\mathbf{q}} = \mathbf{M}^{\text{joint}} + \mathbf{G}(\mathbf{q})g + \mathbf{V}(\mathbf{q}, \dot{\mathbf{q}}) + \mathbf{F}^{\text{non}}(\mathbf{q}, \dot{\mathbf{q}}) \quad (2)$$

where $\mathbf{q}, \dot{\mathbf{q}}, \ddot{\mathbf{q}}$ are vector coordinates, velocities, and accelerations, respectively; $\boldsymbol{I}(\mathbf{q})$ is system mass; $\mathbf{M}^{\text{joint}}$ vector of net joint muscle moments (whereby $\mathbf{M}^{\text{joint}} = R(q)F^{mus}$, with R(q), moment arm matrix (3 directions of motion), and F^{mus}, joint muscle force vector); $\mathbf{G}(\mathbf{q})g$, $\mathbf{V}(\mathbf{q}, \dot{\mathbf{q}})$, $\mathbf{F}^{\text{non}}(\mathbf{q}, \dot{\mathbf{q}})$ are gravity vector, Coriolis and centripetal, and non-muscle contributions (Zajac, 2002). "The force generated by a muscle acts to accelerate instantaneously not only the segments to which it attaches and the joints that it spans, but also all other segments and joints" (Zajac, 2002). It is fundamentally erroneous to conclude muscle only delivers and receives power to and from adjacent segments.

It was not within the budget of this study to perform body composition analysis using DEXA. Basic body metrics, such as height and mass, were collected from participants. This information was used to better estimate subject specific inertial parameters. Due to highly developed musculature found in lower extremities of elite level Olympic weightlifters, anthropomorphic estimations established by Dempster (1955) were likely not representative of participants' segmental inertial characteristics. Chui (2005) performed a study which focused on

differences in kinetic output variables using DEXA or Dempster's data in processing. Chui (2005) found small, yet significant, differences in net muscle moments of force about hip joint in sagittal plane using different anthropometric data (Chui, 2005). The exclusion of DEXA technology was regrettable, but use of standardized anthropometric data in inertial calculations was likely only small contributor to total error in an inverse dynamics approach (Chui, 2005).

Delimitations

Participants in the present study were elite-level male Canadian weightlifters. The sample was not randomly selected from general population. Nor was it representative of all elite-level Canadian lifters, as participants were all male and hailed from the same training facility. This limited external validity of the research and required cautious interpretation and extension of results to the broader lifting community.

Each participant performed three snatch lifts at each of the three lifting intensities. Subject order was blindly selected, and lift order wasbalanced across subjects.Trials from each lifting condition were averaged per participant to limit the effect of outliers on variance analyses. Final averaged data were not representative of any single lift, but of trends in lifting mechanics.

Review of Literature

The ability to move powerfully, performing movements in a rapid manner is required in many sports. Mechanical power, defined as rate of work or as a product of force and velocity, is a variable commonly used to assess athletic ability (Baechle, 2000; Garhammer, 1984; 1993). Many fitness assessments such as the Wingate Anaerobic test, various maximal progressive aerobic tests, and vertical jump tests use mechanical power as a key determinant of fitness or athletic capability (Brooks, 2005). As such, development or improvement of human power output is given much attention in the athletic world.

Typically, training protocols designed to assist athletes in developing muscular power, utilize specific forms of resistance exercises. Increasing muscular power requires improvement of the neuromuscular system's ability to rapidly convert chemical energy stores (ATP and CP) into high rates of mechanical work through the skeletal structure. The principle of specificity of training (specific adaptations to imposed demands) dictates a biological system will respond to applied stress in a mode-specific manner (Brooks, 2005). Regarding development of mechanical power in muscle through resistance training, specificity of training principle demands athletes perform loaded movements—primarily large muscle groups–focusing on variable speed of movement and technical mastery (Cronin, 2001). Olympic Weightlifting (OW) is an ideal training method to develop muscular power in athletes, as lifts and assistance exercises utilize all major muscle groups, over large ranges of joint amplitudes, at high rates of work, and can be performed at various resistance intensities (Naruhiro, 2007; Vorobyev, 1978).

Due to the similarities in movement patterns, OW is often compared with vertical jumping as an example of maximal human power output (Channell, 2008; Garhammer, 1992; Markovic, 2007). OW involves, however, larger knee extensor moments of force, substantial

trunk stabilization (isometric contraction), and shoulder girdle activity not seen in vertical jumping (Garhammer, 1978). OW involves full body musculature in performance of rapid movement against substantial resistance lasting less than one second. From this lens, Olympic Weightlifting is the quintessence of human power output.

As a competitive sport, OW consists of two distinct lifting movements with a precise set of rules controlling their execution. The first is the snatch lift and the second is the clean &jerk. Briefly, the snatch lift involves gripping the barbell wide (past shoulder width), powerfully and continuously lifting the barbell overhead, catching with fully extended elbows (locked out) and standing with the weight under control. The clean and jerk involves two distinct phases:the clean phase involves a narrower grip than the snatch and the goal of the clean is to powerfully lift the barbell from the floor onto the front of the shoulders. The jerk phase involves rapid thrust upwards of the barbell and simultaneous drop-under of the body, resulting in arms locked out and weight held overhead. These above descriptions are rudimentary, for detailed explanation of the subtleties of lifting technique refer to Baumann, 1985; Campos, 2006; Garhammer, 1985; Hiskia, 1997; Kauhanen, 1984; Gourgoulis, 2002; 2004; 2008; and Vorobyev, 1978.

Extensive descriptive research on OW has been conducted (Baumann, 1985; Campos, 2006; Garhammer, 1985; Hiskia, 1997; Kauhanen, 1984; Gourgoulis, 2002; 2004; 2008; Vorobyev, 1978), but only select studies have focused on kinetic variables. Specifically, Garhammer (1978; 1979; 1980; 1982; 1984; 1985; 1991; 1992; 1993) and Enoka (1979; 1983; 1988) established guiding research concerning variables such as segmental energy flow, vertical ground reaction force characteristics, total work and power output. Garhammer (1982) used a 5-link dynamic rigid segment model to examine intersegmental energy flow during weightlifting movements. His analysis demonstrated that during OW, segmental potential energy increases

were significantly greater than segmental kinetic energy increases during both snatch and clean & jerk movements. Weightlifters typically lifted more mass during the clean and jerk than in the snatch. Garhammer (1982) demonstrated, however, *total* work done during each lift to be equivalent. This equality was produced by the inverse relationship between segment and barbell energy curves in OW. The clean and jerk is a more compact movement with both smaller body segment displacements and kinetic energy than the snatch, but larger barbell potential energy due to the relatively larger mass. Conversely, the snatch requires both larger segment displacement and kinetic energy, but possesses smaller barbell potential energy due to relatively smaller barbell load. When summed, total (system) work done during each lift was comparable (Garhammer, 1982).

Enoka (1979) studied OW 'pull' (defined by lifters and academics alike as barbell liftoff to final thrust upwards) and reported several interesting results. First, pull technique of participants in his study did not conform to proposed force-phase relationship of Grieve (1970). Grieve (1970) predicted that for successful lifts, the initial pull of the barbell off the ground to knee height must be more forceful than the second pull. Enoka's (1979) participants were able to successfully complete a series of lifts, and only one of Enoka's (1979) participants fulfilled Grieve's (1970) "requirement" for success. The results of Enoka's (1979) study questioned the predictive validity of Grieve's (1970) force-phase relationship.

Secondly, Enoka (1979) identified a triphasic force pattern exerted on the ground and barbell during OW pull. These results showed OW movements were not performed as a single vigorous lift from the ground to finish. Rather, OW lifts involved two periods of net system acceleration separated by a period of net system negative acceleration. Enoka's (1979) study utilized the vertical ground reaction force as indicator of net system impulse and barbell

kinematics to induce impulse applied to the barbell. While ground reaction force and induced barbell impulse largely agreed, periods of net positive and negative acceleration only described system behaviour and could not account for relative intersegmental motions during these phases.

Thirdly, Enoka (1979) provided mechanical explanation for the use of double-knee bend technique (DKB). DKB technique utilized a period of "unweighting" (referred to as the "rebend") to transition between the two phases of net positive system acceleration. The rebend involved concentric knee flexion and occurred after the knees were initially extended to lift the barbell from the floor to knee height. DKB technique produced a brief period of net negative system acceleration. Intuitively this would seem counterproductive in a sport where the primary objective is to lift a large mass overhead. Enoka (1979) noted, however, DKB technique provided several mechanical advantages, which compensated for the decrease in net system acceleration. Using a quasistatic model of the lifting system at the end of the first pull, Enoka (1979) calculated the resultant muscle moment of force (primarily back and hip extensor moment of force) required to maintain equilibrium with and without DKB technique. Use of DKB technique produced approximately 70% lower back and hip extensor muscle torques through the realignment of the torso and subsequent decrease in moment arm length.

Fourthly, in addition to a reduction of the extensor moment of force about hip, the DKB technique redeployed knee extensors over their optimal range for the second pull. At the end of first pull, Enoka (1979) reported mean knee extension angles of 145±6°. This is at the upper limit of optimal knee extensor capacity as reported by Smidt (1973). After transition, the mean knee extension angle was reported as 136±6°, and within optimal extension range (Smidt, 1973).

Finally, the DKB technique involved concentric contraction of knee flexors, which may contribute to substantial elastic energy storage in the knee extensors as they eccentrically resist.

In this respect, the DBK technique has been likened to the mechanical advantages found in the jumping countermovement. Garhammer (1981) noted the asymptotic relationship between force and velocity in muscle–well documented in isolated muscle contractions (Abbott, 1952; Hill, 1938, Katz, 1939; Wilkie, 1949)–has also been identified in multisegmental movements such as weightlifting. Enoka (1979) identified elastic energy storage in knee flexors as a possible mechanical advantage of the DKB technique.

Enoka (1983) investigated muscular control patterns in rapid learned movements. He tested the "Speed Control Hypothesis" (SCH) under novel movement conditions. The SCH stipulated a movement variable, such as speed, is modulated by contraction intensity only, while contraction duration remains constant (Freund, 1978). Enoka (1983) used the double-knee bend (DKB) technique of skilled and less-skilled weightlifters as means to test the predictive ability of the SCH under conditions of varying intensity, multidirectional and multiarticular motion. Results showed the SCH provided limited predictive validity when the movement paradigm included multiple joints and multiple directions of motion. During the first pull of the clean (from the ground to knee height), contraction duration remained constant while contraction intensity increased with incremental barbell loads. This phase was consistent with predictions based on the SCH. During rebend (period of concentric knee flexion between periods of extension) the more skilled athletes showed, however, increased flexor moment *duration and force* as barbell load increased compared to less-skilled lifters. These findings prompted two important conclusions. First, the results displayed several limitations of the SCH, which predicted only intensity modulations with increasing load. Secondly, Enoka's (1983) research identified a key difference between skilled—and less—skilled lifters independent from force production and related to temporal organization of movement patterns.

Another crucial finding from Enoka's (1983) work was the typical triphasic muscle activation patterns found in rapid single joint movements were not seen in the DKB technique. Rather, a biphasic pattern of concentric muscle activity to create acceleration in a given direction was followed by eccentric activity to slow segments and prepare for the change of direction.

The present study excluded female lifters and confined research to males only. Hoover and colleagues (2006) provided relevant insight into the potential variance found in lifting technique between males and females. Hoover and colleagues noted, in their analysis of U.S. National caliber women weightlifters, three distinct differences in female lifting technique compared to established standards for male lifters. First, few lifters (less than half of their sample population) exhibited standard horizontal barbell kinematics during the snatch lift. Specifically, women often do not replicate the towards-away-towards barbell path established as mechanically desirable in men (Burdett 1982; Garhammer 1985; Hiskia 1997; Gourgoulis *et al* 2002; 2004; 2008). Hoover and colleagues suggested suboptimal barbell trajectories were due to the relative inexperience of female weightlifters, since women's weightlifting competitions are relatively new (Olympic status in Sydney Games, 2000). Popularity, participation, and visibility of women in this sport, while growing, remain largely secondary to males.

Secondly, drop-under depths and times reported by Hoover and colleagues were larger than those reported for elite male lifters. The authors speculated these differences may reflect actual sex-related differences in muscle behaviour. Specifically, they suggested drop-under depth and time differences between males and females were caused by females' limited use of the stretch-shortening cycle to store elastic energy in rapid motions (Hoover, 2006). Thus, it would be inappropriate to use a mixed-sex sample population as sex-related differences could potentially act as confounding variables when attempting to isolate the effects of some other

variable of interest (for example, peak moment power). Hoover and colleagues' work was aligned with previous kinematic comparisons between male and female lifting technique performed by Gourgoulis and colleagues (2002). Gourgoulis and colleagues reported significant differences in selected kinematic variables between male and female lifters. Specifically, female drop-under times were significantly slower than males (Gourgoulis, 2002).

Finally, in comparison to world-class women lifters, U.S. National-level women lifters produced significantly lower maximal vertical barbell velocities during the snatch lift (Hoover, 2006). Difference in output variables must be considered for any statistical comparison between groups of mixed sex.Garhammer (1991) analyzed lifts at the first Women's World Weightlifting Championships in 1987. His review compared power outputs from the women's competition to previous male records. Results showed female power output between 65-75% of male power output. The results were in agreement with women's vertical jump performance compared to male vertical jump once adjusted for body mass. Similar to the results of Hoover and colleagues (2006), Garhammer (1991) found slower transition times, reduced knee flexion amplitude during transition, and slower drop-under phases when compared to male lifters (Garhammer, 1991).

To our knowledge, only one research team has performed a three-dimensional kinetic analysis of snatch lift (Baumann, 1985). Their results indicated two-dimensional motion capture does not accurately measure motions of lower limbs during the snatch lift. Baumann and colleagues (1985) concluded three-dimensional investigations are required for accurate biomechanical analysis of Olympic Weightlifting. Interestingly, they found relatively low knee extensor and flexor moments of force, and could not provide mechanical evidence for common knee injuries reported byweightlifters. Conversely, net hip extensor moments of force were several times larger, reaching values as high as 660 Nm in selected participants. A strong

correlation(r = 0.95) between the barbell load and hip extensor moments was observed.Knee moments of force did not, however, significantly co-vary with the barbell load.

The majority of studies interested in kinetic variables do not account for upper body segmental contribution to lift mechanics. Inspection of lifters' musculature suggests upper limbs do not substantially contribute to lifting mechanics. Burdett (1982) reported, however, drop-under rates faster than could be produced by gravity alone. It is likely upper body musculature actively pulls the lifter under the bar. As such, 'drop-under' may be a misnomer, and 'pull-under' may be more representative of actual mechanics.

Garhammer (1978; 1979; 1980; 1982; 1985) modeled the upper body as series of non-deformable rigid links: torso, head, arm-mass. A variation on this model was used in the present study. The present study used an iterative Newton-Euler approach to resolve net joint moments of force and powers. A brief review of this process is provided below. Classic link mechanics are well described in the seminal work by Elftman (1939), as he investigated forces and energy changes during human locomotion (Elftman, 1939). Traditional Newton-Euler approaches involve modeling the mechanical system as a series of n-link non-deformable segments linked by frictionless joints (Miller, 1979). The body is thus modeled as a series of interconnected segments whose properties such as length, mass, centre of mass and moment (or tensor moment, if 3-dimensional) of inertia may be estimated using anthropometric data developed on cadavers (Dempster, 1955; Pezzack, 1977). To resolve net moments of force, researchers exploit the Newton-Euler equations.

Linear and angular segment accelerations are derived by double differentiation of displacement histories (Pezzack, 1977). As displacement histories are typically non-uniform, differentiation is accomplished by iterative (frame by frame) numerical estimation using finite

difference calculus, and executed by computer routines (Robertson, *et al.*, 2004). Prior to differentiation, as raw kinematic histories contain noise, data are filtered to reveal the signal and minimize the noise (Robertson, 2003). Net moments of force about a joint are determined by working progressively up (or down) the kinematic chain. The process begins at a point of known force application—typically distal in origin, such as a foot pushing against a force platform or a limb pulling on a gauged instrument or wire. The force about the subsequent joints may be induced by their accelerations, mass/inertial properties, and by Newton's Third Law of action and reaction (in this case applied to force couples about a joint). As such, without regard to the validity of modeling segments as rigid bodies, all net moments of force in a bounded and non-looped kinematic chain may be resolved by such an iterative approach (Winter, 1980).

Methods

Participants

The sample selection method was non-probabilistic. Subjects were selected deliberately to ensure competent lifting performances and for convenience. The sample consisted of five elite-level Olympic weightlifters (mean age 23 +/- 4.18 years, mean mass 77.6 +/- 5.81 kg). All subjects were elite-level (international caliber) weightlifters. All lifters train at Centre Sportif Claude Robillard in Montreal, Quebec.A larger sample size would have increased statistical power.It was, however, not possible given the pool of elite-level weightlifting competitors within Canada, to recruit a large sample for analysis. As well, it was not within the research budget to import elite-level weightlifters from other countries. We proceeded with the knowledge of the limit placed on statistical power by our small sample size, and were careful in thegeneralization of results. We readily acknowledge the trade-off between participant caliber and statistical power. The design of this research was purposefully constructed to examine elitelevel lifting mechanics, and as such the limited statistical power was a byproduct of conscious design and was not an implementation oversight.

Research Design

A 14-segment rigid-link model represented the human musculoskeletal system. Segments included were: single link feet, lower legs, thighs, pelvis, torso, head, upper arms, forearms, and a hand-barbell complex. Participants executed three snatch lifts at 80, 85 and 90% of their personal bests in the snatch lift. The research effort confined itself to snatch lift mechanics and did not encompass analysis of the clean & jerk. The snatch was selected for 3 reasons. First, the snatch was mechanically simpler to analyze because it did not involve modeling two phases of

elastic recoil of the barbell as required by analysis of the clean & jerk (Chui, 2008). Secondly, during the snatch lift the barbell did not rest on the lifter's body, as did during the clean & jerk, thus we did not need to account for any period of closed loop mechanics that the clean & jerk required. Finally, on a practical note, the amount of mass lifted and its accommodation within the laboratory necessitated the use of the snatch lift, as clean & jerk loads may have exceeded the safety setup in the laboratory.

Trial order was balanced to minimize order effects. Athletes blindly selected their lift progressions, consisting of ascending slope, descending slope, normal pyramid and inverted pyramid.

As our research was interested in peak powers during the snatch lift, we did not include analysis of the reception of the barbell nor the overhead squatting phase. Inspection of Figure 4 in the results section shows the drop-off the moment-powers about the ankle, knee, and hip once the barbell has been propelled overhead. Large eccentric powers do exist, but they are used stop the descent of the barbell and lifter thus permitting the lifter to stand to full extension. As such, analysis of data began with vertical displacement of the barbell and terminated with the lifter's loss of contact with the ground.

Prior research regarding lifting results by weight category (Kauhanen, 2002) reported lift totals (snatch and clean &jerk combined) as non-normal in distribution. Normality of research variables was tested using the Shapiro-Wilk Normality test (Shapiro, 1965). If the distribution of the output variables proved to be non-normal, then subsequent variance analyses werenon-parametric in nature. Repeated-measures variance analysis of non-parametric data sets were accomplished by using Friedman's Test for analysis of non-normal groups (Friedman, 1937), and paired comparisons were performed using Wilcoxon signed rank test (Wilcoxon, 1945).

Laboratory Setup

Data collection took place at in the Biomechanics Laboratory of the University of Ottawa. The laboratory was modified to allow lifters to perform in the same manner as during training or competition. Crash pads surrounded the force platforms so lifters could drop the loaded barbell, as is customary in OW training.

Five MX cameras and one Panasonic PV-DV601 high-definition camera captured lift kinematics. Cameras sampled the motion at 200 Hz with a calibrated lifting volume of 1.3×2×3 m. Ground reaction forces of both feet were recorded using two fixed Kistler piezoelectric force platforms. Analog data from these force platforms were sampled at 200 Hz.Before analog data was collected, residual voltages were assessed while the force platform was unoccupied. Signal voltages were adjusted manually such that these low-level signals hovered about the zero mark. Due to the substantial vibrations created by participants dropping the loaded barbell, the force platforms became saturated following each collection event. As such, force platforms were zeroed before the collection of a new trial.

The University of Ottawa full-body marker set was used across the body, in addition to segment clusters for marker redundancy. The lifter's body was defined as a 13-segment model and a barbell. The segments were defined by placing reflective markers over prominent musculoskeletal landmarks found through palpation. Their definitions were as follows. The foot was constructed by placing reflective markers at the 1st and 5th metatarsal-phalangeal joints, medial and lateral malleoli, and posterior aspect of the calcaneus. The shank (or lower leg) was defined using the superior aspect of the previous segment (left and right malleoli of the ankle), and the medial and lateral condyles of the femur. The thigh (or upper leg) was defined by the medial and lateral condyles of the femur and by the lateral aspect of the greater trochanter of the

femur. The pelvis was defined using the greater trochanters of the left and right femurs, and the left and right anterior superior iliac spines. The torso was defined using the left and right anterior superior iliac spines for the inferior border, and the left and right acromion processes for the superior border. The upper arm was defined by the acromion process and the medial and lateral epicondyles of the humerus. The lower arm was defined by the medial and lateral epicondyles of the humerus at the proximal end, and the radial prominence and styloid process of the ulna at the distal end. The head was defined using the centre of the forehead, left and right ear centres, and the centre of the occipital plate on the posterior aspect of the cranium.

Three markers were placed on the barbell to track its motion in 3-dimensional space. Markers were placed at both ends of the barbell and one placed in an offset position at the centre. It was crucial to offset one (it did not have to be the central marker, but this was a natural choice) of the markers, because if all three markers were to have possessed 2 common planar positions it would have been impossible to create an object geometry with a full 6 degrees of freedom.

With the lifter and the barbell defined in 3-dimensional space, the determination of the system centre of mass followed from the computation of the centre of mass of a single segment in our system. By using the segment boundaries imposed by the reflective markers on key anatomical landmarks, each segment possessed proximal and distal radii. Based on these values and the longitudinal distance between them a normal frustum was created for all segments, except the torso and head. The head was represented by an ellipsoid with semi-major axis found by front and back head markers, and with semi-minor axis found by left and right ear markers. The trunk was represented by an elliptical cylinder with superior semi-major axis found by the left and right acromion processes, superior semi-minor axis estimated by the distance between sternum and back tracking marker, inferior semi-major axis found by the left and right anterior

superior iliac spines, and the inferior semi-major axis found by the reproduction of its superior analog. Due to the differences between proximal and distal (superior and inferior) segment dimensions, segment volumes were tapered at their distal (or inferior) borders.

Using standard anthropometric data as well as the height and mass of the participant (measured in the laboratory on the date of data collection), a segment's mass was determined as a proportion of the participant's total mass (Miller and Nelson, 1973). The segment's centre of mass and inertial properties were determined by integral calculus. First, for each segment's geometry, mass was assumed to be uniformly distributed (constant density). As such, the centre of mass of each segment was located at the centroid of the volume. The inertial properties were computed by the partial integration (x, y, and z directions) of the mass density function for the given geometry. System centre of mass was thus computed, frame by frame, as the weighted (proportional to the total system mass) average of the positions of the segment centres of mass. Naturally, in a 3D environment this process was carried out in each of the component directions (x, y, and z) and reduced to a single three-dimensional coordinate. This point was thus said to be the system centre of mass, and was tracked during data collection. Segmental motion was oriented first to the global (lab) coordinate system to provide its position within the data collection environment, and secondly to the linked segments to provide the relative motions between adjacent segments. As a segment moved through space its tracking markers provided transformation and rotation values in relation to the global (lab) Cartesian origin (0, 0, 0). Thus, frame by frame, a segment would have a 3D coordinate describing its position, and a coordinate describing its orientation. In order for these data to be used to develop kinematics such as joint angles, angular velocities, or accelerations, first the relationship between linked segments must be established. To accomplish this, an internal (relative) frame of reference for each segment was

established. Convention has established the origin for each segment to be placed at the proximal (or superior) end for axial segments, although the placement of the origin was strictly arbitrary. Following convention was convenient as motion about these joints usually described with the assumption that the limbs to move about a stable proximal anchor. Using the lower leg (shank) as an example, the internal/external rotation axis (z axis) is defined as the line joining the proximal and distal centres of the segment as defined by the proximal and distal segment markers. A plane of best fit is developed using the medial and lateral marker positions from the proximal and distal segment boundaries. The abductor/adductor axis (y axis) was found to be orthogonal with this plane of best fit. Finally, the flexion/extension axis (x axis) was found as the cross product of the z and the y axes.

With respect to the internal frame of reference, the relative motion between linked segments (for example the lower leg and the upper leg) can be developed by the relative differences between the metric of interest (for example the difference between the angular rotation velocities of the upper and lower leg).

Vicon Workstation was used to synchronize force platform data and the labelled kinematic histories into one file (.C3D file format). Data were then processed with Visual3D. Filtered (8 Hz) and differentiated displacement histories were applied to iterative Newton-Euler formulations to resolve net joint moments of force and powers about the joints of interest (see literature review for more details). Visual3D also allowed for modification of segment parameters (mass, inertial properties, geometries, etc.), custom report templates and pipeline commands for data exportation to specialized graphical software such as Excel and BioProc3.

Results and Discussion

Results

For all three research hypotheses, statistical testing resulted in the uniform failure to reject the null hypotheses. Detailed numerical and graphical exploration of data and subsequent variance and deviation testing may be found in Appendix A. Using a Shapiro-Wilk's test of normality (Shapiro, 1965), peak power data about the six joints of the lower extremities in the sagittal plane were found to be normally distributed. When these kinetic data were organized by barbell loadand these individual three sections again tested for normality, peak powers about the six joints of the lower extremities in the sagittal plane were found to be normally distributed. With normality statistically assured, we proceeded with subsequent analyses.

Table 1 listed average peak powers about the six joints of lower extremities. Figures 1-3 display the effect of barbell load on average peak powers about left ankle, knee, and hip, respectively, in the x axis for all lifting participants. In Figures 1-3, average peak power is plotted on the ordinate, and normalized to body mass as W/kg. On the abscissa is plotted relative barbell load as % of maximal snatch lift capacity. Average peak power about left lower extremity joints remained stable across barbell intensities. Statistical tests (repeated measures ANOVA) were used to verify this visual trend. Table 2 lists the results of pairwise t-tests, used to assess bilateral symmetry of peak powers about the lower extremity joints in x axis.

Table 3 displays the results of the nonparametric assessment of bilateral symmetry for peak powers about the lower extremity joints in the y axis.Table 4 displays the results of the nonparametric assessment of bilateral symmetry for peak powers about the lower extremity joints in the z axis.

Lifter code	Barbell load	Left ankle power (W/kg)	Left kneepower (W/kg)	Left hip power (W/kg)	Right ankle power (W/kg)	Right knee power (W/kg)	Right hip power (W/kg)
1	80%	6.53	2.99	14.75	8.19	2.90	13.54
2	80%	6.92	4.74	12.17	10.87	4.60	10.43
3	80%	5.61	6.76	12.83	6.23	6.88	16.57
4	80%	9.76	3.55	17.33	10.10	3.58	14.20
5	80%	6.70	7.69	14.17	8.22	9.74	9.73
1	85%	6.70	3.18	16.55	8.19	3.35	14.13
2	85%	7.15	5.06	15.89	10.87	3.94	13.46
3	85%	8.06	7.48	11.76	6.23	7.87	11.90
4	85%	9.45	3.37	14.28	10.10	4.12	16.14
5	85%	5.77	6.04	11.17	8.22	8.15	10.09
1	90%	8.54	5.74	14.85	8.42	6.24	13.07
2	90%	6.75	5.10	15.37	8.24	4.88	12.70
3	90%	10.01	6.90	13.38	7.40	7.28	14.83
4	90%	9.61	2.48	16.17	9.66	4.88	13.88
5	90%	7.78	6.43	14.48	8.35	7.92	10.88

Table 1. Averaged peak power about six joints of lower extremity in sagittal plane across barbell intensities. Powers are normalized to body mass (W/kg).

	Paired Differences					t	df	Sig. (2-tailed)
	Mean	Std. Deviation	Std. Error Mean	Lower 99% CI	Upper 99% CI			
Ankle peak power	-0.931	1.761	0.455	-2.284	0.422	-2.048	14	0.060
Knee peak power	-0.588	0.997	0.257	-1.354	0.178	-2.284	14	0.038
Hip peak power	1.308	2.224	0.574	-0.401	3.018	2.278	14	0.039

Table 2. Summary table of the dependent t-tests performed on the mean peak power about the x-axis across the left and right side joints of the lower extremity inclusive of all barbell intensities. Bonferroni correction (α/n) results in alpha = 0.016.

Test Statistics[a]			
	RANK power about y axis - LANK power about y axis	RKNE power about y axis - LKNE power about y axis	RHIP power about y axis - LHIP power about y axis
Z	-1.022[a]	- 738[b]	- 568[a]
Asymp. Sig. (2-tailed)	307	460	570

a Wilcoxon Signed Ranks Test

Table 3. Summary table of the Wilcoxon sign rank test performed on the mean peak power about the y-axis across the left and right side joints of the lower extremity inclusive of all barbell intensities.

Test Statistics[b]			
	RANK power about z axis - LANK power about z axis	RKNE power about z axis - LKNE power about z axis	RHIP power about z axis - LHIP power about z axis
Z	-1 590[a]	- 738[a]	-1 931[a]
Asymp Sig (2-tailed)	112	460	053

b Wilcoxon Signed Ranks Test

Table 4. Summary table of the Wilcoxon sign rank test performed on the mean peak power about the z-axis across the left and right side joints of the lower extremity inclusive of all barbell intensities.

To simply further variance analysis and to test the assumptions of previous research efforts, we evaluated whether statistical differences existed between the average peak power values of the left and right halves of the lower body. The average peak power data in the sagittal plane of motion was normally distributed. Thus, three dependent t-tests were performed with Bonferroni corrections to limit the effect of family-wise error arising from performing multiple pairwise comparisons. For the non-normal average peak power data about the y and z axes, Wilcoxon signed rank tests (Wilcoxon, 1945) were employed to test for differences between left and right side joints of the lower extremities.

No significant differences in averaged peak moment powers in the sagittal planewere identified between the left and right sides of the body at any of the joints of lower extremity. For

ankle, knee, and hip, t (14) = 0.06, 0.038, 0.039, p = 0.016, respectively (refer to Table 2). Similarly, in the y axis of motion the Wilcoxon signed rank test found no significant differences in peak power values about the joints of the lower extremity. Ankle, knee, and hip produced significance values of 0.307, 0.460, 0.570, p = 0.05, respectively (refer to Table 3).Finally, the average peak moment powers about the z axis showed no significant differences between the left and right side joints of the lower extremity. Wilcoxon test statistic for the comparison between the ankles, knees and hips were 0.112, 0.460, 0.053, p = 0.05 (refer to Table 4).

These results greatly simplified further variance analysis, as we preceded but only considered one side of the lower body. This reduced test joints from six to three. Arbitrarily we chose the left side of the body for further variance analyses, both parametric and non-parametric in nature.

Having satisfied our query into the symmetry between left and right side average peak moment powers in three dimensions, we preceded with analyses of variance of average peak moment powers in response to varied barbell resistance.

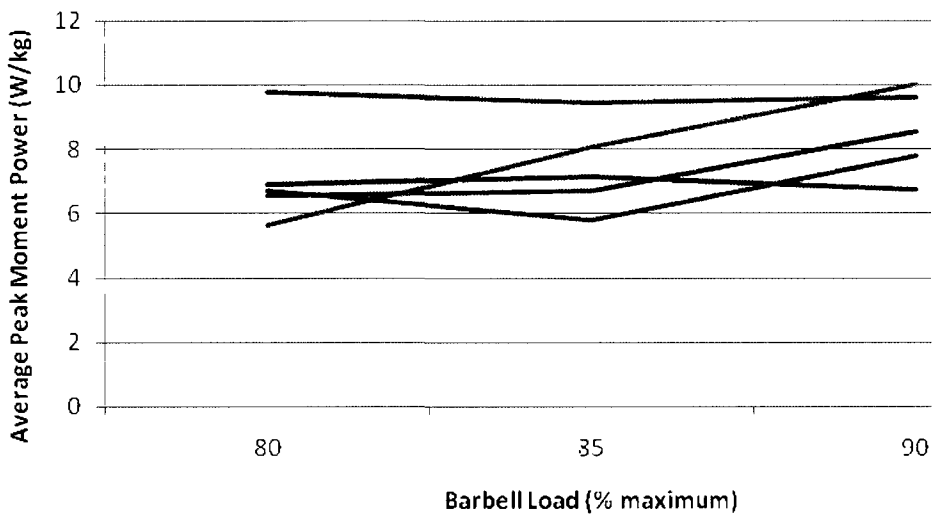

Figure 1. Average left ankle peak moment power about the x-axis (sagittal plane of motion) across barbell intensities for all lifting participants. Power is normalized to body mass (W/kg) on the ordinate and relative barbell load is on the abscissa.

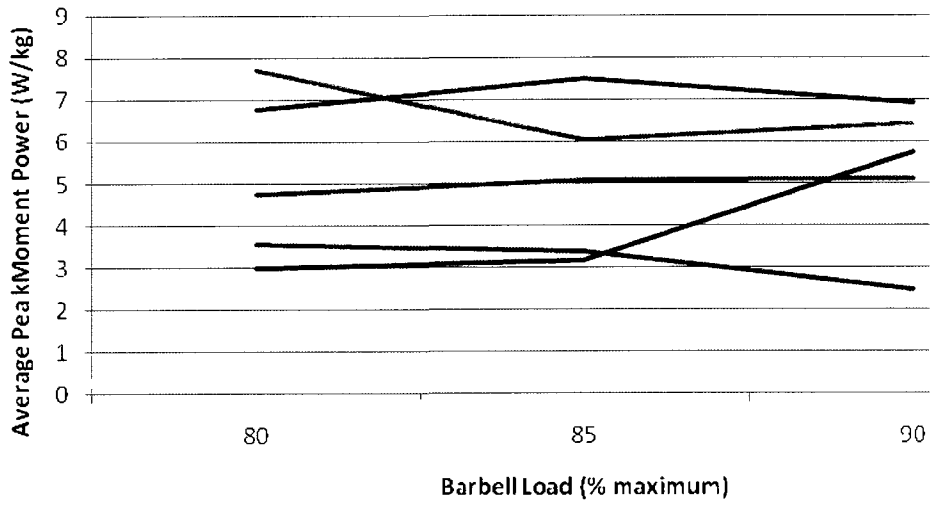

Figure 2. Average left knee peak moment power about the x axis (sagittal plane of motion) across barbell intensities for all lifting participants. Power is normalized to body mass (W/kg) on the ordinate and relative barbell load is on the abscissa.

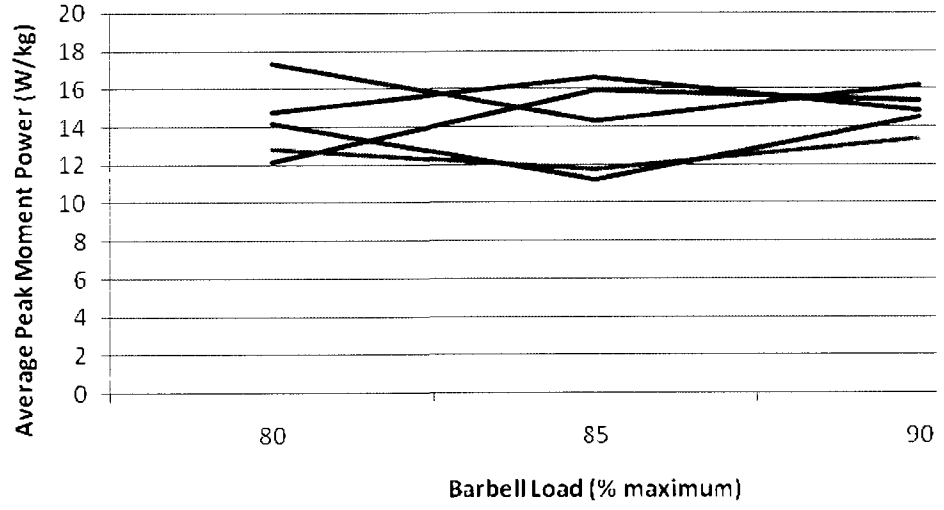

Figure 3. Average left hip peak moment power about the x axis (sagittal plane of motion) across barbell intensities. Power is normalized to body mass (W/kg) on the ordinate and relative barbell load is on the abscissa.

As illustrated in Figures 1-3, averaged peak moment powers in the sagittal plane of motion about the joints of left lower extremity appeared constant despite changes in barbell load. Repeated-measures ANOVA's were performed across averaged peak power values about ankle, knee, and hip about the x axis for 80, 85 and 90% barbell intensities to verify the visual summaries found in Figures 1-3. As the intensity factor had 3 levels, correlation between factor levels was also assessed. Mauchly's test of sphericity resulted in the failure to reject the null hypothesis for all three joints. We therefore proceeded with within-subject effects without analysis of homogeneity of variance. No significant differences were identified across intensities for averaged peak ankle powers in the sagittal plane, $F(2, 8) = 2.594$, $p = 0.135 > 0.05$. Power of this ANOVA was only 37.5% indicating if differences existed, the current data set size and statistical methods produced only a 37.5% chance of identification. Thus, very small differences were likely overlooked and only large differences illuminated using this test. About the left knee in the sagittal plane, $F(2, 8) = 0.133$, $p = 0.878 > 0.05$, therefore we failed to reject the null hypothesis. No significant differences in averaged peak left knee powers in the sagittal plane existed across lifting intensities. At the hip, within-subject effects revealed no significant differences in average peak hip powers in the sagittal plane across lifting intensities with $F(2, 8) = 0.420$, $p = 0.671 > 0.05$, therefore we failed to reject null hypothesis.

Regarding the peak abductor/adductor moment powers about the ankle, knee, and hip, statistical tests revealed results similar to the peak moment powers in sagittal plane (above). About the left ankle, the Friedman rank test determined no significant differences in average peak abductor/adductor moment power values across barbell intensities. Friedman test statistic, $FTS (5, 2) = 0.819$, $p = 0.05$, thus we failed to reject the null hypothesis. About the left knee, average peak abductor/adductor moment power values across barbell intensities showed no

significant differences. FTS (5, 2) = 0.247, p = 0.05, thus we fail to reject the null hypothesis. About the left hip, average peak abductor/adductor moment power values across barbell intensities showed no significant differences. FTS (5, 2) = 0.819, p = 0.05, thus we fail to reject the null hypothesis. Average peak abductor/adductor moment powers about the left ankle, knee, and hip, were not significantly different across 80, 85, 90% barbell resistance levels.

In line with the average peak moment powers about the x and y axes, statistical tests revealed no significant differences across barbell loads in terms of average peak moment powers about the z axis for the left ankle, knee, and hip. As the power data about the z axis was non-normal in its distribution, Friedman signed rank tests were used to assess significant across repeated measures. About the ankle, knee, and hip, FTS (5, 2) = 0.091, 0.247, 0.165, p = 0.05, respectively. Thus, we fail to reject the null hypothesis at each of the joints of the left lower extremity. No significant differences in average peak internal/external rotation moment powers were found across the range of barbell loads.Detailed statistical reports may be found in Appendix B.

We next turned our attention to assessment of the second research hypothesis. We were testing effect of barbell load on range of anterior-posterior displacement of system centre of mass (COM). Results from Mauchly's Test of Sphericity and within-subject effects are detailed in Appendix C. Mauchly's Test of Sphericity reported significance value of $p = 0.401 > 0.05$, therefore we failed to reject test null hypothesis and proceed with repeated-measures analysis of within-subject effects. Repeated-measures ANOVA produced $F(2, 4) = 0.765$, $p = 0.523 > 0.05$, therefore we failed to reject the research null hypothesis. No significant differences in system COM range of motion in the anterior-posterior plane were found across barbell intensities.

Moment power analysis. Figure 4 (below) provided the visual explanation for the trial boundaries alluded to in the methods section.

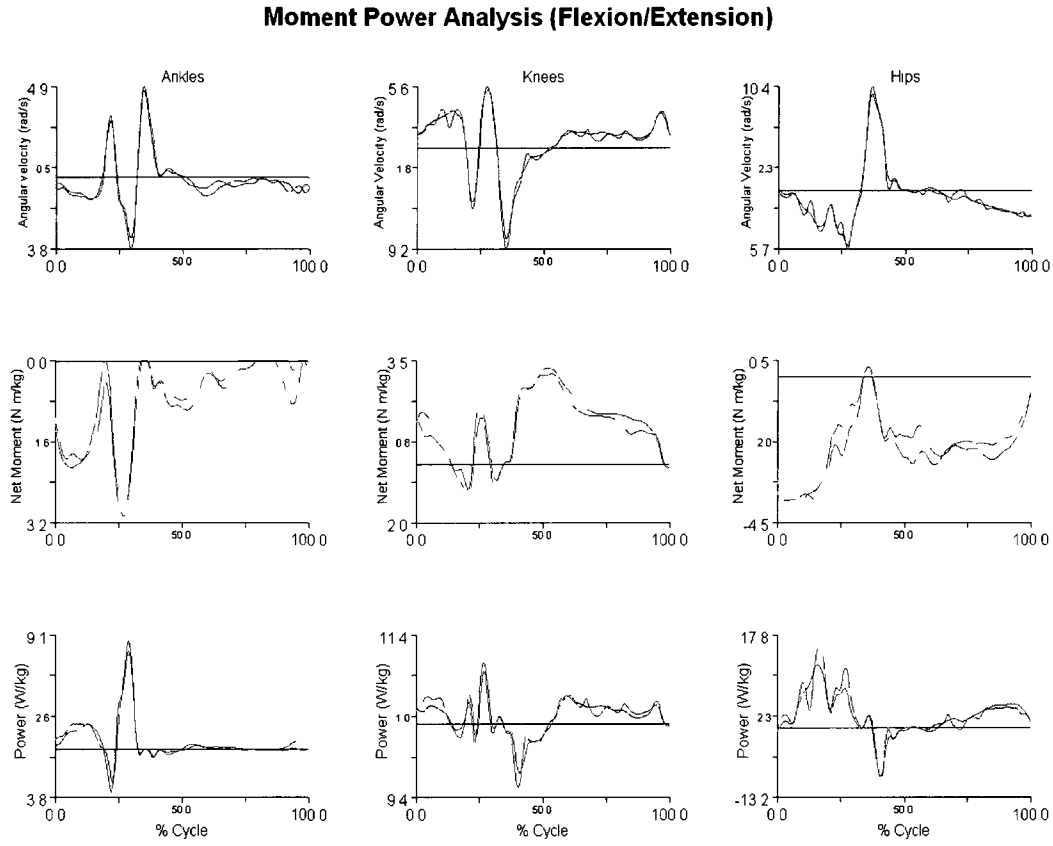

Figure 4. Moment power curves of participant 5's 90% snatch. The blue series represents angular velocities (rad/s), the red series net moment of force (N.m/kg), and the green series represents power (W/kg). The first column holds data about the x-axis for motion about the ankles, second about the knees, and third about the hips.

Positive moment powers relating to the propulsive phases of the snatch lift were seen to drop-off rapidly once the lifter has left the ground. As such, the analysis of each trial began with vertical barbell displacement and was terminated by the lifter's loss of contact with the force platform.

Participants executed the snatch lift with similar phase organization. Results showed key power bursts slightly earlier or later both within and between participants. For clarity, a series of plots of several variables are presented with only one lifter represented in each figure. Within a single lifting condition, the same lifter showed varying relative and absolute timing of key power bursts. Figure 5 displayed the results of the snatch lifts performed by participant 5 at selected barbell load. Complete graphical displays for all lifters at all intensities are located in Appendix D.

Figure 5displays the key kinematic and kinetic histories from the lower extremities of participant 5's snatch lifts 90% of his maximal capacity. Figure 5 contains data for motion about the x-axis (sagittal plane), while Figure 6 superimposes the moment power curves about the internal y-and z-axes with those from the x-axis. The top rows in these figures (blue) contain histories of the angular velocities, the middle rows (red) contain histories of the net moments of force normalized to body mass and the bottom rows (green) contain the moment powers normalized to body mass. The abscissas for these plots are normalized to lift cycle. Each row contains three plots: one plot containing histories for the left and right ankle, knee and hip joints, respectively.

Figure 5 was selected as an example of typical organization of kinetic and kinematic events. In Figure 5 are found a series alphanumeric codes and event bars superimposed on the graphs. These codes and bars were placed at specific points along the curves defining key phases of the lift. Key kinetic events such as bursts of moment of force and power are denoted by alphanumeric codes. For example the first ankle moment of force is coded as Am1, and the first ankle power as Ap1. Key kinematic events are identified with a superimposed vertical bar. As subject parameters varied between lifters, as well as lift timing and organization, caution must be

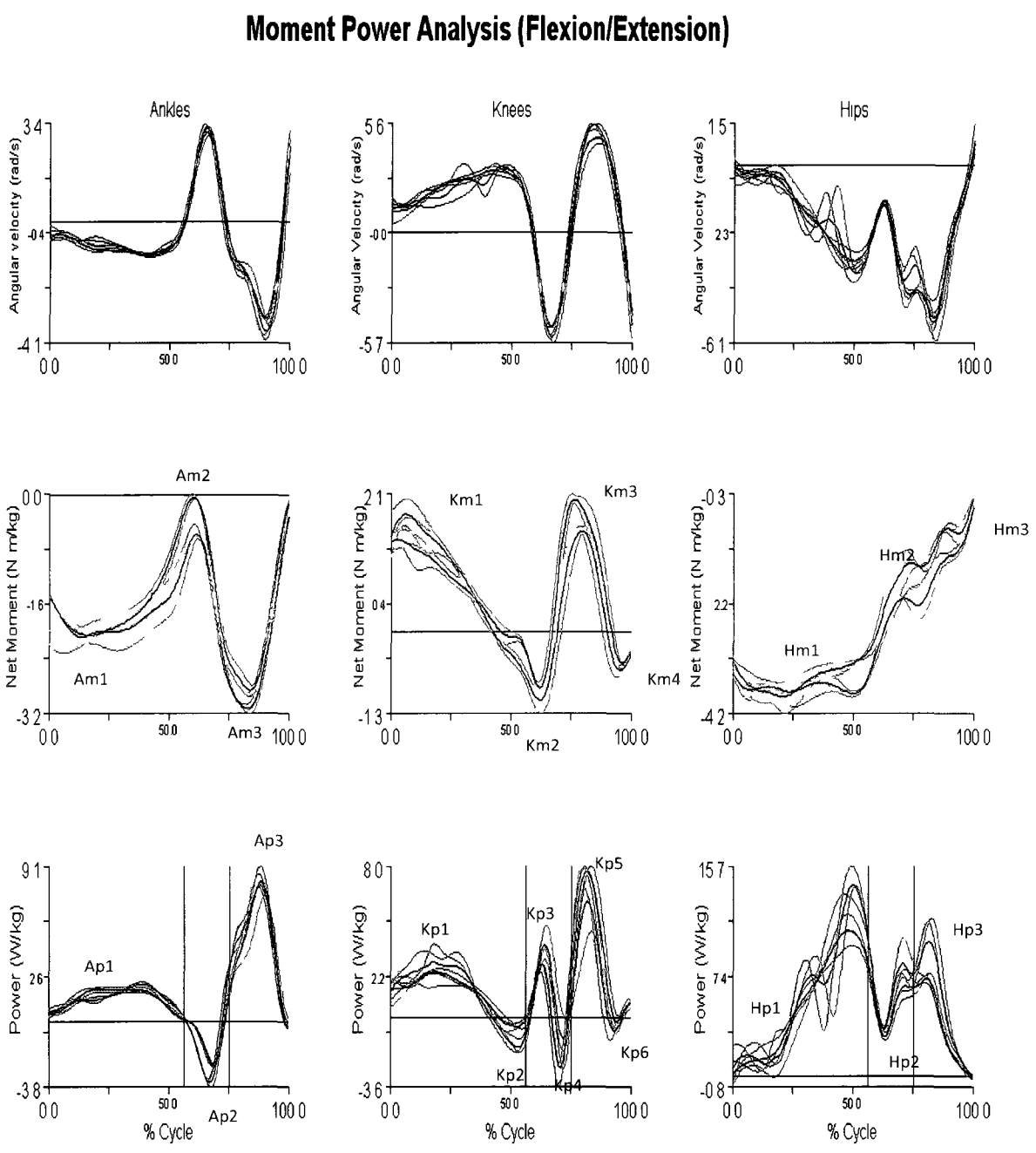

Figure 5. Participant 5 executing a 130 kg (90%) snatch lift. On the ordinate axes, the first row displays angular velocity (rad/s), the second net moment of force normalized to body mass (N.m/kg), and the third moment power normalized to body mass (W/kg). The first column plots both right and left ankles, the second right and left knees, and the third right and left hips. All plotted variables concern motion in the sagittal plane (about the internal frame of reference y-axis), time is plotted on the abscissa and is normalized to 100% of lift cycle from barbell liftoff until the feet left the floor in the final propulsion.

taken when using kinematics to denote phase boundaries. Meaningful kinetic events should be criteria for phase boundaries and these kinetic events should largely coincide with the kinematic boundaries. Our defined stages show close agreement between kinetic and kinematic descriptors.

We have defined the phases of the opening of the snatch lift as follows: the first knee extension phase ranges from the barbell liftoff, to the first vertical event bar (Figure 5). This first vertical bar denotes a kinematic event at the point at which the lifter's knees have extended maximally for the first time. This phase boundary closely coincides with an important kinetic event. The role of the musculature changes from positive to negative plantiflexor and extensor powers about the ankle and knee, respectively, as the lifter moves from the first knee extension phase to the transition phase. The power curves are seen to change scale to negative, denoting a change role of the musculature.

The transition phase is found between the two vertical bars on Figure 5. Using lift kinematics the transition phase is defined as beginning with the lifter's knees reaching maximal local extension ranging to the knees reaching maximal local flexion. The kinetic event defining this range is active flexion of the knee through positive flexor power about the knee joint. Muscular power about the ankle joint reinforces the transition phase boundary, as a burst of negative power (eccentric contraction by plantiflexors) pre-stretches the plantiflexors in preparation for the final propulsion of the barbell.

The final knee extension phase is found from the second vertical bar to when the feet loose contact with the ground (Figure 5). Lift kinematics define this phase from the lifter's knees reaching second maximal flexion angle to the first point where both feet have left the ground. The kinetic event defines this phase from the beginning of the final positive power burst about

the knee until power returns to zero (or trial ends).The moment power patterns from Figure 5 were quite stable. We saw similar trends across all lifting conditions and between lifters.

First knee extension phase. The first knee extension phase of the snatch lift ranges from the barbell liftoff to the lifter's first maximal knee extension. The point at which the knees reach a local maximum in extension is indicated by first of two vertical lines. Three simultaneous muscular efforts were performed during the first knee extension phase. About the ankle joint, net moment of force was negative indicating net plantiflexor effort found on Figure 5 by code Am1 (Ankle moment of force 1). The ankle was extending during this phase, as such the power about the ankle was positive indicating positive work done by the plantiflexors (Ap1 – Ankle power 1).

Motion about the knee joint during the first extension phase was extension as seen in the second column and first row of Figure 5. Net moment of force about the knee was net extensor moment of force (Km1 – knee moment of force 1) correlating with a small positive burst of power about the knee (Kp1 – knee power 1). At the end of this first phase, net moment of force and power about the knee changed and became negative (Kp2). Angular velocity graph showed the knee was still extending. As such, the knee flexors were performing negative work to control the rate of knee extension, likely in preparation for the next phase of lift.

The hips were continually extending during the first extension phase (and throughout the entire movement in general). Net moment of force about the hip was negative throughout the first phase (Hm1 – hip moment of force 1). This net moment of force corresponded to positive power and work during the first extension phase (Hp1 – hip power 1). The ankle, knee and hip were all extending during the first extension phase. The ankle and hip were actively extending, while the knee initially exhibited an extensor moment of force and positive power (Kp1), then a net flexor moment of force and negative power (Kp2) to control knee extension.

Transition phase. During the transition from the first extension phase (barbell lift off to local knee flexion maximum) to the second extension phase (extension of lower extremity joints from position of second maximum in knee flexion), the ankle and hip both showed similar mechanical trends

The ankle briefly and rapidly dorsiflexed (as seen in Figure 5, first column and row) as the lifter executed the double knee-bend technique This technique required the simultaneous reorientation of the trunk to a more vertical position, with concurrent lowering and forward movement of the hips to align closely with the barbell centre of mass prior to the final extension phase The ankle was dorsiflexed allowing the hips to move in the anterior direction and approach the barbell Regarding the timing of muscular bursts, knee net moment of force (Km2) was the key muscular burst of the transition phase The ankle kinematics approached net dorsiflexion, but retained net plantiflexor moment of force (Am2) Ankle power was distinctly negative during the transition phase as the ankle plantiflexors resisted relative dorsiflexion (Ap2) This likely served to pre-stretch the plantiflexors in preparation for the final extension phase

Active knee flexion (Km2) coincided with negative power seen about the ankle joint (Ap2) The knee was the crucial joint during the transition phase acting as controller bringing the lifter and barbell centres of mass close together The knee musculature changed role from the previous phase as power about the knee became positive as the knee was actively flexed (Kp3) At end of the transition phase the role of the musculature about the knee changed, however, from net flexor dominance to net extensor dominance and negative power at end of the transition phase (Kp4) The burst of positive flexor power (Kp3) followed immediately by a burst of negative power by the knee extensors (Kp4) may have served to pre-stretch quadriceps prior to

the final extension phase The rapid oscillation between net flexor and extensor moment of force, and oscillation between positive and negative power about knee were commonalities seen between the mechanics of weightlifting (in particular the snatch lift) and the countermovement vertical jump (Carlock, 2004, Channell, 2008, Nuzzo, 2008) In fact, the prevalence and potential mechanical advantages found in countermovements (pre-stretch) should entice investigators to predict the presence of countermovements in all ballistic or explosive athletic movements, weightlifting included

The hips continued to extend under the influence of net extensor moment of force (Hm2) and positive power (Hp2), although both decreased in magnitude as the rate of hip extension dropped dramatically This brief drop in power coincides with a rapid decrease in the hips angular velocity during transition Thisbrief perturbation in the slope of the moment of force and power curves was never pronounced enough to result in change of scalar sign, but likely reflected efforts to reorient the trunk to more vertical position while respecting the precise timing requirements of reorientation for the final extension phase

Second extension phase. The second extension phase was bounded by the end of the transition phase (second local maximum in knee flexion) and the extension of the joints of the lower extremity culminating in the loss of contact with the ground About the ankle, net plantiflexor moment of force was seen (Am3) and the joint was plantiflexed Work was positive resulting from the burst of positive power (Ap3) as the ankle rapidly extended

Similar to the ankle behaviour, about the knee rapid extension with net extensor moment of force (Km3) occurred Knee extensor moment of force (Km3) and power (Kp5) were the earliest muscular actions seen in the second extension phase Knee power burst (Kp5) preceded, slightly, both the ankle (Ap3) and hip (Hp3) power bursts At the end of the second extension

phase the muscular action about the knee was resistive in nature. This was evidenced by net moment of force about knee (Km4) and negative power (Kp6) as the flexors acted eccentrically to resist hyperextension of the knee at the end of the explosive final extension. In addition, this action was likely anticipatory of the flexion required for catching the barbell after propulsion.

The hips continued in their path towards extension from initial flexed position at barbell liftoff when the lifter was in a crouched position. The lifter has completed the transition phase with concurrent reorientation of the trunk, and produced a burst of positive power (Hp3) as the hips fully extended in the final extension phase. Net moment of force was extensor (Hm3), and was reduced in magnitude in comparison to the first extension phase (Hm1).

Characteristic of the second extension phase was the extension of all joints of lower extremity. Both the knee and hip extensors showed peak phase activity earlier in the second extension phase, while the ankle plantiflexors showed a longer and more consistent burst of positive power. By the end of the second extension phase the knee and hip musculature was preparing for the barbell reception and the extensor activity was completed.

Figure 6 displays flexor/extensor, abductor/adductor and internal/external rotation moment-power curves for a selected participant completing a 90% snatch. These data series are plotted in blue, red and green respectively The same axes labels apply from Figure 4 and 5. The moment powers for motion about the internal y and z axes were very small in comparison to those about the internal x axis (flexion and extension) As such, the detailed analysis of the data has focused primarily on motion about the x axis. Statistical analyses were performed on y and z axes data, and are presented in the statistics section.

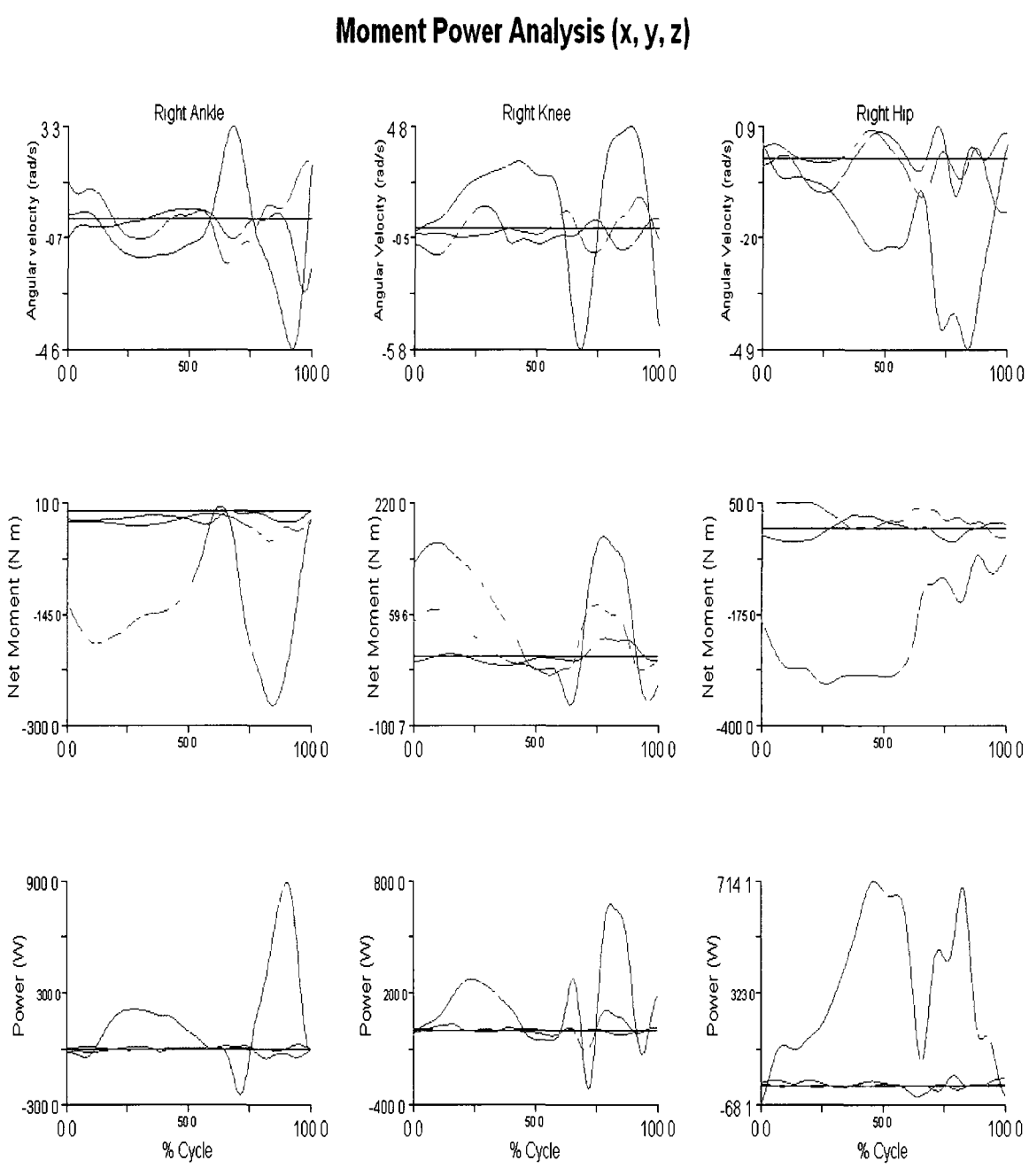

Figure 6. Participant DM executing three attempts at 130 kg (90%) snatch lift. On the ordinate axes, the first row displays angular velocity (rad/s), the second net moment of force normalized to body mass (N.m/kg), and the third moment power normalized to body mass (W/kg). The first column plots right ankle, the second the right knee, and the third the right hip. Flexion/extension was the blue series, abductor/adductor motion was the red series and internal/external rotation was the green series. Time was plotted on the abscissa and is normalized to 100% of lift cycle from barbell liftoff until the feet left the floor in the final propulsion.

To view the angular velocity, net moment of force and power curves for remaining lifters please refer to Appendix D.

The statistics section tested the bilateral symmetry of the peak power values about the joints of the lower extremity. Numerical tests (displayed in Table 2 and 3) indicated no significant differences between left and right joints of the lower extremities in terms of mean peak power about the x and y axes. To highlight this symmetry between left and right outputs, presented are selected lifts from a variety of participants.

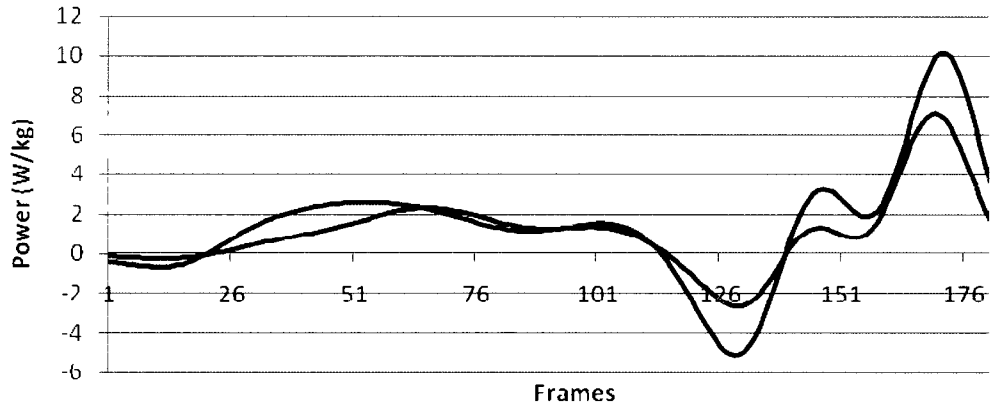

Figure 7. Left ankle power (blue series) and right ankle power (red series) for sagittal plane of participant's FLG first snatch of 110 kg load. The abscissa shows frame number (200 Hz) and ordinate has power in watts normalized to body mass.

The two series had Pearson's correlation of $r = 0.9634$, and showed substantial similarity between overall power histories. Left ankle showed greater peak negative power during transition phase and greater peak positive power during second extension phase.

Stronger correlation between left and right ankle power across capture range was seen in Figure 8. Left and right ankle power series showed close pairing. Pearson's correlation of $r = 0.9728$, substantiated this observation. In this trial, the left ankle plantiflexor moment showed

greater eccentric power during transition phase between propulsion phases, and right ankle showed greater peak plantiflexor power during final propulsion.

To see complete comparison between left and right ankle, knee and hip power for remaining lifting participants please refer to Appendix E.

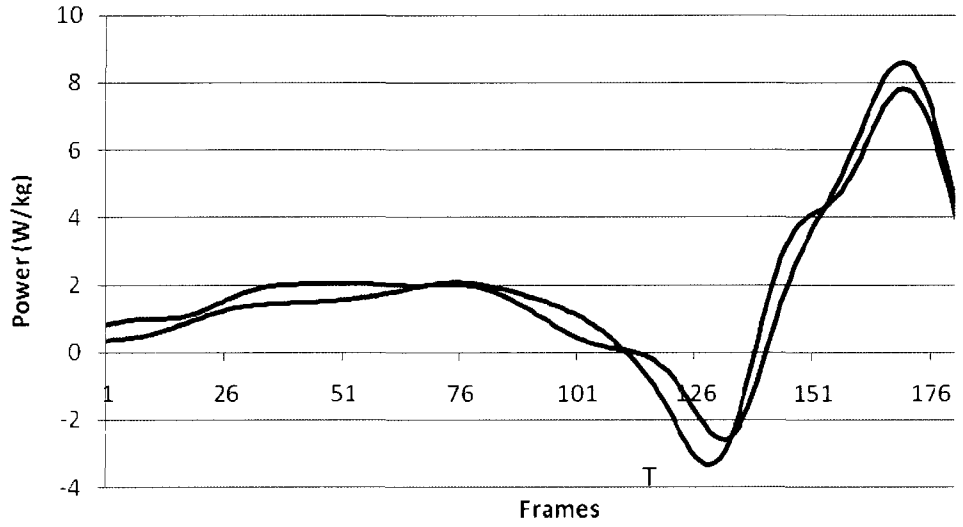

Figure 8. Left ankle power (blue series) and right ankle power (red series) for sagittal plane of participant's DM first snatch of 130 kg load. The abscissa shows frame number (200 Hz) and ordinate has power in watts normalized to body mass.

Kinematic analysis of selected variables. Having completed kinetic analysis of various snatch lifts, we proceeded with kinematic examination of selected variables across lifting intensities. We examined the possibility a kinematic variable, such as shoulder symmetry or trajectory of system centre of mass (COM), distinguished between the two lifts. First we described trends seen in shoulder trajectory and system COM by examining selected snatch lifts. Complete displays of shoulder trajectory are available in Appendix F.

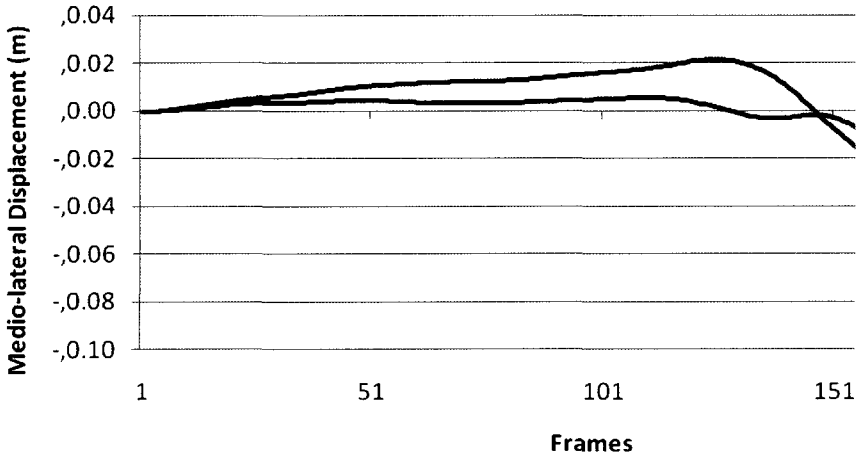

Figure 9. Participant DM first attempt at 130 kg snatch lift. Plotted is mediolateral displacement of left (blue series) and right (red series) shoulder markers. Starting position bias was offset by zeroing the starting positions. Pearson's correlation between the two curves is, $r = 0.9515$.

Figures 9 through 11 show the shoulders to have moved primarily in the anterior-posterior and vertical directions. Observed were small amounts of mediolateral displacements of left and right shoulder markers. Maximal range of the mediolateral shoulder movement across the entire trial was approximately 10 cm, indicating this motion was small but indeed present.

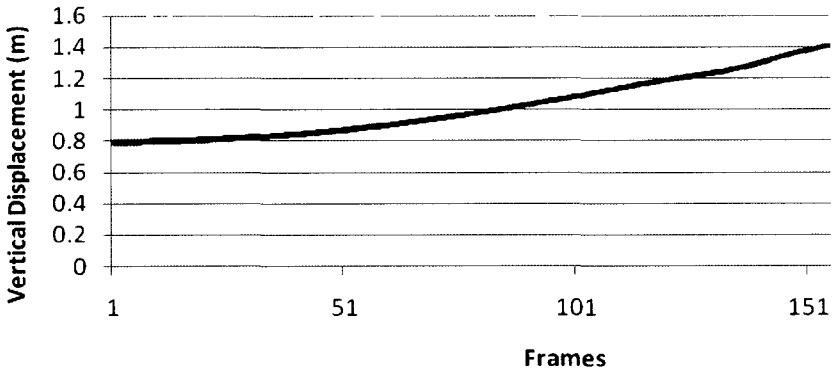

Figure 10. Vertical displacement of left (blue series) and right (red series) shoulder markers for participant DM's first lift at 130 kg snatch lift. Starting position was offset by zeroing the starting positions. Pearson's correlation between the two curves is, $r = 0.999$.

Vertical displacement of shoulder markers showed extremely close correlation between left and right markers. The trajectory was sigmoid, as the greatest rate of increase in vertical position of the shoulders occurred during the transition phase of the lift. This was due to a rapid

reorientation of the trunk (and consequently shoulders) from crouched position of the first propulsion phase until maximal extension of second propulsion phase

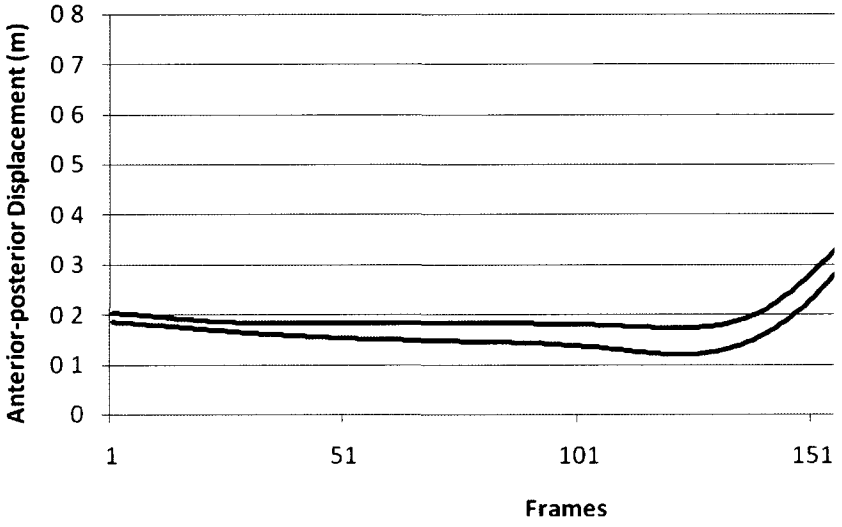

Figure 11 Anterior-posterior displacement of left (blue series) and right (red series) shoulder markers for participant DM's first lift at 130 kg snatch lift Starting position was offset by zeroing the starting positions Pearson's correlation between the two curves is, r = 0 9968

In Figure 11 we observed initial shoulders motion slightly towards the anterior direction during the first knee extension and transition phases Once the transition phase was completed and continuing into the final extension phase, the shoulders moved rapidly towards the posterior direction as the lifter reoriented their trunk towards the vertical accommodating the final extension of the barbell Figure 11 showed larger anterior displacement of the left shoulder during this particular trial and lifter The larger anterior motion of the left shoulder may have been indicative of a lifting pattern of this lifter This lifter often makes a small rotation of 5-10° to the negative (right hand rule) direction when completing the snatch lift

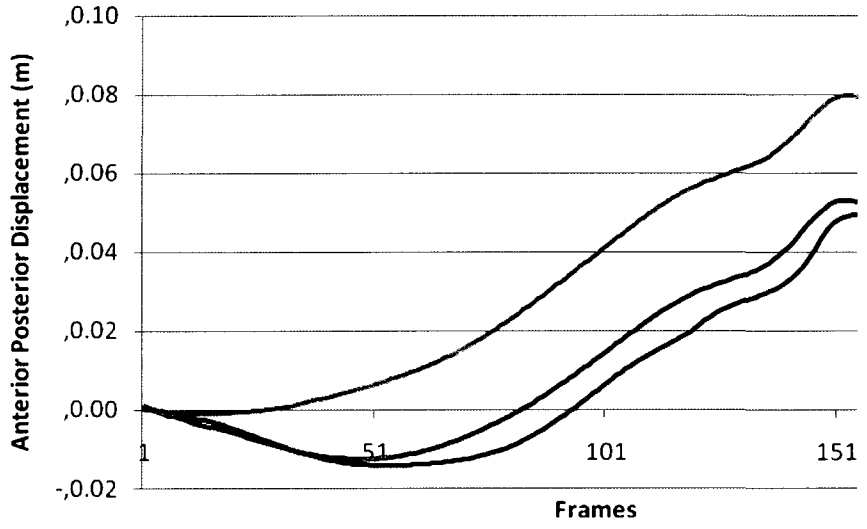

Figure 12. Participant DM system centre of mass (COM) trajectory in anterior-posterior direction for first (blue), second (red), and third (green) attempts at 130 kg snatch. Displacement is plotted on y axis (metres) and time in frames (200 Hz) is plotted on x axis. Bias removal has been used to zero varied starting positions between individual trials.

The participant showed two notable features in the history of the anterior-posterior motion of the system centre of mass. First and second attempts (blue and red series) showed an initial movement of the system COM anteriorly as the barbell moved through the first extension phase and into the transition phase. During the transition and continuing into the second extension phase, the system COM moved posteriorly as the lifter extended the joints of the lower extremities and propelled the barbell overhead. The third attempt (green series) showed immediate and continuous posterior motion of the system COM. The ranges of anterior-posterior system COM motion were fairly small and consistent, approximately 8-10cm across all trials.

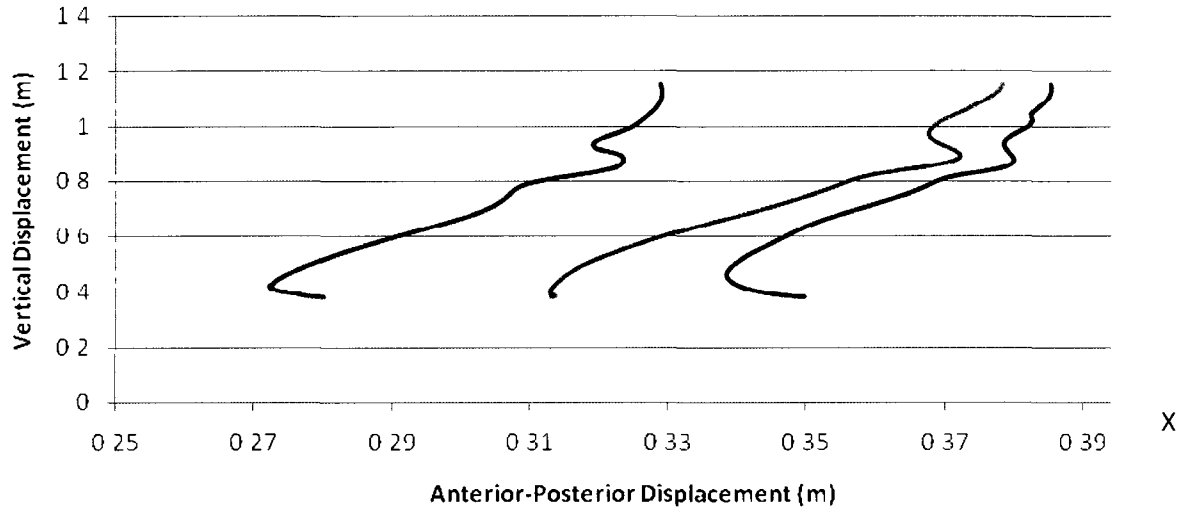

Figure 13. Total COM trajectories of participant DM's three 110 kg snatch lifts. Subject faced the negative anterior-posterior direction.

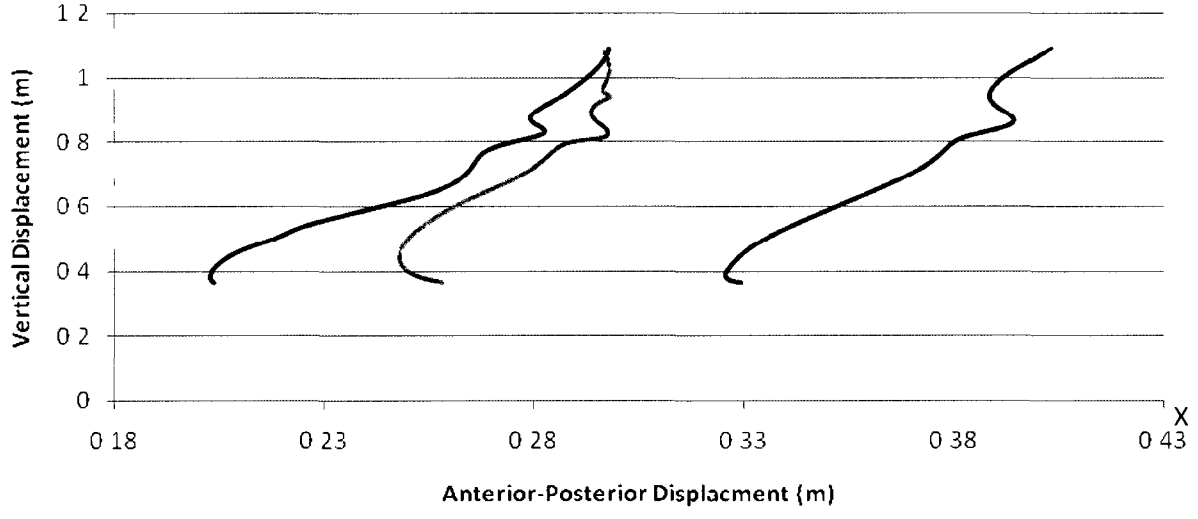

Figure 14. Total COM trajectories of participant DM's three 120 kg snatch lifts. Subject faced the negative anterior-posterior direction.

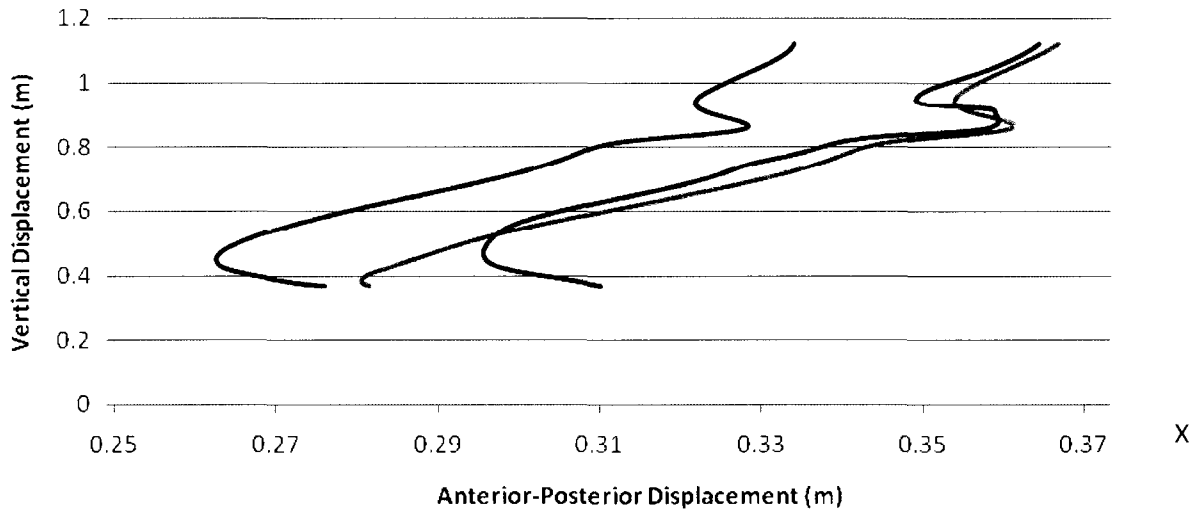

Figure 15. Total COM trajectories of participant DM's three 130 kg snatch lifts. Subject faced the negative anterior-posterior direction.

Figures 13-15 display participant DM's three attempts at 110, 120, and 130 kg respectively. In each figure system COM vertical displacement, in metres, is plotted against anterior-posterior displacement, in metres, for the three attempts at the given barbell load. The participant did not begin each lift at the same location on the force platforms, hence the small differences in anterior-posterior starting position. What is largely consistent across all attempts by participant DM is the trajectory of the system COM displacement as the lift progresses. Immediately following liftoff, DM's system COM was displaced forward (between 2 and 5 cm), and then proceeded to move posteriorly for the rest of the first extension and transition phases. Just as the barbell reached hip height and the second extension phase began, the barbell made contact with the lifter's hips and this caused a displacement of the barbell in the anterior direction. This accounted for the brief anterior movement of the system COM during the second extension phase, seen as the characteristic 'zigzag' motion near the termination of most trials' second knee extension phase.

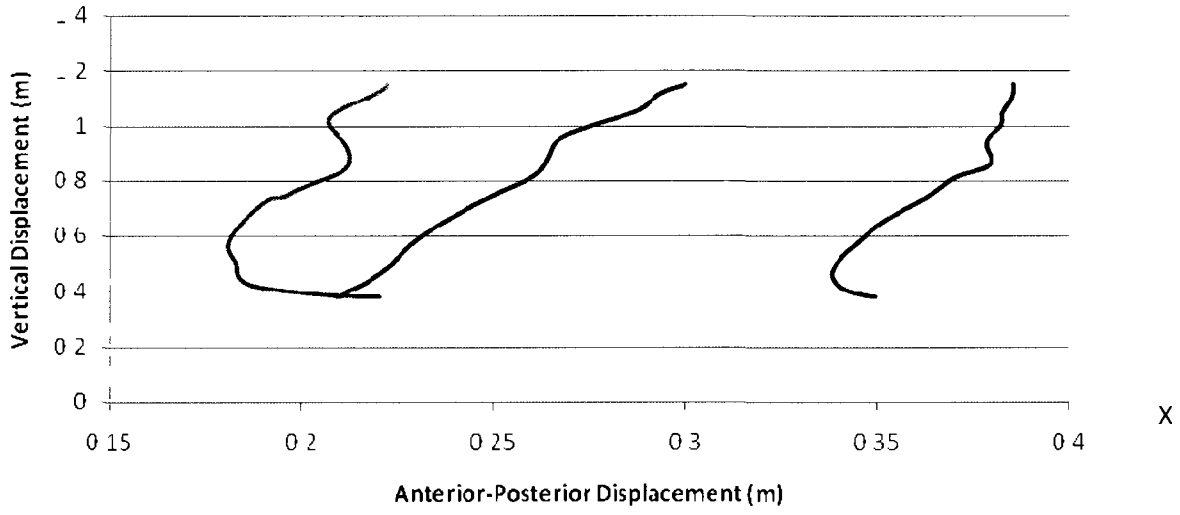

Figure 16. Total COM trajectories of three participants' attempts at 80% snatch lifts. Subjects faced the negative anterior-posterior direction.

Figure 16 plots the vertical against the anterior-posterior displacement (in metres) of the system COM for three separate lifters. Plots of participant MRC, LGD, and DM are found as green, blue, and red respectively. Participants DM and, to a larger extent, MRC (red and green series, respectively) showed an initial anterior displacement of their system COMs in conjunction with vertical displacement. Both showed posterior displacement of system COM as their lifts progressed, as well as the characteristic zigzag feature seen all trials. Participant LGD's trajectory of system COM was different than the other lifters. He demonstrated immediate posterior displacement of system COM following the barbell liftoff. Similar to other lifters, LGD's system COM proceeded to move posteriorly immediately after liftoff, but in contrast to other lifters LGD showed minimal zigzag feature at hip contact.

Discussion

Repeated measures ANOVAs found no significant differences in the average peak moment power about the ankle, knee, or hip in three dimensions across the barbell loads. Above 80% capacity of maximal snatch lift, elite-level lifters did not impart greater peak power about the ankle, knee, or hip as the barbell load increased. These results were in accordance with Enoka (1988), who showed no significant increase in lower extremity joint power across 77% to 86% relative barbell load. Three-dimensional motion capture only confirmed the results of previous 2-dimensional research on the effects of load variations on power output. These results strongly suggest to coaches and athletes that above 80% snatch capacity lifters do not increase peak powers about the joints of the lower extremities. Thus, training exercises designed to improve muscle power in the lower extremities should not exceed 80% snatch capacity. As well, the coach and athlete should realize that above 80% snatch capacity, the lifter must make other accommodations to the heavier barbell loads. These accommodations may include faster pull under times, and/or lower reception depth. These accommodations would require power production, but outside of the propulsion phase.

The inverse relationship between muscle force and contraction velocity has been well documented by physiologists and sport scientists alike (Abbott, 1952; Brooks, 2005; Carlock, 2004; Hill, 1938; Katz, 1939; Nuzzo, 2008; Zatsiorsky, 1995). The central challenge of the sport of weightlifting is to lift a large load from the ground, through a range of poor leverage, and hold it overhead. Proficient lifters overcome the poor leverage positions by propelling the barbell from a position of excellent leverage (second knee extension phase) and then quickly positioning themselves under to catch the barbell. The crux of competitive weightlifting is then to successfully accomplish this task with heaviest total mass between two lifts (snatch and clean &

jerk). This is where the competitive difficulty arises. As noted from foundation research on muscle physiology and muscle mechanics, the highest levels of muscle tension cannot coexist (intramuscularly) with the highest rates of muscle contraction velocity. So the problem facing weightlifting athletes and coaches is how to impart sufficient upward velocity to the massive barbell load to allow the athlete to drop-under and catch the barbell.

Our results indicate that between 80–90% of maximal snatch capacity average peak moment powers in three dimensions about the joints of the lower extremities did not vary. Thus, other variables must accounts for the ability to lift larger barbell loads. Lifters may adjust to heavier barbell loads by making subtle modifications to lifting parameters not captured in this research effort. Possible quantifiable adjustments include drop-under time and depth and/or shorter transition phase times. These are interesting alternative variables because they each provide explanation for why kinetic variables such as peak moment power may not capture differences across intensities. Drop-under time and depth are kinematic variables measuring time and range of motion from peak vertical barbell velocity to local minimum in barbell height prior to stand. Potentially, lifters accommodate heavier barbell loads not with increase in muscular power, but by moving more quickly or deeper under barbell to receive weight. This adaption may be seen as a skill or technique based accommodation for heavier barbell loads, and would not be detected across intensities using only peak power or some other kinetic variable to discriminate. Additionally, transition phase time may provide explanation for the lack of power variation above 80% threshold. To exploit elastic properties of musculoskeletal system, the stretch shortening cycle must be completed as rapidly as possible (Komi, 1984). Athletes may complete the transition phase of lift in shorter time frame as barbell load becomes heavier. Shortening the transition phase could potentially increase the myoelastic effect of the stretch-

shortening cycle allowing lifters to apply more impulse to the barbell by conserving some kinetic energy loss during the transition phase of the lift and applying it to the second extension phase. The mechanical advantages available to a weightlifter through use of the stretch-shortening cycle during the transition phase should prompt coaches and athletes to utilize lifting techniques and develop assistance exercises that incorporate and develop the elastic properties of muscle.

In the course of data analysis we simultaneously verified assumptions of early researchers that the snatch lift could be numerically modelled as bilaterally symmetrical (Enoka, 1979; Garhammer, 1978; 1982). We performed multiple dependent *t*-tests with appropriate alpha corrections across left and right pairs of joints of the lower extremities. No significant differences in average peak moment powers were found. This result agrees with previous research on barbell mechanics (Rossi, 2007) provides strong support for the symmetrical nature of elite-lifters' mechanics. This simplifies future academic investigations into lifting, and coaching evaluations of lifters as an observer may focus only on one side of the lifter and be confident trends are symmetrical.

Barbell trajectory has been a key evaluative tool of researchers and coaches alike in the field of weightlifting (Baumann, 1985; Vorobyev, 1978). We chose to analyze the total system (lifter and barbell) centre of mass as a key descriptive variable. The lifter and barbell masses both contribute to the position of the system centre of mass throughout the lift. Even during the lowest lift intensity (80% of maximal snatch load), the barbell load was 15 kg to 40 kg more massive than the lifter. Lifter *and* barbell have been seen to move (not always in synchronous fashion) in both the vertical and anterior-posterior planes of motion in elite lifters (Bai, 2008; Bartonietz; 1996; Baumann, 1985; Enoka, 1979; 1983; 1988; Garhammer, 1978; 1979; 1980; 1982; 1985; 1992; Gourgoulis, 2002; 2004; 2009; Hiskia, 1997; Hoover, 2006; Kauhanen, 1984;

Rossi, 2007; Salammi, 2008; Schilling, 2002; Vorobyev, 1978; Winchester, 2009). We contended that system COM trajectory was a preferable analytical variable than either lifter or barbell centre of mass trajectory alone. Critical points or inflections for system COM series have not been established in the literature; hence our analysis of the system COM motion was largely descriptive. We did quantitatively assess maximal anterior-posterior system COM range of motion. The averages of selected lifters are presented below in Table 3.

Lifter Code	Range of Anterior-Posterior System COM motion (cm)		
	80 % barbell load	85% Barbell Load	90% Barbell Load
DM	T1: 4.7	T1: 7.8	T1: 7.1
	T2: 5.7	T2: 9.5	T2: 6.9
	T3: 6.6	T3: 5.0	T3: 8.6
MRC	T1: 4.0	T1: 13.5	T1: 3.7
	T2: 9.5	T2: 5.0	T2: 7.8
	T3: 4.6	T3: 8.5	T3: 5.4
LGD	T1: 9.2	T1: 8.4	T1: 6.0
	T2: 10.3	T2: 9.8	T2: 9.8
	T3: 9.2	T3: 11.2	T3: 5.6

Table 5. Summary of anterior-posterior system centre of mass (COM) motion for selected lifters across barbell intensities.

Results of variance analysis indicated no significant differences in anterior-posterior range of motion of system COM. Repeated measures ANOVA produced $F(2, 4) = 0.765$, $p =$

$0.523 > 0.05$, therefore we failed to reject the null hypothesis. Statistical power for variance analysis of system COM was small. As such, the numerical tests may not have revealed important features regarding system COM motion if the differences across barbell load were subtle. In addition, qualitative differences in anterior-posterior motion of system COM may not have been captured by numerical testing of COM range of motion. System COM anterior-posterior range of motion is useful for identifying lifting technique with large or inefficient horizontal translation of system COM, but anterior-posterior range alone does not provide information regarding trends or qualitative behaviour of system COM trajectory. To assess the trends in system COM, we relied on graphical analysis for reporting.

The statistical tests performed on the mean peak powers about the joints of the lower extremities in the x and y axes clearly indicate no significant differences exist between the left and right sides of the body. The statistical tests considered the mean peak power taken from the entire group, and thus is representative of the central tendency in this population. These results are in accord with the established practice within both the athletic and scientific community, in regards to weightlifting, to consider the performance of the snatch lift as a symmetrical event. Our results support this contention in as much as the peak powers from our elite-level sample are, on average, symmetrical between left and right side joints of the lower extremity for motion in the x and y axes.

Enoka (1979) noted, and confirmed by detailed study of barbell trajectory of elite lifters (Bai, 2008; Bartonietz; 1996; Baumann, 1985; Enoka, 1979; 1983; 1988; Garhammer, 1978; 1979; 1980; 1982; 1985; 1992; Gourgoulis, 2002; 2004; 2009, Hiskia, 1997; Hoover, 2006; Kauhanen, 1984; Rossi, 2007; Salammi, 2008; Schilling, 2002; Vorobyev, 1978; Winchester, 2009), barbell trajectory does not follow a strictly vertical path. Rather, most elite-level lifters

demonstrate an elongated 'S-shaped' barbell trajectory (Hiskia, 1997) with initial backwards barbell displacement. If the barbell load is large or to allow for a large barbell load, the moment arm between barbell and lifter centres of mass must be minimized. This reduces the moment of force created by the product of gravity's action on the barbell and the perpendicular distance to the rotation axis (low back and hips). In doing so, this reduces the muscle force required to overcome the inertial loads of the barbell (Enoka, 1979).

As the mass of the barbell was substantially larger than the body mass of the lifter, we contended that system COM profile would be slightly biased towards the posterior and follow similar trends as the barbell trajectory. Due to the mass inequality between the lifter and the barbell (even at the lowest relative intensity) it is a logical conclusion that barbell position trajectory would dominate the calculation of the system centre of mass. Graphical inspection of system COM trajectory largely confirmed our prediction. All COM trajectories, for each athlete sampled, showed distinct posterior displacement. The absolute value of the anterior-posterior system COM range of motion and trial specific trends in system COM trajectory were varied somewhat. Selected trials showed initial anterior displacement followed by net posterior displacement in system COM trajectory (example Figure 13), while others demonstrated immediate posterior displacement (example Figure 17). Several trials showed a distinct interruption of the smooth and continuous posterior displacement as the barbell made contact with the hips during the second knee extension phase (Figures 13-16). At this point, the body was fully extended, typically with a small posterior lean as the hips were rapidly thrust upwards with the barbell during the final explosive thrust.

We investigated another kinematic variable, shoulder position, to see if the symmetry trend seen in the lower body moment-power curves would be mimicked by shoulder position.

Left and right shoulder markers showed very high linear correlation in vertical and anterior-posterior displacement. Pearson's *r*-values were typically above $r = 0.95$. Vertical and anterior-posterior positions showed greatest left-right symmetry with Pearson's $r > 0.98$ in many cases. Thus, no substantial differences in shoulder position were seen across lifting intensities.

Conclusions and Recommendations

The primary purpose of this research was to investigate the effects of varying barbell load on peak powers about joints of the lower extremity (ankle, knee and hip) and selected kinematic variables with elite-level weightlifters performing the snatch lift. The results of this research prompt the following conclusions. First, variance analysis determined no significant differences in average peak moment power in three dimensions about any of the joints of the lower extremities across the 80–90% relative barbell load range. The statistical power of the variance analysis was weak due to the small sample size of elite-level lifting participants, thus it is possible differences existed across barbell loads, but were too small to be detected using these data and statistical tools. Secondly, paired sample t-tests revealed no significant differences between left and right side average peak moment powers in three dimensions about the ankle, knee, and hip. The left and right shoulder displacements showed very high linear correlations between their displacement trajectories during the snatch lift. This strong linear correlation did not change as barbell load was varied between 80-90% maximal snatch capacities. We conclude that the shoulders follow symmetrical displacement trajectories during the snatch lift. Finally, system centre of mass (COM) anterior-posterior displacement range did not vary significantly across the 80-90% barbell load. Therefore, we conclude that the lifters did not change their lifting mechanics in such a way as to affect the range of anterior-posterior system COM displacement.

References

Abbott, B C , Wilkie, D R (1952) The relation between velocity of shortening and the tension-length curve of skeletal muscle *Journal of Physiology, 120*, 214-223

Andrews, J G (1982) On the relationship between resultant joint torques and muscular activity *Medicine and Science in Sports and Exercise,14(5),* 361-367

Baechle, T R , Earle, R W (2000) *Essentials of Strength Training* Champagne, IL Human Kinetics

Bai, X , Wang, H , Zhang, X , Ji, W , Wang, C (2008) Three-dimension kinematics simulation and biomechanics analysis of snatch technique In *Proceedings of 1st International Pre-Olympic Conference of Sports Science & Sports Engineering, Najing, China,* Vol 1

Bartonietz, K E (1996) Biomechanics of the Snatch Toward a Higher Training Efficiency *Strength and Conditioning, 18*(3), 24-31

Baumann, W , Gross, V , Quade, K , Galbrierz, P , Schwirtz, A (1985) The Snatch Technique of World Class Weightlifters at the 1985 World Championships *International Journal of Sport Biomechanics, 4*, 68-89

Brooks, G A , Fahey, T D , Baldwin, K M (2005) *Exercise Physiology Human Bioenergetics and Its Applications* (4th ed) Toronto McGraw Hall

Burdett, R G (1982) Biomechanics of the Snatch Technique of Highly Skilled and Skilled Weightlifters *Research Quarterly for Exercise and Sport, 53*, 193-197

Campillo, P , Chollet, D , Micallef, J P (1997) Localisation de point critiques lors du tirage a l'arrache en halterophilie *Science and Sports, 13,* 90-92

Campos, J , Poletaev, P , Cuesta, A , Pablos, C , Carratala, V (2006) Kinematical Analysis of the Snatch in Elite Male Junior Weightlifters of Different Weight Categories *Journal of Strength and Conditioning Research, 20*(4), 843-850

Cappello, A , Stagni, R , Fantozzi, S , & Leardini, A (2005) Soft Tissue Artifact Compensation in Kinematics by Double Anatomical Landmark Calibration Performance of a Novel Method During Selected Motor Tasks *IEEE Transactions on Biomedical Engineering, 52*(6), 992-998

Carlock, J M , Smith, S L , Hartman, M J , Morris, R T , Ciroslan, D A , Pierce, K C , Newton, R U , Harman, E A , Sands, W A , Stone, M H (2004) The Relationship Between Vertical Jump Power Estimates and Weightlifting Ability A Field-Test Approach *Journal of Strength and Conditioning Research, 18*(3), 534-539

Chambers, J M , et al (1983) *Graphical methods for data analysis* Boston Duxbury Press

Channell, B T , Barfield, J P (2008) Effects of Olympic and Traditional Resistance Training on Vertical Jump improvement in High School Boys *Journal of Strength and Conditioning Research, 22(5),* 1522-1527

Chui, L Z F , Salem, G J (2005) Net Joint Moment Calculation Errors During Weightlifting Dempster versus DEXA *Clinical Kinesiology, 59*(1), 6

Chui, L Z F , Schilling, B K , Fry, A C , Salem, G J (2008) The influence of deformation on barbell mechanics during the clean pull *Sports Biomechanics, 7*(2), 260-273

Cronin, J , McNair, P J , Marshall, R N (2001) Velocity Specificity, Combination Training and Sport Specific Tasks *Journal of Science and Medicine in Sport, 4*(2), 168-178

Davies, C T M , Rennie, R (1968) Human power output *Nature, 217*

Dempster, W T (1955) *Space Requirements of the Seated Operator* (No 55) United States Aerospace Medical Research Laboratory

Elftman, H (1939) Forces and energy changes in the leg during walking *American Journal of Physiology, 125*, 339-356

Enoka, R M (1979) The pull in Olympic weightlifting *Medicine and Science in Sports, 11*(2), 131-137

Enoka, R M (1983) Muscular Control of a Learned Movement The Speed Control System Hypothesis *Experimental Brain Research, 51*, 135-145

Enoka, R M (1988) Load- and Skill-related changes in segmental contribution to a weightlifting movement *Medicine and Science in Sports and Exercise, 20*(2), 178-187

Escamilla, R F , Fleisig, G S , Lowry, T M , Barrentine, S W , Andrews, J R (2001) A Three-Dimensional Biomechanical Analysis of the Squat during Various Stance Widths *Medicine and Science in Sports and Exercise, 33(6),* 984-998

Freund, H J , Buidingen, H J (1978) The Relationship between Speed and Amplitude of the Fastest Voluntary Contractions of Human Arm Muscles *Experimental Brain Research, 31,* 1-12

Friedman, M (1937) The Use of Ranks to Avoid the Assumption of Normality Implicit in the Analysis of Variance *Journal of the American Statistical Association, 32*(200), 675-701

Funato, K , Matsuo, A , Fukunaga, T (2000) Measurement of Specific Movement Power Application Evaluation of Weightlifters *Ergonomics, 43(1),* 40-54

Gallucci, N (2008) *Sport Psychology Performance, Enhancement, Performance Inhibition, Individuals, and Teams* Hove Psychology

Garhammer, J (1978) Biomechanical Analysis of Selected Snatch Lifts at the U S Senior National Weightlifting Championships In *Biomechanics of Sport and Kinanthropometry,* Landry, F , Orban, W A R (eds) Miami Symposia Specialists

Garhammer, J (1979) Performance Evaluation of Olympic Weightlifters *Medicine and Science in Sports, 11*(3), 284-287

Garhammer, J (1980) Power Production by Olympic Weightlifters *Medicine and Science in Sports and Exercise, 12*(1), 54-60

Garhammer, J (1981) Biomechanical Characteristics of the 1978 World Weightlifting Championships In *Biomechanic, VII-B, 300-304* Baltimore University Park

Garhammer, J (1982) Energy Flow during Olympic Weightlifting *Medicine and Science in Sports and Exercise, 14*(5), 353-360

Garhammer, J (1984) Power Kinesiological Evaluation *National Strength and Conditioning Journal June-July*

Garhammer, J (1985) Biomechanical Profiles of Olympic Weightlifters *International Journal of Sport Biomechanics, 1*, 122-130

Garhammer, J (1991) A Comparison of Maximal Power Outputs Between Elite Male and Female Weightlifters in Competition *International Journal of Sport Biomechanics, 7*, 3-11

Garhammer, J (1993) A Review of Power Output Studies of Olympic and Powerlifting Methodology, Performance Prediction, and Evaluation Tests *Journal of Strength and Conditioning Research, 7*(2), 76-89

Garhammer, J , and Gregor, Robert (1992) Propulsion Forces as a Function of Intensity for Weightlifting and Vertical Jumping *Journal of Applied Sport Science Research, 6*(3), 129-134

Gourgoulis, V , Aggeloussis, P , Antoniou, Christoforidis, C , Mavromatis, G , Gara, A (2002) Comparative 3-dimensional Kinematic Analysis of the Snatch Technique in elite Male and Female Greek Weightlifters *Journal of Strength and Conditioning Research, 16*, 359-366

Gourgoulis, V , Aggeloussis, P , Antoniou, Kalivas, V , Mavromatis, G (2004) Snatch Lift Kinematics and Bar Energetics in Male Adolescent and Adult Weightlifters *Journal of Sports Medicine and Physical Fitness, 44*, 126-131

Grieve, D W (1970) The defeat of gravity in weightlifting *British Journal of Sports Medicine, 5*, 37-41

Hill, A V (1938) The heat of shortening and the dynamic constants of muscle *Proceedings of the Royal Society on Biomechanics, 126*, 136-195

Hiskia, G (1997) *Biomechanical Analysis of World and Olympic Champion Weightlifters*, Budapest, Hungary

Hoover, D L , Carlson, K M , Christensen, B K , Zebas, C J (2006) Biomechanical Analysis of Women Weightlifters During the Snatch *Journal of Strength and Conditioning Research, 20*(3), 627-633

Hori, N , Newton, R U , Nosaka, K , McGuigan, M R (2006) Comparison of different methods of determining power output in weightlifting exercises *Journal of Strength and Conditioning Research, 28(2),* 34-40

Jarvis, M (1999) *Sport Psychology* New York Routledge

Katz, B (1939) The relation between force and speed in muscular contraction *Journal of Physiology, 96*, 45-64

Kauhanen, H Hakkinen, K , Komi, P V (1984) A biomechanical analysis of the snatch and clean & jerk techniques of Finnish elite and district level weightlifters *Scandinavian Journal of Sports Science, 6(2),* 47-56

Kauhanen, H , Komi, P V , Hakkinen, K (2002) Standardization and Validation of the Body Weight Adjustment Regression Equations in Olympic Weightlifting *Journal of Strength and Conditioning Research, 16*(1), 58-74

Komi, P V (1984) Physiological and Biomechanical Correlates of Muscle Function Effects of Muscle Structure and Stretch-Shortening Cycle on Force and Speed *Exercise and Sport Sciences Reviews, 12*(1), 81-122

Marieb, E N , Mallatt, J , Wilhelm, P B (2008) *Human Anatomy* (5th ed) San Francisco Pearson

Markovic, G , Jaric, S (2007) Is vertical jump height a body size-independent measure of muscle power? *Journal of Sports Sciences,25(12),* 1355-1363

McGibbon, C A , Krebs, D E (1998) The influence of segment endpoint kinematics on segmental power calculations *Gait and Posture, 7*(3), 237-242

McGuigan, R M , and Kane, M K \ (2004) Reliability of Performance of Elite Olympic Weightlifters *Journal of Strength and Conditioning Research, 18*(3), 650-653

Miller, D I (1979) Modelling in biomechanics an overview *Medicine and Science in Sports, 11*(2), 115-122

Miller, D I , Nelson, R C (1973) *Biomechanics of Sport* Philadelphia, PA Lea & Febiger

Naruhiro, H , Newton, R U , Warren, A A , Kawamori, N , McGuigan, M R , Nosaka, K (2007) Comparison of Four Different Methods to Measure Power Output During the Hang Power Clean and the Weighted Jump Squat *Journal of Strength and Conditioning Research, 21*(2), 314-320

Nuzzo, J L , McBride, J M , Cormie, P , McCaulley, G O (2008) Relationship Between Countermovement Jump Performance and Multijoint Isometric and Dynamic Tests of Strength *Journal of Strength and Conditioning Research, 22*(3), 699-707

Pezzack, J C , Norman, R W , Winter, D A (1977) An Assessment of Derivative Determining Techniques Used for Motion Analysis *Journal of Biomechanics, 10*, 377-382

Robertson, D G E , Dowling, J J (2003) Design and Responses of Butterworth and Critically Damped Digital Filters *Journal of Electromyography and Kinesiology, 13*, 569-573

Robertson, D G E , *et al* (2004) *Research Methods in Biomechanics* Windsor Human Kinetics

Robertson, D G E , Winter, D A (1980) Mechanical Energy Generation, Absorption, and Transfer Amongst Segments During Walking *Journal of Biomechanics, 13*, 845-854

Rossi, S J , Buford, T W , Smith, D B , Kennel, R , Haff, E E , Haff, G G (2007) Bilateral Comparison of Barbell Kinetics and Kinematics During a Weightlifting Competition *International Journal of Sports Physiology and Performance, 2*, 150-158

Salaami, F , Jamshidi, N , Rostami, M , Najarian, S (2008) Power enhancement of weightlifters during Snatch through reducing torque on joints by particle swarm optimization *American Journal of Applied Sciences 5(12),* 1670-1675

Schilling, B K , Stone, M H , O'Bryant, H S , Fry, A C , Coglianese, R H , Pierce, K (2002) Snatch Technique of Collegiate National Level Weightlifters *Journal of Strength and Conditioning Research, 16*(4), 551-555

Shapiro, S S , Wilk, M B (1965) An analysis of variance test for normality (complete samples) *Biometrika, 52*(3 and 4), 591-611

Smidt, G L (1973) Biomechanical Analysis of Knee Flexion and Extension *Journal of Biomechanics, 6*, 79-92

Stone, M H , O'Bryant, H S , Williams, F E , Pierce, K C , Johnson, R L (1998) Analysis of bar paths during the snatch in elite male weightlifters *Journal of Strength and Conditioning, 20,* 56-64

Stone, M H , Sands, W A , Pierce, K C , Carlock, J , Cardinale, M , Newton, U (2005) Relationship between maximum strength to weightlifting performance *Medicine and Science in Sports and Exercise, 37(6),* 1037-1043

Vorobyev, A N (1978) *Weightlifting* Budapest International Weightlifting Federation

Wilcoxon, F (1945) Individual comparisons by ranking methods *Biometrics, 1*, 80-83

Wilkie, D R (1949) The relation between force and velocity in human muscle *Journal of Physiology, 110*, 249-280

Winchester, J B , Porter, J M , McBride, J M (2009) Changes in bar path kinematics and kinetics through the use of summary feedback in power snatch training *Journal of Strength and Conditioning Research, 23(2),* 444-454

Winter, D A (1976) Analysis of instantaneous energy of normal gait *Journal of Biomechanics, 9,* 253-257

Winter, D A , Robertson, D G E (1978) Joint torque and energy patterns in normal gait *Biological Cybernetics, 29,* 137-142

Winter, D A , Robertson, D G E (1980) Mechanical Energy Generation, Absorption and Transfer Amongst Segments During Walking *Journal of Biomechanics, 13*, 845-854

Zajac, F E , Neptune, R R , Kautz, S A (2002) Biomechanics and muscle coordination of human walking Part 1 Introduction to concepts, power transfer, dynamics and simulations *Gait and Posture, 16*, 215-232

Zatsiorsky, V M (1995) *Science and Practice of Strength Training* Windsor Human Kinetics

Appendix A

The first step in quantitative data analysis was to perform thorough data exploration. Descriptive statistics were performed including graphical displays of frequency distributions, stem and leaf plots, q-q plots of experimental data against Gaussian cumulative distribution frequency, and box plots. These statistics allowed for visual inspection and interpretation of characteristics of data distribution.

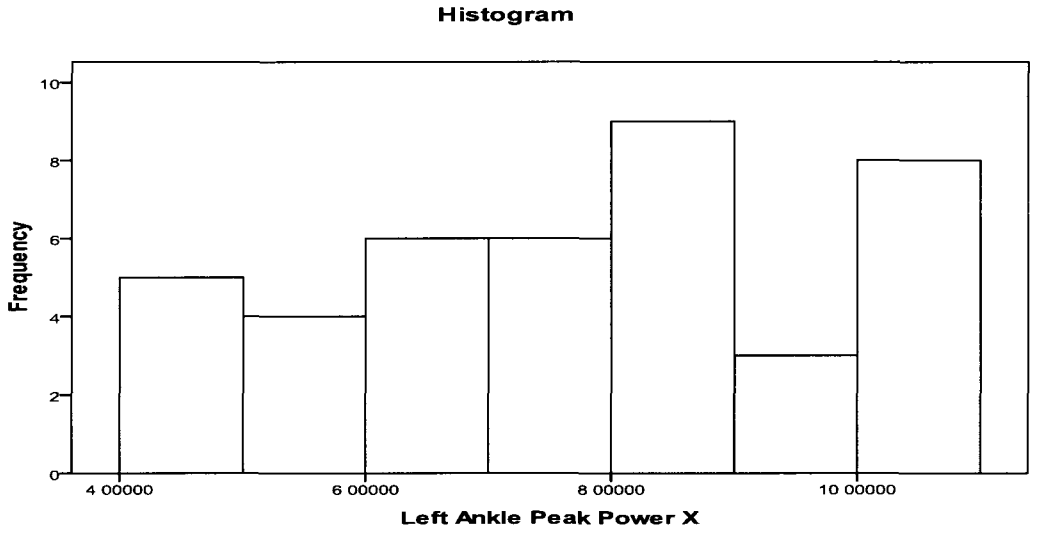

Figure A1. Histogram displaying frequency counts of average peak left ankle powers about the x axis (internal reference frame). These data are inclusive of all barbell intensities.

The histogram is perhaps the most popular graphical method to quickly visually inspect a data set for normality trends, as a Gaussian line plot may be superimposed on this graph to help identify regions of data concentration indicative of skewed distributions. Similar to the histogram above, stem and leaf plots provide tabular accounts of the frequency distribution of a given data set.

Left Ankle Peak Power X Stem-and-Leaf Plot

Frequency	Stem &	Leaf
5.00	4 .	35789
4.00	5 .	1229
6.00	6 .	002299
6.00	7 .	234558
9.00	8 .	000222267
3.00	9 .	022
8.00	10 .	01222456

Stem width: 1.00000

Each leaf: 1 case(s)

Figure A2 Stem and leaf plot summarizing average peak left ankle powers about the x axis Leaf values are rounded to nearest whole integer

To more rigorously analyze data trends, we used an instructive and powerful graphical assessment tool the quantile-quantile (q-q) plot The default division of this data set performed by SPSS software broke ordered data sets into octiles or 8 quantiles

We see large scale conformity to the normal line (y = x), with deviations greatest at the tails of the data set Below is a summary of numerical tests of normality performed on average peak power about each joint (bilateral), for each trial across all intensities Given the sample size, n = 45, numerical assessment of normality requires use of Shapiro-Wilk test (Shapiro, 1965) This evaluates whether a sample population can statistically be said to come from a normally distributed population Explicitly, null hypothesis states there no significant difference between empirical data and normal distribution

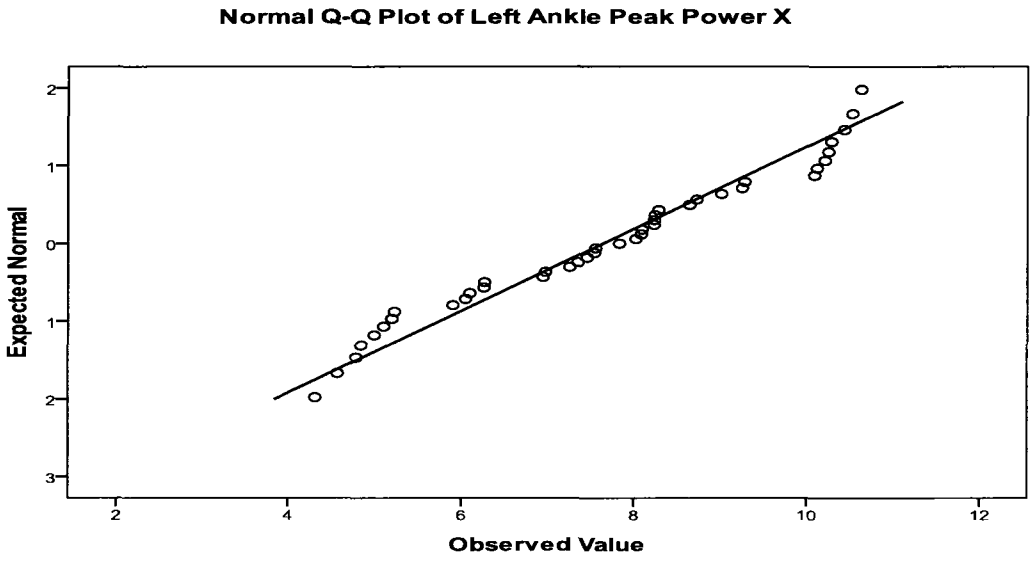

Figure A3 Quantiles plot (q-q) of average peak left ankle powers for all intensities plotted against expected (normal) cumulative frequency distribution Note the small oscillations over and under the normal line of y = x These oscillations signal regions of trend deviation from ideal normal distribution in the empirical data set

Only variables about x axis (sagittal movements) were normally distributed Exception to this trend was right knee peak power statistic This results in rejection of null hypothesis (normality assumption) for right knee peak power Characteristics of right knee peak power about x axis were further investigated

The q-q plot above shows the deviations from normality were small in magnitude (p = 0 042 < 0 05) and oscillated above and below expected normal distribution (y = x) The oscillation made it difficult to locate the exact region of deviance in sample set Typically a sample distribution steeper than the normal line is *more* dispersed than the normal curve A flatter empirical distribution is *less* dispersed than the normal curve (Chambers, 1983) Figure 5 showed both of these trends requiring further development From inspection of the histogram (Figure 6), data were bimodal in nature The first concentration was a leptokurtic distribution and the second mesokurtic These two concentrations had a net cancelling effect on each other, explaining Shapiro-Wilk statistic's proximity to alpha

	Kolmogorov-Smirnov[a]			Shapiro-Wilk		
	Statistic	df	Sig	Statistic	df	Sig
Left Ankle Peak Power X	0 097	45	0 200*	0 949	45	0 063
Left Ankle Peak Power Y	0 260	45	0 000	0 525	45	0 000
Left Ankle Peak Power Z	0 165	45	0 006	0 835	45	0 000
Right Ankle Peak Power X	0 107	45	0 200*	0 964	45	0 217
Right Ankle Peak Power Y	0 179	45	0 002	0 719	45	0 000
Right Ankle Peak Power Z	0 192	45	0 001	0 807	45	0 000
Left Knee Peak Power X	0 110	45	0 200*	0 956	45	0 111
Left Knee Peak Power Y	0 234	45	0 000	0 766	45	0 000
Left Knee Peak Power Z	0 163	45	0 008	0 922	45	0 008
Right Knee Peak Power X	0 135	45	0 058	0 944	45	0 042
Right Knee Peak Power Y	0 188	45	0 001	0 867	45	0 000
Right Knee Peak Power Z	0 166	45	0 006	0 891	45	0 001
Left Hip Peak Power X	0 123	45	0 123	0 952	45	0 084
Left Hip Peak Power Y	0 152	45	0 018	0 908	45	0 003
Left Hip Peak Power Z	0 211	45	0 000	0 873	45	0 000
Right Hip Peak Power X	0 125	45	0 105	0 957	45	0 128
Right Hip Peak Power Y	0 196	45	0 000	0 904	45	0 002
Right Hip Peak Power Z	0 154	45	0 016	0 845	45	0 000

[a] Lilliefors Significance Correction* This is a lower bound of the true significance

Table A1 Summary sheet of normality tests performed on entire data set Relevant result is Shapiro-Wilk statistic for all average peak powers in 3 dimensions about lower extremity joints Alpha is set to 0 05

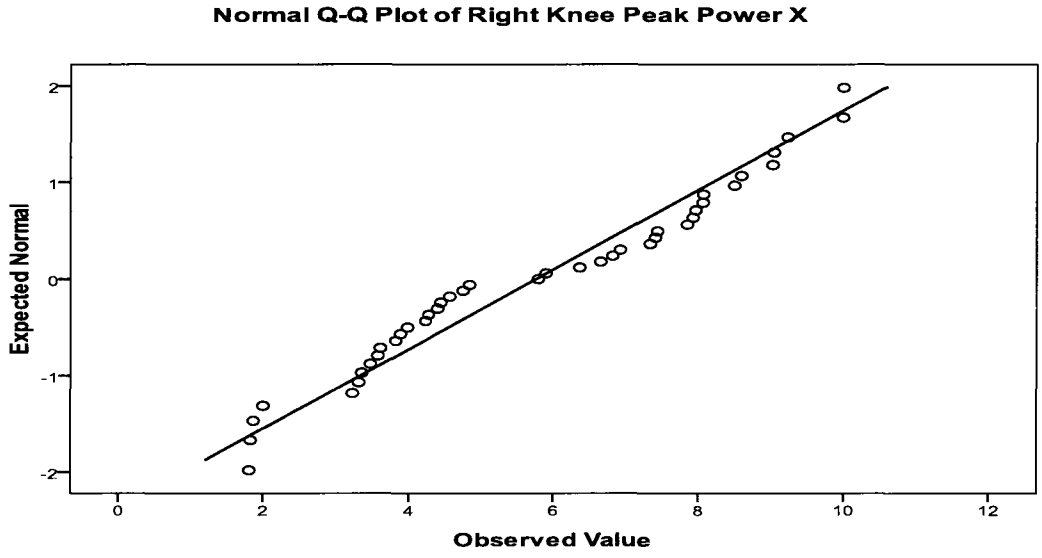

Figure A4. Q-q plot of average peak right knee power about the x axis for all data across intensities. The central quantiles highlight two antagonistic deviations from the normal line (y = x). This reflects the slight bimodal feature in the data distribution. The modes are of different amplitudes making for a more complicated assessment of data fit.

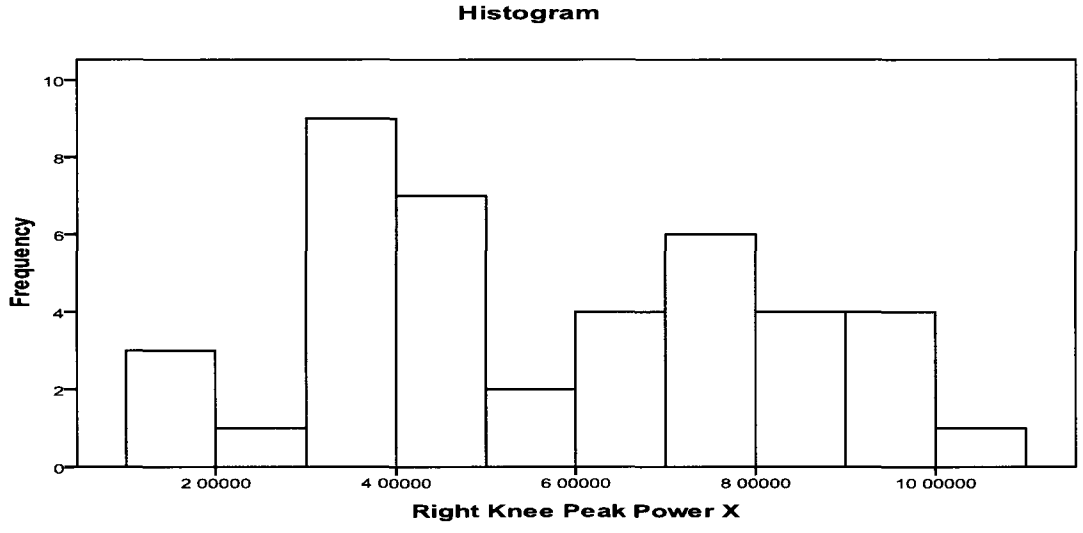

Figure A5. Histogram of frequency distribution for average peak right knee powers about the x axis inclusive of all barbell intensities. Note bimodal distribution.

Variance analyses employed to test the research hypotheses were not performed on the data as a whole, but rather across data grouped by barbell intensity level within larger body of data. Therefore we

similarly inspected data sections for normality and distribution trends as they were the actual sections of data for comparison and testing Summaries of these results may be found in Appendix A All cohorts showed normal data distribution for peak power variable about x axis (sagittal plane of motion) for all joints of lower extremities We failed to reject null hypothesis regarding data normality

Variance analysis was performed across dependent variables for all barbell intensities Barbell intensity had more than two levels, therefore it was necessary to test the correlation of data across these levels Mauchly's Test of Sphericity assessed the correlation of data across factor levels While ANOVA assumed homogeneity of variance across repeated measures or cohorts, it will remain robust despite violation of homogeneity of variance only if data were uncorrelated across factor conditions If intensity grouped data were correlated, homogeneity of variance across cohorts would be required for ANOVA to remain robust This did not prove necessary, as Mauchly's test of Sphericity, produced 'P' values all greater than *alpha* 'P' values for 80, 85 and 90% were 0 432, 0 549 and 0 258, respectively This resulted in failure to reject null hypothesis across all cohorts Therefore we continued with variance analysis

	Kolmogorov-Smirnov[a]			Shapiro-Wilk		
	Statistic	df	Sig	Statistic	df	Sig
Left Ankle Peak Power X	171	15	200*	925	15	228
Left Ankle Peak Power Y	213	15	066	890	15	067
Left Ankle Peak Power Z	179	15	200*	897	15	085
Right Ankle Peak Power X	194	15	133	947	15	484
Right Ankle Peak Power Y	119	15	200*	939	15	370
Right Ankle Peak Power Z	213	15	066	888	15	063
Left Knee Peak Power X	157	15	200*	943	15	428
Left Knee Peak Power Y	113	15	200*	966	15	798
Left Knee Peak Power Z	188	15	159	894	15	077
Right Knee Peak Power X	223	15	043	896	15	083
Right Knee Peak Power Y	184	15	185	881	15	050
Right Knee Peak Power Z	206	15	087	909	15	132
Left Hip Peak Power X	116	15	200	951	15	535
Left Hip Peak Power Y	105	15	200*	985	15	993
Left Hip Peak Power Z	179	15	200*	907	15	123
Right Hip Peak Power X	162	15	200*	923	15	211
Right Hip Peak Power Y	189	15	156	897	15	085
Right Hip Peak Power Z	158	15	200*	924	15	221

a Lilliefors Significance Correction * This is a lower bound of the true significance

Table A2 Statistical summary sheet of the normality tests performed on the 80% barbell intensity cohort for all subjects and joints Note peak power data about the x axis, again passes the test for normality as we fail to reject the null hypothesis regarding normality of data for all cases about the x axis

	Kolmogorov-Smirnov[a]			Shapiro-Wilk		
	Statistic	df	Sig	Statistic	df	Sig
Left Ankle Peak Power X	167	15	200*	923	15	309
Left Ankle Peak Power Y	264	15	020	831	15	022
Left Ankle Peak Power Z	178	15	200	910	15	212
Right Ankle Peak Power X	203	15	187	909	15	210
Right Ankle Peak Power Y	242	15	051	847	15	033
Right Ankle Peak Power Z	140	15	200	954	15	690
Left Knee Peak Power X	171	15	200	951	15	656
Left Knee Peak Power Y	351	15	000	781	15	006
Left Knee Peak Power Z	205	15	173	898	15	147
Right Knee Peak Power X	206	15	168	890	15	117
Right Knee Peak Power Y	221	15	110	873	15	072
Right Knee Peak Power Z	268	15	017	858	15	046
Left Hip Peak Power X	164	15	200*	948	15	605
Left Hip Peak Power Y	234	15	067	802	15	010
Left Hip Peak Power Z	244	15	047	888	15	111
Right Hip Peak Power X	240	15	055	913	15	231
Right Hip Peak Power Y	307	15	003	785	15	006
Right Hip Peak Power Z	123	15	200*	963	15	824

[a] Lilliefors Significance Correction *This is a lower bound of the true significance

Table A3 Summary sheet of normality tests performed on 85% barbell intensity cohort Results mimic those of in text 80% set

	Kolmogorov-Smirnov[a]			Shapiro-Wilk		
	Statistic	df	Sig	Statistic	df	Sig
Left Ankle Peak Power X	101	15	200*	966	15	817
Left Ankle Peak Power Y	320	15	000	509	15	000
Left Ankle Peak Power Z	187	15	200*	898	15	104
Right Ankle Peak Power X	139	15	200*	942	15	447
Right Ankle Peak Power Y	258	15	012	715	15	001
Right Ankle Peak Power Z	296	15	002	783	15	003
Left Knee Peak Power X	145	15	200*	918	15	208
Left Knee Peak Power Y	349	15	000	746	15	001
Left Knee Peak Power Z	150	15	200*	918	15	207
Right Knee Peak Power X	143	15	200*	910	15	156
Right Knee Peak Power Y	238	15	030	844	15	019
Right Knee Peak Power Z	252	15	016	866	15	037
Left Hip Peak Power X	184	15	200*	910	15	158
Left Hip Peak Power Y	215	15	080	796	15	004
Left Hip Peak Power Z	271	15	006	766	15	002
Right Hip Peak Power X	182	15	200*	941	15	429
Right Hip Peak Power Y	130	15	200*	943	15	458
Right Hip Peak Power Z	203	15	123	889	15	078

Table A4. Summary sheet of normality tests performed on 90% barbell intensity cohort. Results mimic both 80% and 85% lifting sets.

Appendix B

Measure·MEASURE_1

Within Subjects Effect	Mauchly's W	Approx Chi-Square	df	Sig	Epsilon[a] Greenhouse-Geisser	Huynh-Feldt	Lower-bound
leftanklepower	.571	1 681	2	.432	700	961	500

Tests the null hypothesis that the error covariance matrix of the orthonormalized transformed dependent variables is proportional to an identity matrix

a May be used to adjust the degrees of freedom for the averaged tests of significance Corrected tests are displayed in the Tests of Within-Subjects Effects table

b Design· Intercept

Within Subjects Design leftanklepower

Table B1. Summary sheet of Mauchly's test of data sphericity for average peak left ankle power about the x axis inclusive of all barbell intensities.

Measure·MEASURE_1

Source		Type III Sum of Squares	df	Mean Square	F	Sig	Partial Eta Squared	Noncent Parameter	Observed Power[a]
leftanklepower	Sphericity Assumed	5 646	2	2 823	2 594	135	.393	5 189	.375
	Greenhouse-Geisser	5.646	1 400	4 034	2 594	162	393	3.631	295
	Huynh-Feldt	5 646	1 922	2.937	2 594	139	393	4.987	365
	Lower-bound	5.646	1 000	5 646	2 594	183	393	2.594	238
Error(leftanklepower)	Sphericity Assumed	8 705	8	1 088					

Greenhouse-Geisser	8 705	5 599	1 555
Huynh-Feldt	8 705	7 689	1 132
Lower-bound	8 705	4 000	2 176

a Computed using alpha = 05

Table B2 Summary sheet of within subject effects from repeated measures ANOVA for average peak left ankle powers about the x axis

Measure MEASURE_1

Within Subjects Effect	Mauchly's W	Approx Chi-Square	df	Sig	Epsilon[a] Greenhouse-Geisser	Huynh-Feldt	Lower-bound
leftkneepowe	670	1 200	2	549	752	1 000	500

Tests the null hypothesis that the error covariance matrix of the orthonormalized transformed dependent variables is proportional to an identity matrix

a May be used to adjust the degrees of freedom for the averaged tests of significance Corrected tests are displayed in the Tests of Within-Subjects Effects table

b Design Intercept

Within Subjects Design leftkneepower

Table B3 Mauchly's test of sphericity for average peak left knee power about the x axis across all barbell intensities

Source		Type III Sum of Squares	df	Mean Square	F	Sig.	Partial Eta Squared	Noncent. Parameter	Observed Power[a]
leftkneepowe	Sphericity Assumed	232	2	.116	133	878	.032	.265	.064
	Greenhouse-Geisser	232	1 504	154	133	.823	032	200	.062
	Huynh-Feldt	232	2 000	116	133	878	032	265	064
	Lower-bound	232	1 000	232	133	734	032	133	059
Error(leftkneepowe)	Sphericity Assumed	7 003	8	875					
	Greenhouse-Geisser	7 003	6 016	1 164					
	Huynh-Feldt	7 003	8 000	875					
	Lower-bound	7 003	4 000	1 751					

Table B4. Summary sheet of within subject effects test for average peak left knee power about the x axis across all lifting intensities.

Measure:MEASURE_1

Within Subjects Effect	Mauchly's W	Approx. Chi-Square	df	Sig.	Epsilon[a] Greenhouse-Geisser	Huynh-Feldt	Lower-bound
lefthippower	.433	2.511	2	.285	.638	.804	500

Table B5. Mauchly's test of sphericity for average peak left hip power about the x axis across all lifting intensities.

Measure MEASURE_1

Source		Type III Sum of Squares	df	Mean Square	F	Sig	Partial Eta Squared	Noncent Parameter	Observed Power[a]
lefthippower	Sphericity Assumed	2 181	2	1 090	420	671	095	841	097
	Greenhouse-Geisser	2 181	1 276	1 708	420	593	095	536	085
	Huynh-Feldt	2 181	1 609	1 355	420	633	095	676	091
	Lower-bound	2 181	1 000	2 181	420	552	095	420	080
Error(lefthippower)	Sphericity Assumed	20 753	8	2 594					
	Greenhouse-Geisser	20 753	5 105	4 065					
	Huynh-Feldt	20 753	6 435	3 225					
	Lower-bound	20 753	4 000	5 188					

Table B6 Summary sheet of within subject effects test for average peak left hip power about the x axis across all lifting intensities

Non parametric statistical procedures were conducted to test differences in average peak abductor/adductor moment power values about the left ankle, knee and hip across repeated trials of varied barbell loads Detailed results of these statistical tests follow below

Descriptive Statistics

	N	Mean	Std Deviation	Minimum	Maximum	Percentiles 25th	50th (Median)	75th
LANKYT1	5	3363	17490	12	60	1918	3400	4791
LANKYT2	5	3204	18824	14	60	1458	3528	4789
LANKYT3	5	3461	12269	16	46	2388	3355	4587

Table B7. Descriptive statistics summary for average peak abductor/adductor moment power values about the left ankle joint across all barbell intensities.

Test Statistics[a]

N	5
Chi-Square	400
df	2
Asymp Sig	819

a Friedman Test

Table B8. Summary sheet of test statistic result for the Friedman singed rank test of average peak abductor/adductor moment power values about the left ankle joint across all barbell intensities.

Descriptive Statistics

	N	Mean	Std Deviation	Minimum	Maximum	Percentiles 25th	50th (Median)	75th
LKNEYT1	5	7375	31600	38	1 16	4500	6887	1 0494
LKNEYT2	5	6832	34533	16	1 09	3792	7036	9770
LKNEYT3	5	9249	64125	43	2 02	4597	7984	1 4534

Table B9. Descriptive statistics summary for average peak abductor/adductor moment power values about the left knee joint across all barbell intensities.

Test Statistics[a]	
N	5
Chi-Square	2 800
df	2
Asymp Sig	247

a Friedman Test

Table B10. Summary sheet of test statistic result for the Friedman singed rank test of average peak abductor/adductor moment power values about the left knee joint across all barbell intensities.

Descriptive Statistics

	N	Mean	Std Deviation	Minimum	Maximum	Percentiles 25th	50th (Median)	75th
LHIPYT1	5	4915	13910	32	66	3636	4709	6296
LHIPYT2	5	5011	14091	35	70	3679	5217	6240
LHIPYT3	5	4982	13731	35	70	3714	5101	6189

Table B11. Descriptive statistics summary for average peak abductor/adductor moment power values about the left hip joint across all barbell intensities.

Test Statistics[a]	
N	5
Chi-Square	400
df	2
Asymp Sig	819

a Friedman Test

Table B12. Summary sheet of test statistic result for the Friedman singed rank test of average peak abductor/adductor moment power values about the left hip joint across all barbell intensities.

Non parametric statistical procedures were conducted to test differences in average peak abductor/adductor moment power values about the left ankle, knee and hip across repeated trials of varied barbell loads. Detailed results of these statistical tests follow below.

Descriptive Statistics

	N	Mean	Std Deviation	Minimum	Maximum	Percentiles 25th	50th (Median)	75th
LANKZT1	5	3197	06414	21	36	2688	3448	3581
LANKZT2	5	1839	.08755	09	29	.0977	1867	2688
LANKZT3	5	1922	13876	04	42	0879	1832	3011

Table B13. Descriptive statistics summary for average peak internal/external rotation moment power values about the left ankle joint across all barbell intensities.

Test Statistics[a]

N	5
Chi-Square	4 800
df	2
Asymp Sig	091

a Friedman Test

Table B14. Summary sheet of test statistic result for the Friedman singed rank test of average peak abductor/adductor moment power values about the left ankle joint across all barbell intensities.

Descriptive Statistics

	N	Mean	Std Deviation	Minimum	Maximum	Percentiles 25th	50th (Median)	75th
LKNEZT1	5	3934	15201	21	62	2759	3437	5358
LKNEZT2	5	3269	18640	15	53	1487	2975	5197
LKNEZT3	5	2535	10969	13	39	1408	2957	3450

Table B15. Descriptive statistics summary for average peak internal/external rotation moment power values about the left knee joint across all barbell intensities.

Test Statistics[a]

N	5
Chi-Square	2 800
df	2
Asymp Sig	247

a Friedman Test

Table B16. Summary sheet of test statistic result for the Friedman singed rank test of average peak internal/external rotation moment power values about the left knee joint across all barbell intensities.

Appendix C

Within Subjects Effect	Mauchly's W	Approx. Chi-Square	df	Sig	Epsilon[a] Greenhouse-Geisser	Huynh-Feldt	Lower-bound
COM	.161	1 827	2	.401	.544	.692	500

Table C1. Summary sheet of the test of data sphericity for system centre of mass (COM) in the x direction (anterior-posterior).

Source		Type III Sum of Squares	df	Mean Square	F	Sig	Partial Eta Squared	Noncent Parameter	Observed Power[a]
COM	Sphericity Assumed	000	2	000	765	523	277	1 530	112
	Greenhouse-Geisser	000	1 087	000	765	480	277	832	087
	Huynh-Feldt	000	1 383	000	765	497	277	1 058	096
	Lower-bound	000	1 000	000	765	474	277	765	085
Error(COM)	Sphericity Assumed	001	4	000					
	Greenhouse-Geisser	001	2 175	000					
	Huynh-Feldt	001	2 767	000					
	Lower-bound	001	2 000	000					

Table C2. Summary sheet of within subject effects from repeated-measures ANOVA for system centre of mass (COM) in the x direction (anterior-posterior).

Appendix D

Participant 4

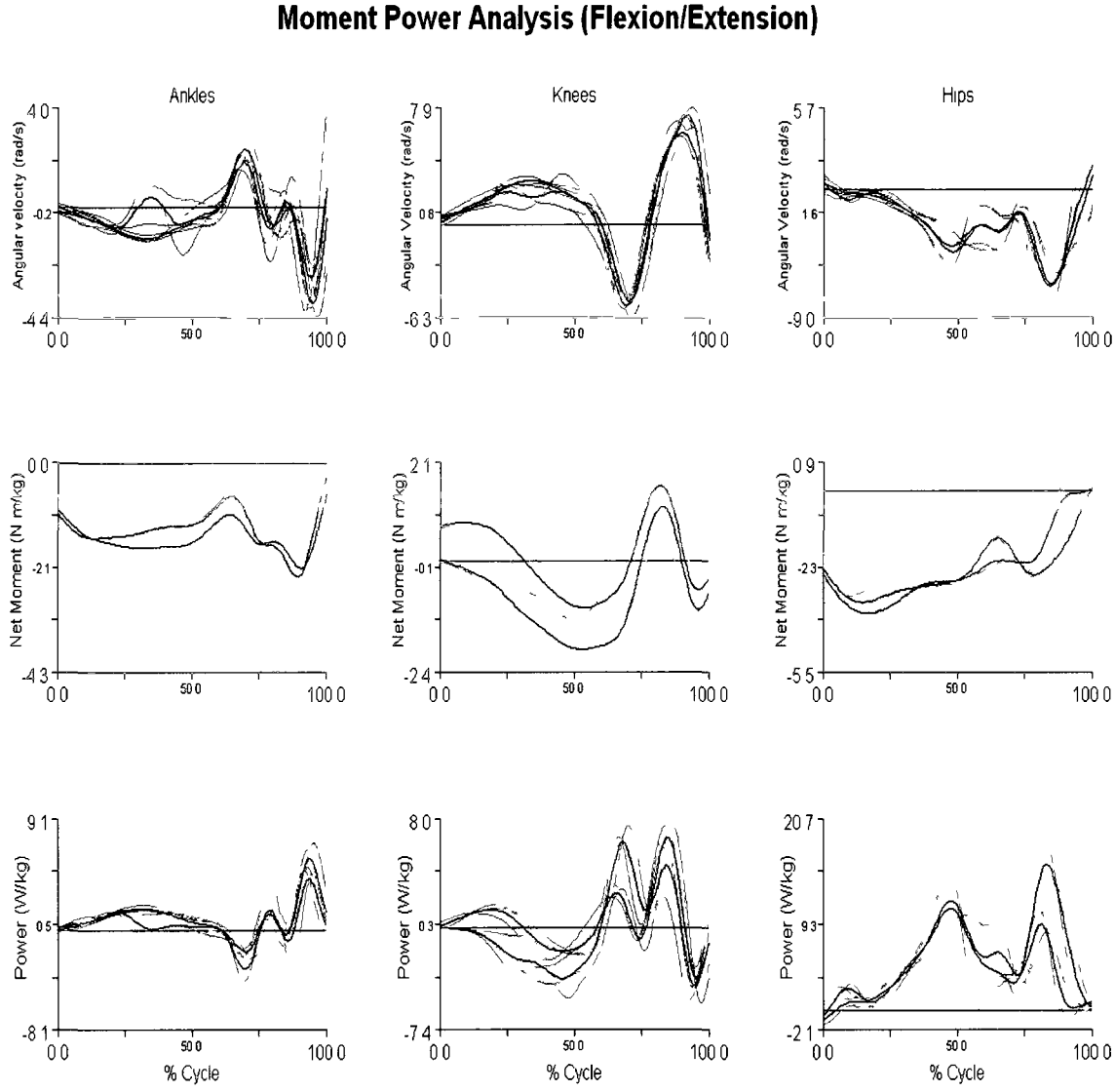

Figure D1. Participant 4's three combined attempts at snatching 100 kg (80%). On the ordinate axes, the first row displays angular velocity (rad/s), the second net moment of force normalized to body mass (N.m/kg), and the third net power normalized to body mass (W/kg). The first column plots both right and left ankles, the second right and left knees, and the third right and left hips. All plotted variables concern motion in the sagittal plane (about the internal frame of reference x axis), Time is plotted on the abscissa and is normalized to 100% of lift cycle from barbell liftoff until feet leave the floor in final propulsion.

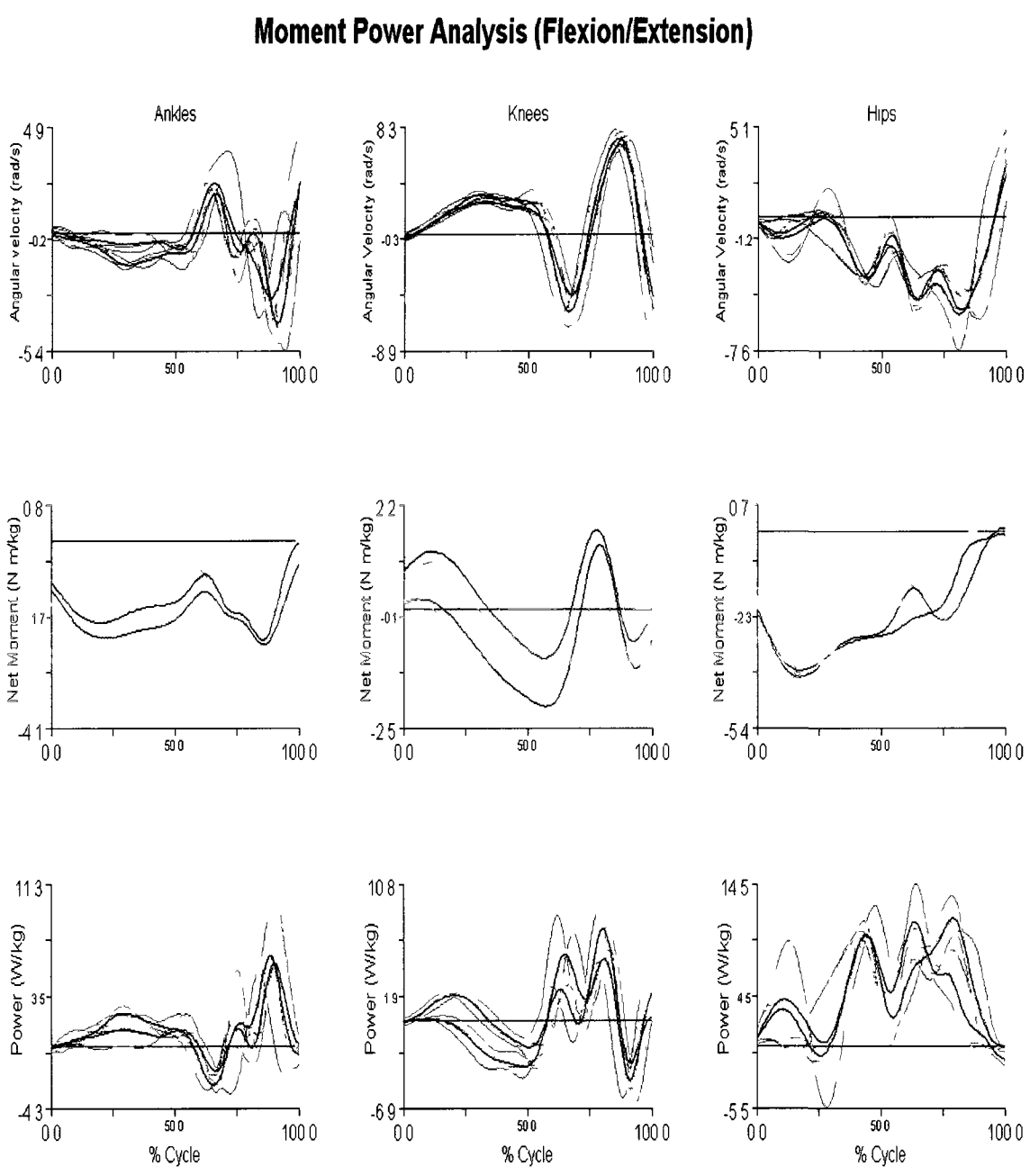

Figure D2. Participant 4's three combined attempts at snatching 105 kg (85%). On the ordinate axes, the first row displays angular velocity (rad/s), the second net moment of force normalized to body mass (N.m/kg), and the third net power normalized to body mass (W/kg). The first column plots both right and left ankles, the second right and left knees, and the third right and left hips. All plotted variables concern motion in the sagittal plane (about the internal frame of reference x axis), Time is plotted on the abscissa and is normalized to 100% of lift cycle from barbell liftoff until feet leave the floor in final propulsion.

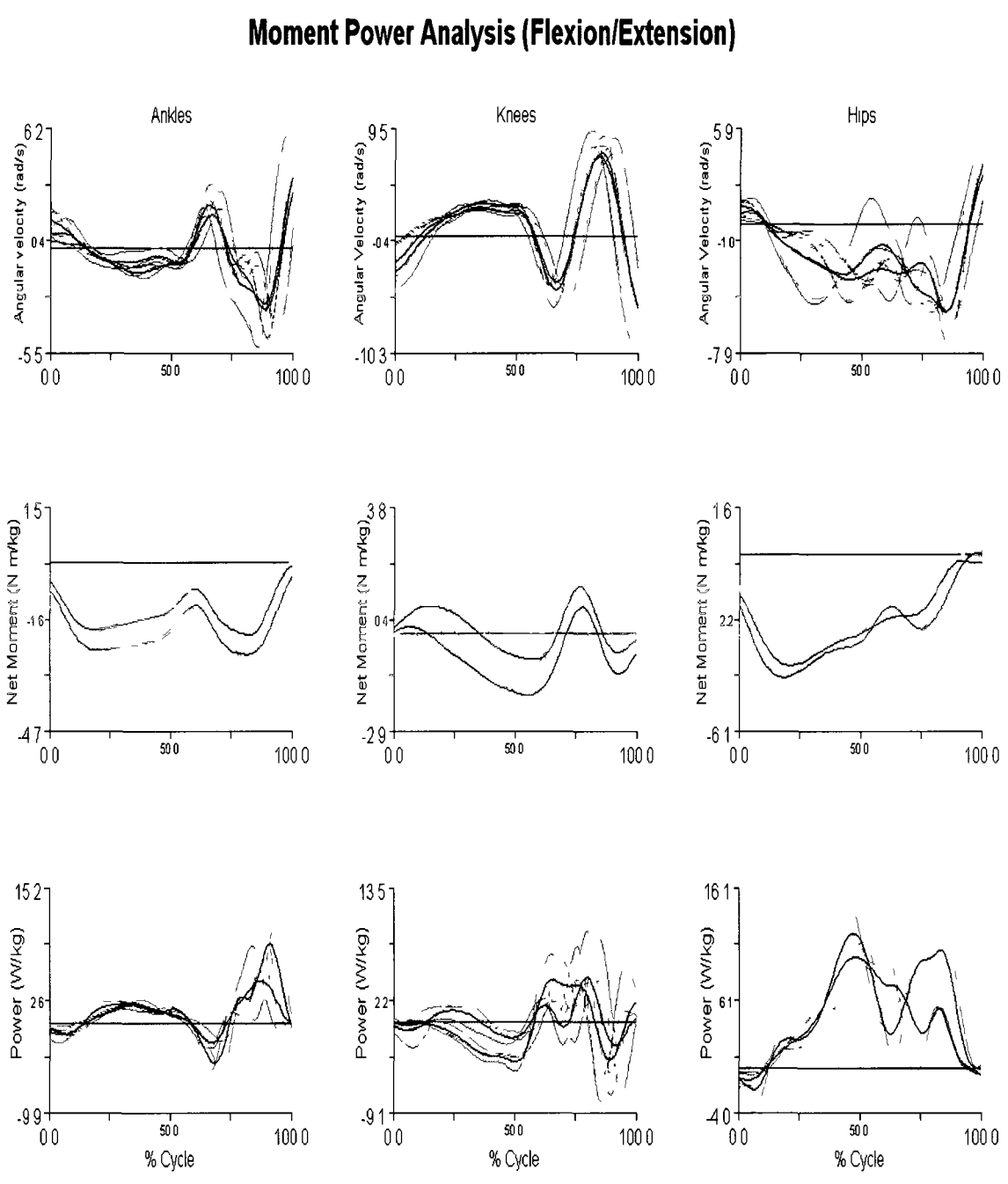

Figure D3. Participant 4's three combined attempts at snatching 110 kg (90%). On the ordinate axes, the first row displays angular velocity (rad/s), the second net moment of force normalized to body mass (N.m/kg), and the third net power normalized to body mass (W/kg). The first column plots both right and left ankles, the second right and left knees, and the third right and left hips. All plotted variables concern motion in the sagittal plane (about the internal frame of reference x axis), Time is plotted on the abscissa and is normalized to 100% of lift cycle from barbell liftoff until feet leave the floor in final propulsion.

Participant 2

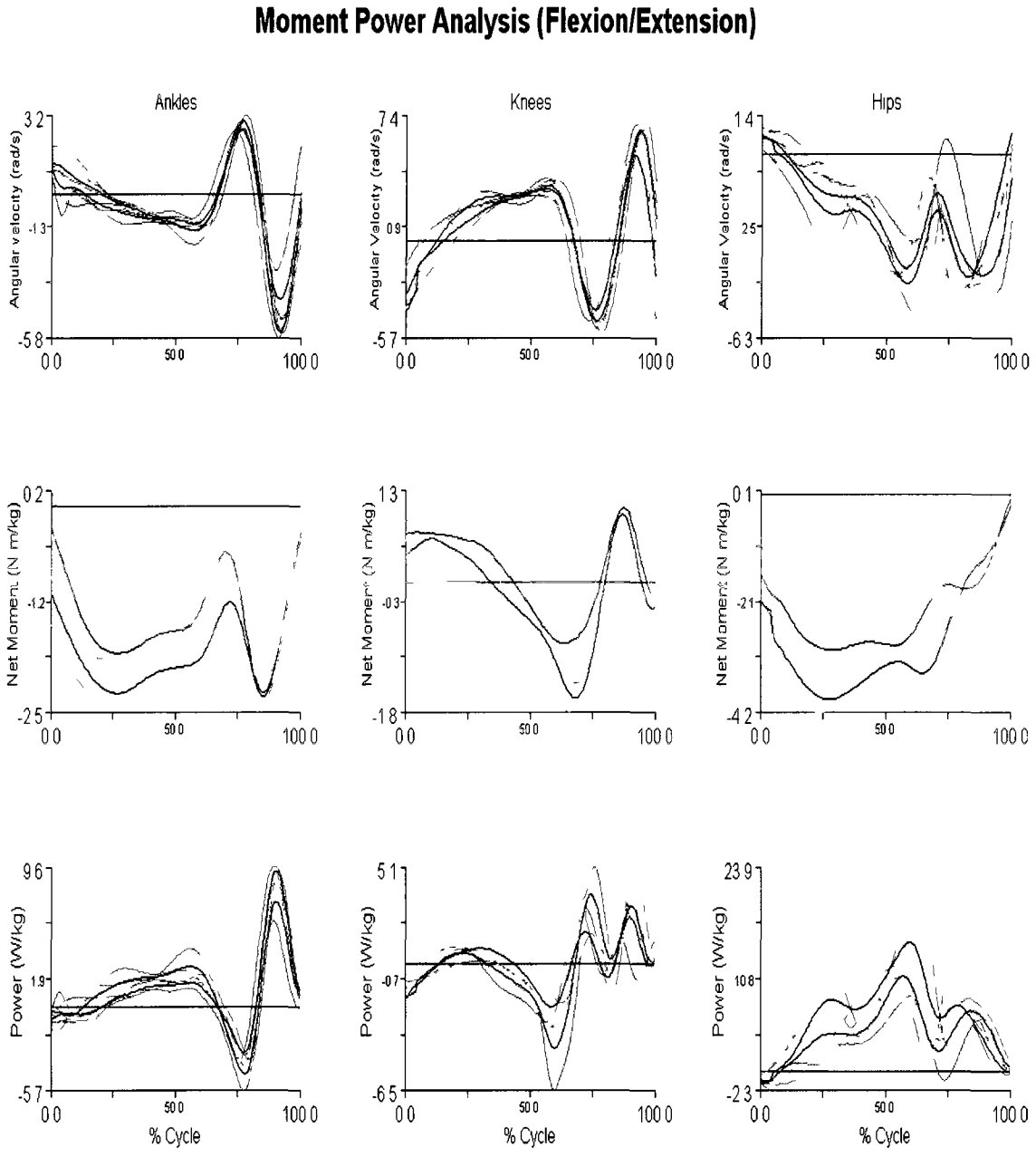

Figure D4.Participant 2's three combined attempts at snatching 100 kg (80%). On the ordinate axes, the first row displays angular velocity (rad/s), the second net moment of force normalized to body mass (N.m/kg), and the third net power normalized to body mass (W/kg). The first column plots both right and left ankles, the second right and left knees, and the third right and left hips. All plotted variables concern motion in the sagittal plane (about the internal frame of reference x axis), Time is plotted on the abscissa and is normalized to 100% of lift cycle from barbell liftoff until feet leave the floor in final propulsion.

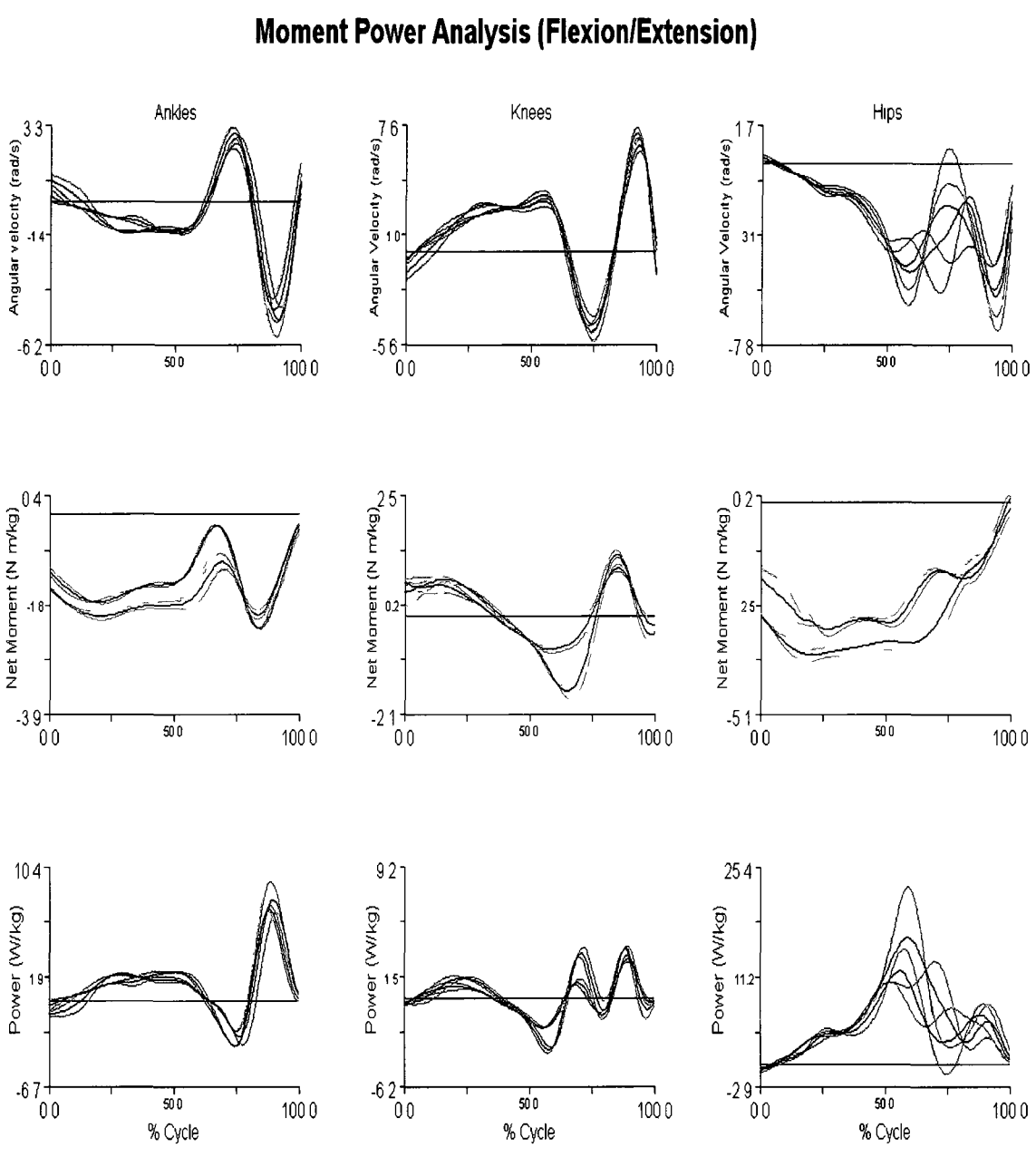

Figure D5. Participant 2's two combined attempts at snatching 105 kg (85%). On the ordinate axes, the first row displays angular velocity (rad/s), the second net moment of force normalized to body mass (N.m/kg), and the third net power normalized to body mass (W/kg). The first column plots both right and left ankles, the second right and left knees, and the third right and left hips. All plotted variables concern motion in the sagittal plane (about the internal frame of reference x axis), Time is plotted on the abscissa and is normalized to 100% of lift cycle from barbell liftoff until feet leave the floor in final propulsion.

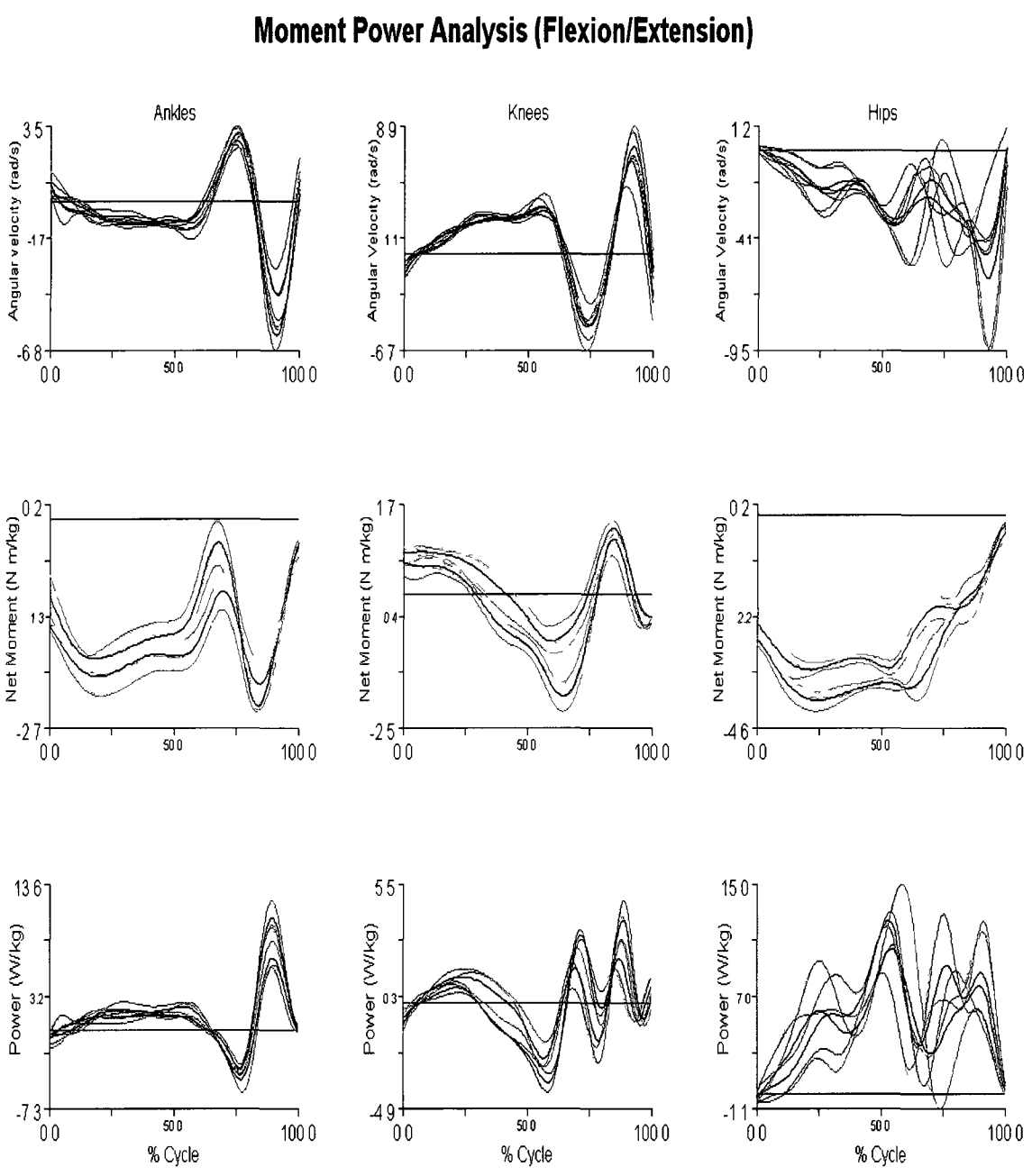

Figure D6. Participant 2's three combined attempts at snatching 110 kg (90%). On the ordinate axes, the first row displays angular velocity (rad/s), the second net moment of force normalized to body mass (N.m/kg), and the third net power normalized to body mass (W/kg). The first column plots both right and left ankles, the second right and left knees, and the third right and left hips. All plotted variables concern motion in the sagittal plane (about the internal frame of reference x axis), Time is plotted on the abscissa and is normalized to 100% of lift cycle from barbell liftoff until feet leave the floor in final propulsion.

Participant 4

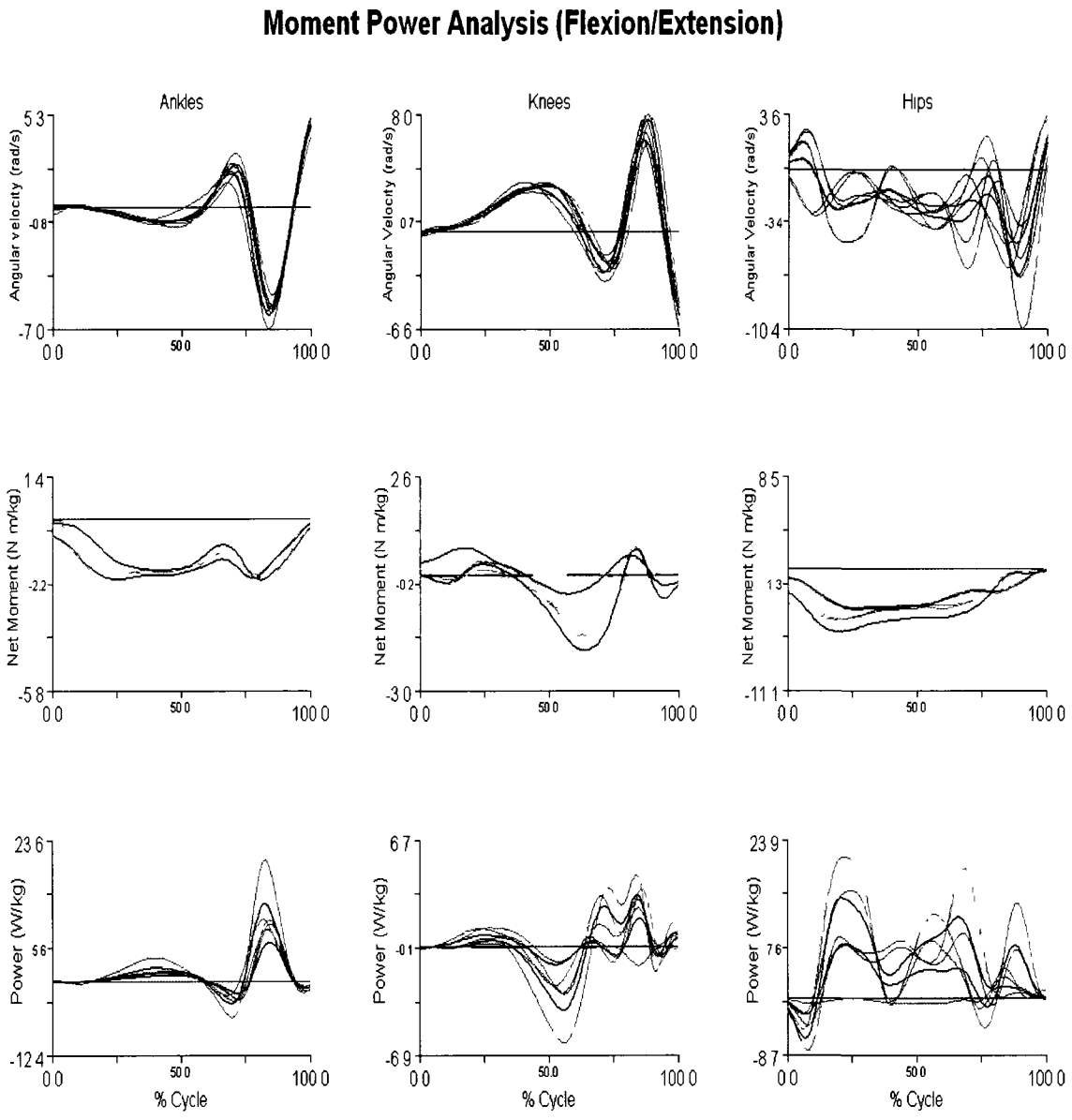

Figure D7. Participant 4's three combined attempts at snatching 90 kg (80%). On the ordinate axes, the first row displays angular velocity (rad/s), the second net moment of force normalized to body mass (N.m/kg), and the third net power normalized to body mass (W/kg). The first column plots both right and left ankles, the second right and left knees, and the third right and left hips. All plotted variables concern motion in the sagittal plane (about the internal frame of reference x axis), Time is plotted on the abscissa and is normalized to 100% of lift cycle from barbell liftoff until feet leave the floor in final propulsion.

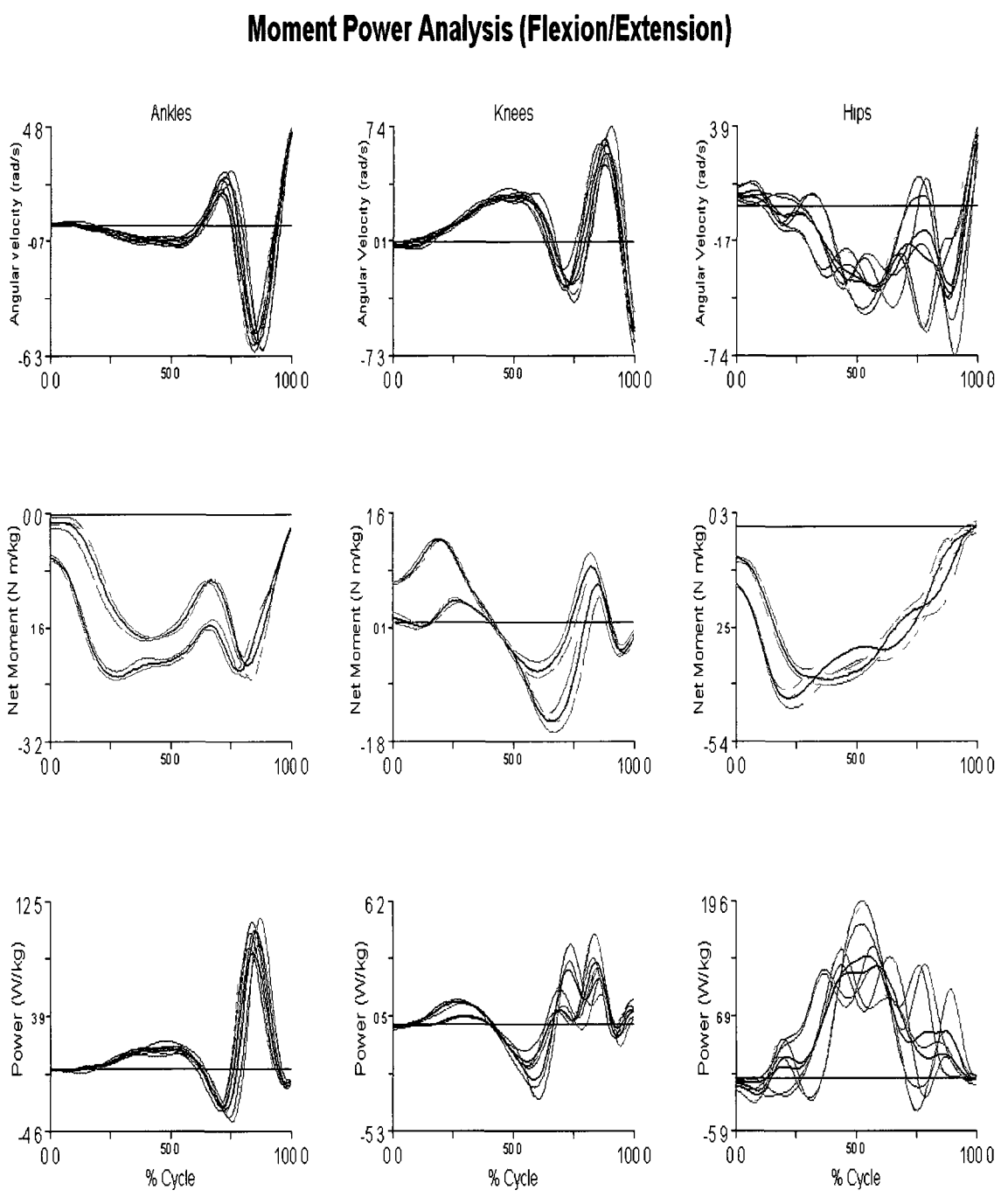

Figure D8. Participant 4's three combined attempts at snatching 95 kg (85%). On the ordinate axes, the first row displays angular velocity (rad/s), the second net moment of force normalized to body mass (N.m/kg), and the third net power normalized to body mass (W/kg). The first column plots both right and left ankles, the second right and left knees, and the third right and left hips. All plotted variables concern motion in the sagittal plane (about the internal frame of reference x axis), Time is plotted on the abscissa and is normalized to 100% of lift cycle from barbell liftoff until feet leave the floor in final propulsion.

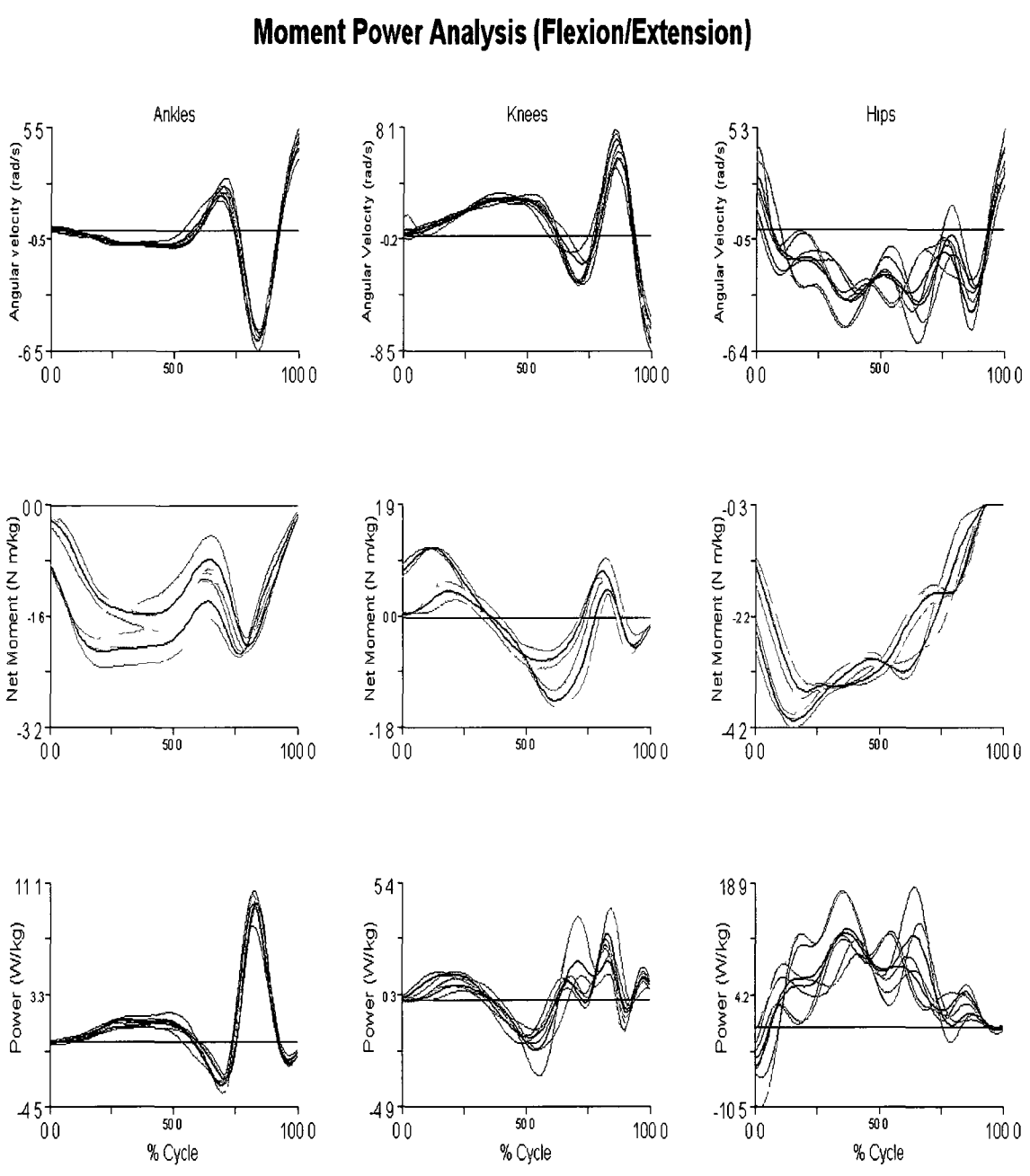

Figure D9. Participant 4's three combined attempts at snatching 100 kg (90%). On the ordinate axes, the first row displays angular velocity (rad/s), the second net moment of force normalized to body mass (N.m/kg), and the third net power normalized to body mass (W/kg). The first column plots both right and left ankles, the second right and left knees, and the third right and left hips. All plotted variables concern motion in the sagittal plane (about the internal frame of reference x axis), Time is plotted on the abscissa and is normalized to 100% of lift cycle from barbell liftoff until feet leave the floor in final propulsion.

Participant 1

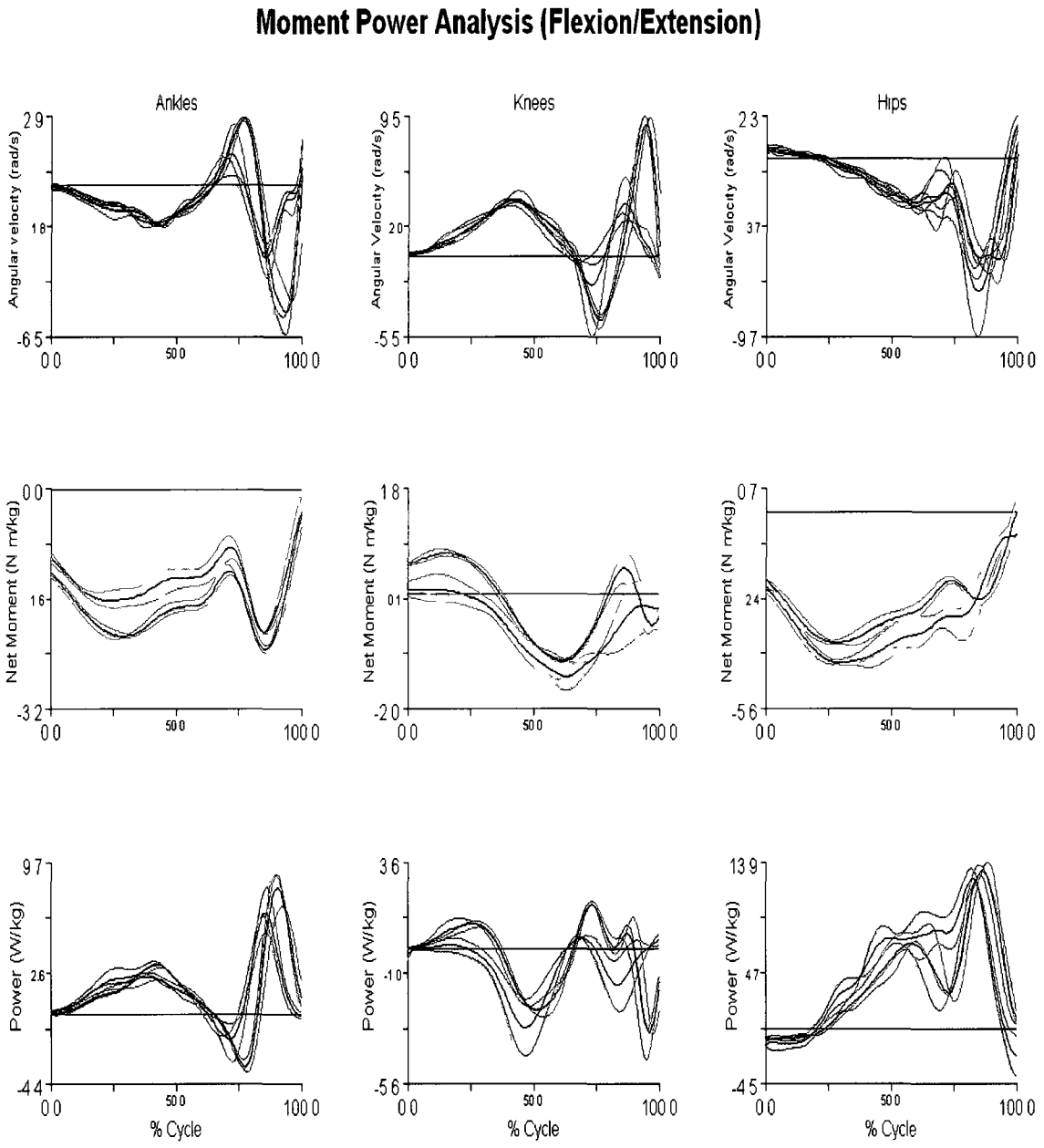

Figure D10. Participant 1's three combined attempts at snatching 100 kg (80%). On the ordinate axes, the first row displays angular velocity (rad/s), the second net moment of force normalized to body mass (N.m/kg), and the third net power normalized to body mass (W/kg). The first column plots both right and left ankles, the second right and left knees, and the third right and left hips. All plotted variables concern motion in the sagittal plane (about the internal frame of reference x axis), Time is plotted on the abscissa and is normalized to 100% of lift cycle from barbell liftoff until feet leave the floor in final propulsion.

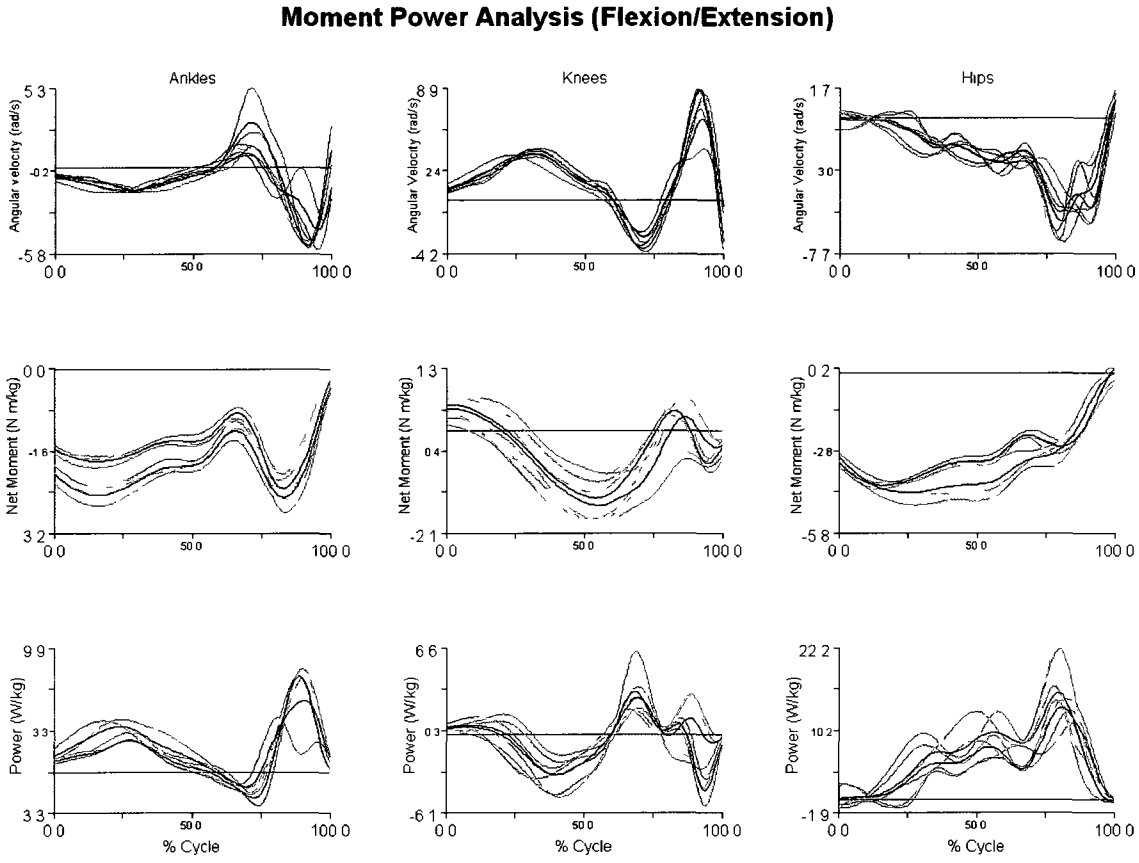

Figure D11. Participant 1's three combined attempts at snatching 110 kg (85%). On the ordinate axes, the first row displays angular velocity (rad/s), the second net moment of force normalized to body mass (N.m/kg), and the third net power normalized to body mass (W/kg). The first column plots both right and left ankles, the second right and left knees, and the third right and left hips. All plotted variables concern motion in the sagittal plane (about the internal frame of reference x axis), Time is plotted on the abscissa and is normalized to 100% of lift cycle from barbell liftoff until feet leave the floor in final propulsion.

Appendix E

Participant 3

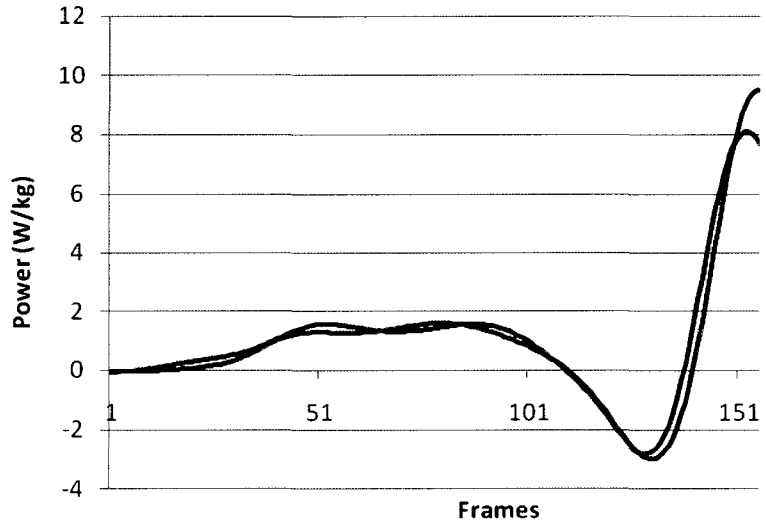

Figure E1. Left ankle (blue series) and right ankle (red series) powers about the ankle joint in the x axis (sagittal plane of motion) of participant 3 snatching 100 kg load, first attempt at 100 kg. The abscissa holds frames (200 Hz) and the ordinate holds power (Watts normalized to body mass).

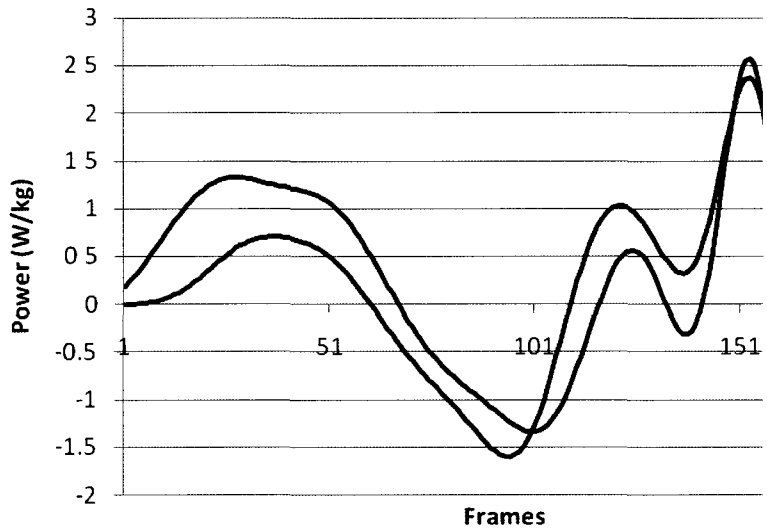

Figure E2. Left knee (blue series) and right knee (red series) powers about the knee joint in the x axis (sagittal plane of motion) of participant 3 snatching 95 kg load, second attempt at 95 kg. The abscissa holds frames (200 Hz) and the ordinate holds power (Watts normalized to body mass).

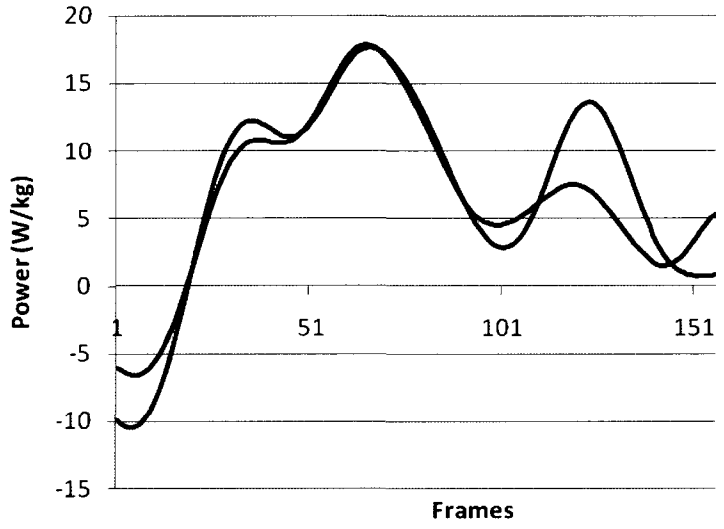

Figure E3 Left hip (blue series) and right hip (red series) powers about the hip joint in the x axis (sagittal plane of motion) of participant 3 snatching 95 kg load, second attempt at 95 kg The abscissa holds frames (200 Hz) and the ordinate holds power (Watts normalized to body mass)

Participant 2

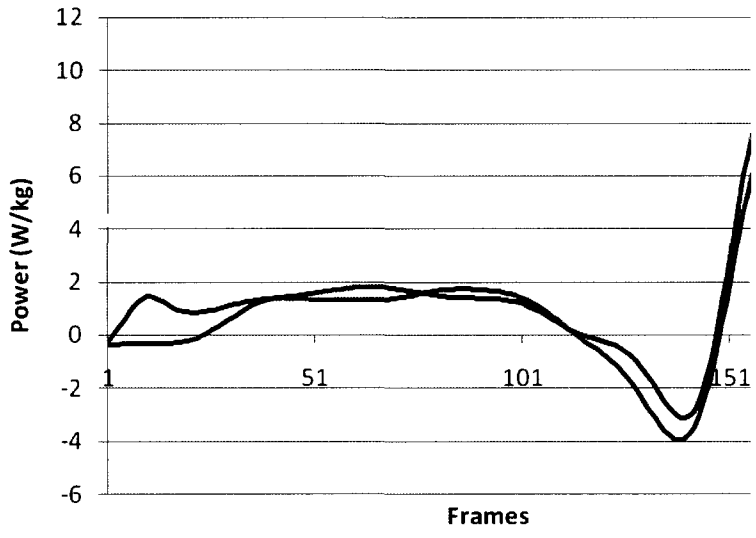

Figure E4 Left ankle (blue series) and right ankle (red series) powers about the ankle joint in the x axis (sagittal plane of motion) of participant 2 snatching 100 kg load, second attempt at 100 kg The abscissa holds frames (200 Hz) and the ordinate holds power (Watts normalized to body mass)

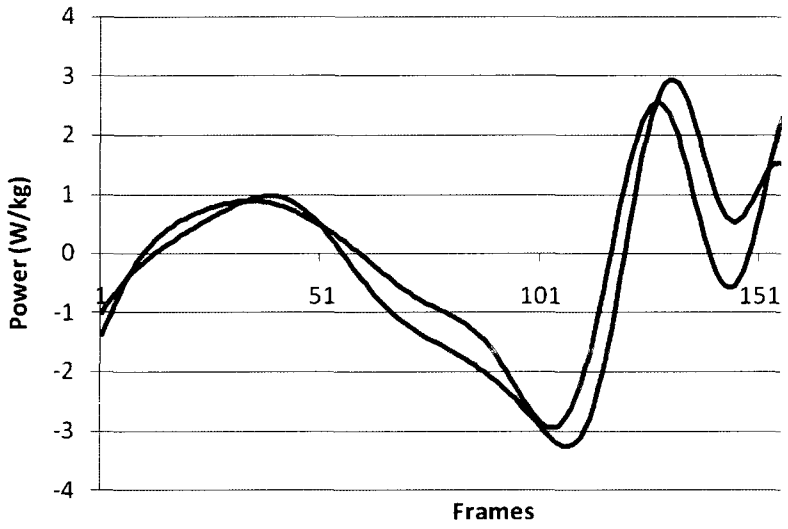

Figure E5 Left knee (blue series) and right knee (red series) powers about the knee joint in the x axis (sagittal plane of motion) of participant 2 snatching 100 kg load, second attempt at 100 kg The abscissa holds frames (200 Hz) and the ordinate holds power (Watts normalized to body mass)

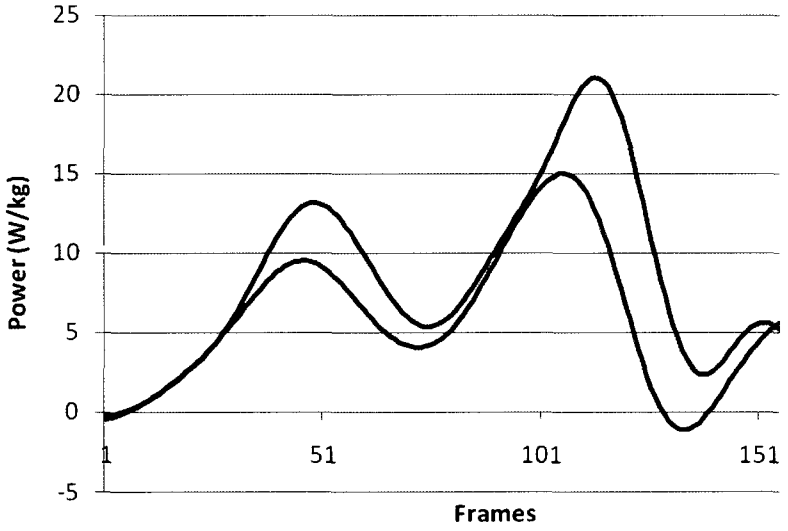

Figure E6 Left hip (blue series) and right hip (red series) powers about the hip joint in the x axis (sagittal plane of motion) of participant 2 snatching 100 kg load, first attempt at 100 kg The abscissa holds frames (200 Hz) and the ordinate holds power (Watts normalized to body mass)

Participant 1

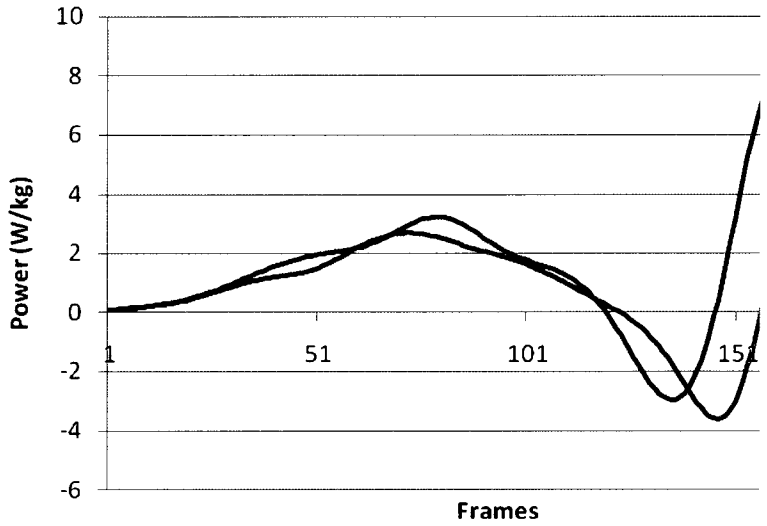

Figure E7 Left ankle (blue series) and right ankle (red series) powers about the ankle joint in the x axis (sagittal plane of motion) of participant 1 snatching 100 kg load, first attempt at 100 kg The abscissa holds frames (200 Hz) and the ordinate holds power (Watts normalized to body mass)

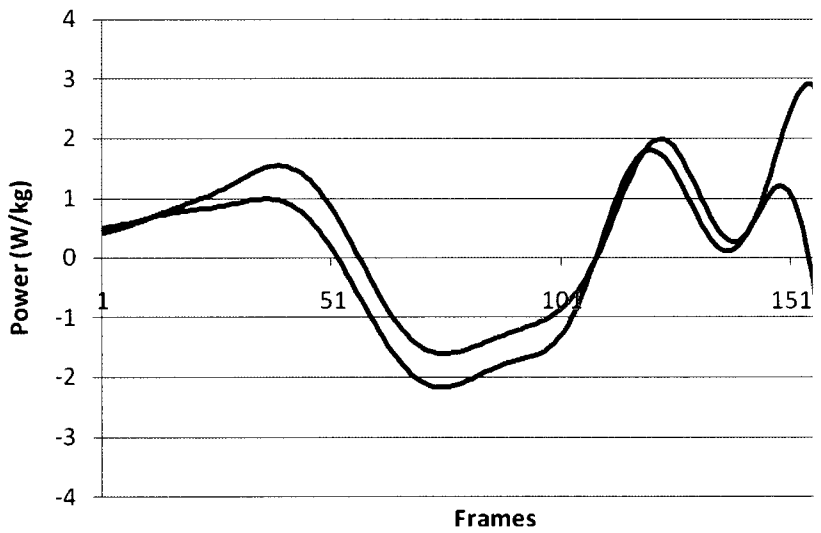

Figure E8 Left knee (blue series) and right knee (red series) powers about the knee joint in the x axis (sagittal plane of motion) of participant 1 snatching 110 kg load, first attempt at 110 kg The abscissa holds frames (200 Hz) and the ordinate holds power (Watts normalized to body mass)

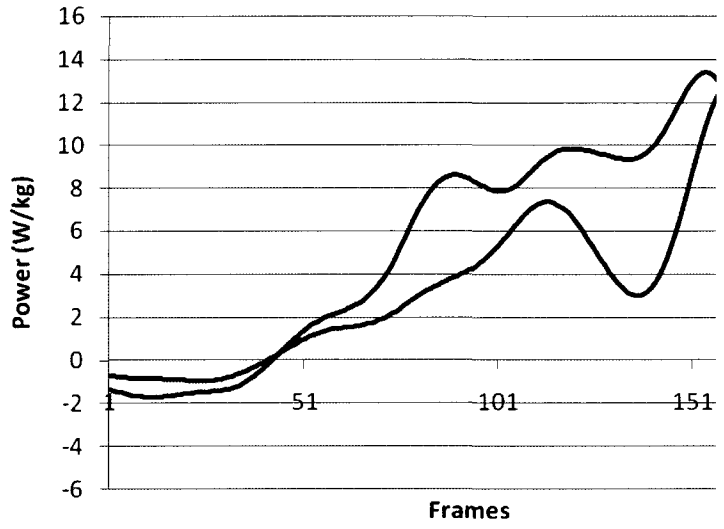

Figure E9 Left hip (blue series) and right hip (red series) powers about the hip joint in the x axis (sagittal plane of motion) of participant 1 snatching 100 kg load, second attempt at 100 kg The abscissa holds frames (200 Hz) and the ordinate holds power (Watts normalized to body mass)

Appendix F

Participant 2

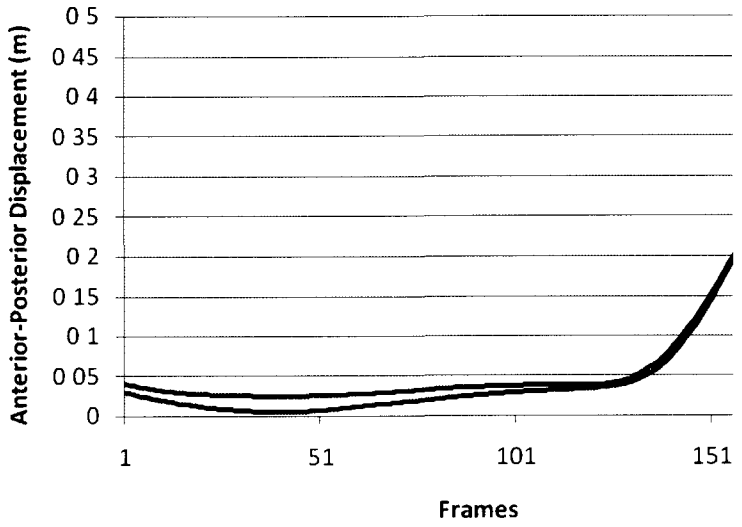

Figure F1 Participant 2's first attempt at 100 kg snatch lift (80%) Plotted is the anterior posterior displacement of the left (blue series) and right (red series) shoulder markers against frames (200 Hz) The Pearson's correlation between trajectories is r = 0 9990

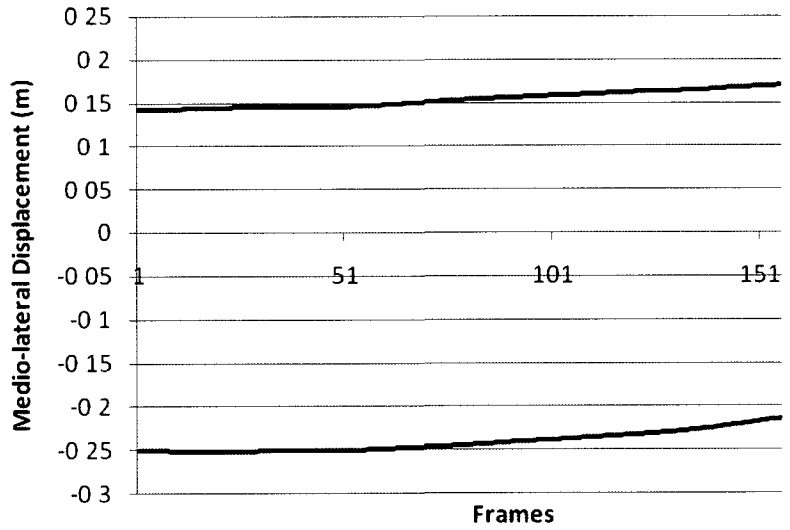

Figure F2 Participant 2's first attempt at 100 kg snatch lift (80%) Plotted is the mediolateral displacement of the left (blue series) and right (red series) shoulder markers against frames (200 Hz) No zeroing of the starting positions was performed, this is raw data The Pearson's correlation between mediolateral trajectories is r = 0 9841

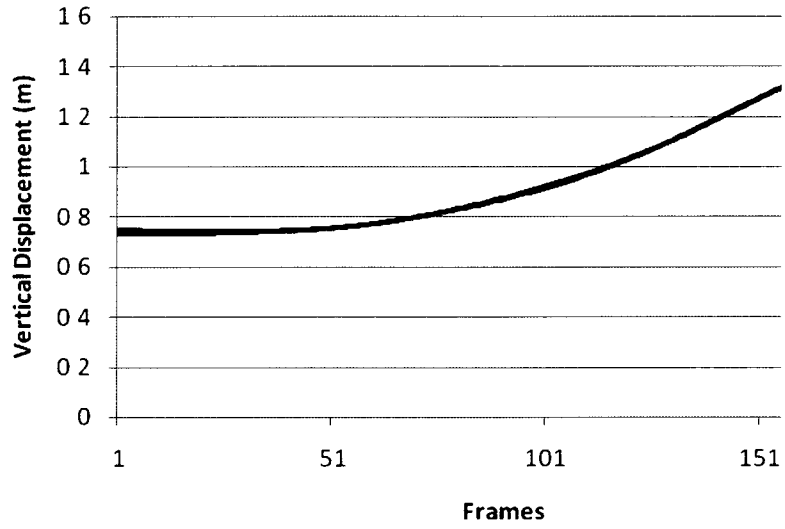

Figure F3 Participant 2's first attempt at 100 kg snatch lift (80%) Plotted is the vertical displacement of the left (blue series) and right (red series) shoulder markers against frames (200 Hz) No zeroing of the starting positions was performed, this is raw data The Pearson's correlation between vertical trajectories is r = 0 9999

Participant 1

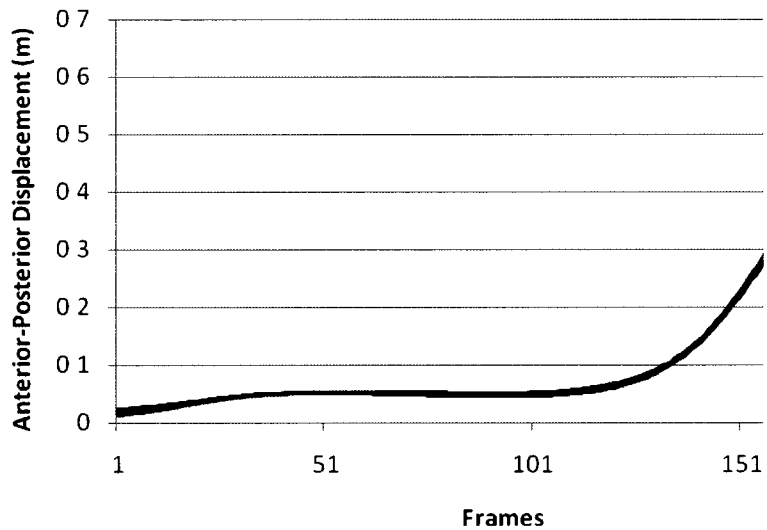

Figure F4 Participant 1's first attempt at 100 kg snatch lift (80%) Plotted is the anterior posterior displacement of the left (blue series) and right (red series) shoulder markers against frames (200 Hz) The Pearson's correlation between trajectories is r = 0 9998

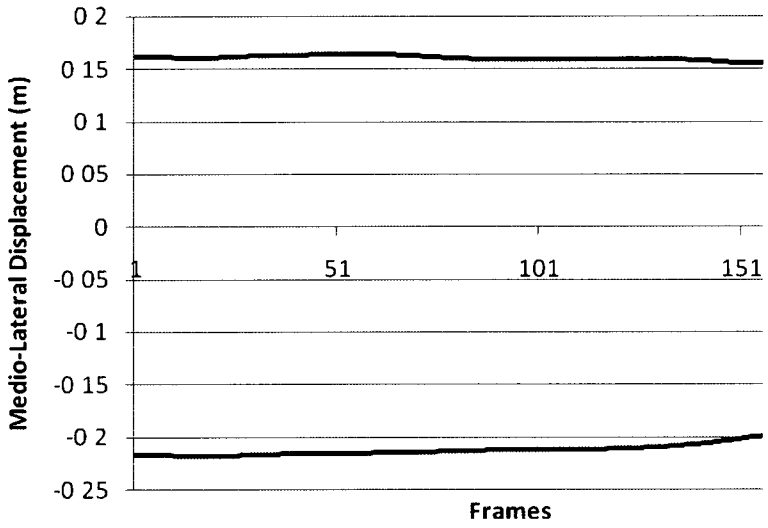

Figure F5 Participant 1's third attempt at 100 kg snatch lift (80%) Plotted is the mediolateral displacement of the left (blue series) and right (red series) shoulder markers against frames (200 Hz) No zeroing of the starting positions was performed, this is raw data The Pearson's correlation between mediolateral trajectories is r = 0 9124

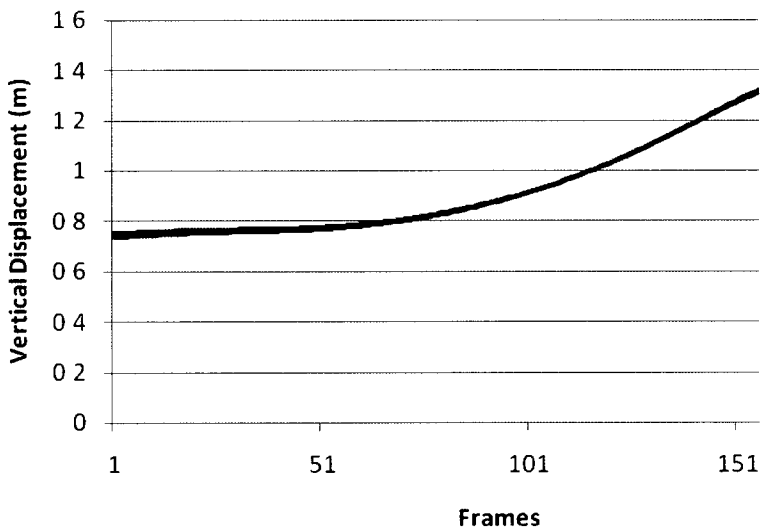

Figure F6 Participant 1's first attempt at 100 kg snatch lift (80%) Plotted is the vertical displacement of the left (blue series) and right (red series) shoulder markers against frames (200 Hz) No zeroing of the starting positions was performed, this is raw data The Pearson's correlation between vertical trajectories is r = 0 9998